

CR 151449

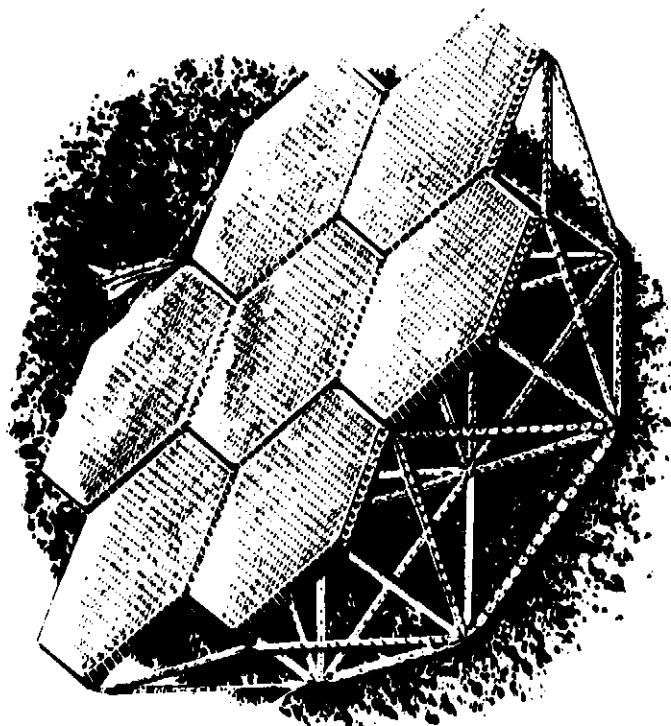
# Large Space Erectable Structures

## **BUILDING BLOCK STRUCTURES STUDY**

(NASA-CR-151449) LARGE SPACE ERECTABLE  
STRUCTURES - BUILDING BLOCK STRUCTURES STUDY  
Final Report (Boeing Aerospace Co., Seattle,  
Wash.) 119 p HC A06/MF A01 CSCI 22A

N77-27156

Unclas  
G3/12 36723



**FINAL REPORT**

**CONTRACT NAS9-14914**

**APRIL, 1977**



**BOEING AEROSPACE COMPANY**

# **Large Space Erectable Structures**

## ***BUILDING BLOCK STRUCTURES STUDY***

**FINAL REPORT  
CONTRACT NAS9-14914  
APRIL, 1977**

**Prepared For  
LYNDON B. JOHNSON SPACE CENTER  
NATIONAL AERONAUTICS AND SPACE ADMINISTRATION  
HOUSTON, TEXAS 77058**

**By  
W. H. ARMSTRONG, D. E. SKOUMAL AND J. W. STRAAYER  
BOEING AEROSPACE COMPANY  
SEATTLE, WASHINGTON 98124**

**D-180-20607-2**

## FOREWORD

This report was prepared by the Boeing Aerospace Company, Seattle, Washington, in compliance with Contract NAS9-14914. This final report describes the work completed during the period between February 1976 and April 1977.

This program was sponsored by the National Aeronautics and Space Administration, Lyndon B. Johnson Space Center, Houston, Texas. Dr. Fred J. Stebbins was the contracting officer's technical representative.

Performance of this contract was under the management of Mr. J. W. Straayer. Mr. D. E. Skoumal was the Program Technical Leader and Mr. W. H. Armstrong performed the structural strength and dynamic analyses.

## TABLE OF CONTENTS

<u>Section</u>	<u>Page</u>
Title	i
Foreword	ii
Table of Contents	iii
List of Illustrations	iv
List of Tables	vi
1.0 Summary and Introduction	1
2.0 Study Approach	4
3.0 Planar Array Development	7
3.1 Truss Configurations and Selection	7
3.2 Packaging Study	10
3.3 Material Selection	23
3.4 Joint Investigations	24
3.5 Weight Estimates	29
3.6 Deployment Analysis	29
3.7 Frequency and Strength Analysis	42
3.8 Area Scale-Up and Concept Drawings	55
4.0 Compression Strut Development	74
4.1 Configuration Trades	75
4.2 Packaging Characteristics	75
4.3 Structural Characteristics and Payload Effects	79
5.0 Concept/Performance Parametric Study & Applications	82
5.1 EVA Requirements	82
6.0 Concept Viability Analysis	83
6.1 Low Cost Manufacturing Options	83
6.2 Manufacturing Approach for Tetratruss Modules	85
7.0 Structure Development Planning	91
7.1 Development Plan	91
7.2 Development Tests	91
7.3 Model Verification Tests	93
8.0 Concluding Remarks	105

## ILLUSTRATIONS

<u>Figure No.</u>		<u>Page</u>
2.0-1	LARGE SPACE ERECTABLE STRUCTURE PROGRAM PLAN	5
2.0-2	BUILDING-BLOCK DESIGN CRITERIA	6
3.0-1	BASIC TETRAHEDRAL MODULE	8
3.0-2	TWO-RING TRUSS ARRAY	9
3.2-1	STS CARGO BAY WITH R.M.S. OPERATORS VIEW FIELD	10
3.2-2	CARGO WEIGHT VERSUS CIRCULAR ORBITAL ALTITUDE-KSC LAUNCH	11
3.2-3	CARGO CG LIMITS ALONG X-AXIS	12
3.2-4	CONCEPT FOR ARTICULATION OF TETRAHEDRAL TRUSS	13
3.2-5	PACKAGED AND DEPLOYED CHARACTERISTICS OF TETRATRUSSE MODULE	14
3.2-6	STRUT DIAMETER VS. NUMBER OF HEXAGONAL RINGS FOR PACKAGED TRUSS	15
3.2-7	STRUT LENGTH VS. NUMBER OF HEXAGONAL RINGS FOR VARIABLE $L/\rho$	16
3.2-8	NUMBER OF TRUSS STRUTS VS. NUMBER OF HEXAGONAL RINGS	18
3.2-9	NUMBER OF ATTACHMENT POINTS VS. NUMBER OF HEXAGONAL RINGS	22
3.2-10	PACKAGING GEOMETRY FOR 14 RING TETRATRUSSE	22
3.4-1	CLUSTER FITTING JOINT CONCEPTS	25
3.4-2	FOLDING HINGE JOINT CONCEPT	26
3.4-3	RIGIDIZING CONCEPT FOR CLEVIS-LUG INTERFACE	27
3.4-4	LOCKING CONCEPTS FOR TELESCOPING STRUTS	28
3.6-1	PARTIALLY DEPLOYED INNER RING OF TETRATRUSSE	30
3.6-2	RIGID BODY DEPLOYMENT TIME VS. SPRING CONSTANT WITH SPRINGS AT MID-HINGE OF FOLDING MEMBERS	32
3.6-3	MAXIMUM RADIAL VELOCITY OF REFERENCE NODE VS. SPRING CONSTANT	33
3.6-4	MAGNITUDE OF RADIAL ACCELERATION OF REFERENCE NODE VS. SPRING CONSTANT WHEN DEPLOYMENT ANGLE $\theta=0^+$ RADIAN	33
3.6-5	RIGID BODY RADIAL DISPLACEMENT, VELOCITY, AND ACCELERATION OF REFERENCE NODE	34
3.6-6	RIGID BODY ROTATION OF UPPER SURFACE FOLDING MEMBERS ABOUT MEMBER CG	35
3.6-7	RIGID BODY MOTION OF TRUSS IN Z-DIRECTION	36
3.6-8	RIGID BODY MOTION OF DIAGONAL MEMBERS ABOUT MEMBER CG	37
3.6-9	LOAD DISTRIBUTION IN RADIAL TRUSS MEMBERS	39

# ILLUSTRATIONS (Continued)

<u>Figure No.</u>		<u>Page</u>
3.6-10	LOWER SURFACE MEMBERS OF 14 RING TETRATRUS	39
3.6-11	KINETIC ENERGY OF ROTATION OF 14 RING TRUSS	41
3.6-12	MAXIMUM AVERAGE COULOMB TORQUE PER HINGE TO ACHIEVE SPIN DEPLOYMENT OF 14 RING ARRAY TRUSS	41
3.6-13	DEPLOYMENT TIME VS. INITIAL ROTATION RATE FOR DEPLOYMENT OF 14 RING TRUSS WITH NO HINGE FRICTION	42
3.7-1	NASTRAN MODEL OF 14 RING ARRAY	43
3.7-2	RELATIVE DISPLACEMENTS OF ONE QUADRANT OF 14 RING ARRAY	45
3.7-3	NATURAL FREQUENCIES AND NODAL LINES OF 14 RING TRUSS	46
3.7-4	NASTRAN PLATE MODEL OF 14 RING ARRAY	47
3.7-5	NASTRAN PLATE-ELEMENT MODEL OF SEVEN MODULE PLANAR ARRAY	48
3.7-6	NATURAL FREQUENCIES AND NODAL LINES FOR FIRST AND SECOND MODES OF SEVEN MODULE PLANAR ARRAY	49
3.7-7	UNDAMPED FUNDAMENTAL FREQUENCY VS. PLANFORM AREA OF ALUMINUM TRUSS PLANAR ARRAY	50
3.7-8	TWO-TIER TETRATRUS CONCEPT UTILIZING DEPLOYABLE TRUSS MODULES	51
3.7-9	EFFECT OF STRUCTURAL DEPTH ON FUNDAMENTAL FREQUENCY OF 1300 m DIAMETER (5-RING) PRIMARY TRUSS	52
3.7-10	EFFECT OF MASS AND STRUCTURAL DEPTH ON FUNDAMENTAL FREQUENCY OF 1000 m DIAMETER PLANAR ANTENNA	53
3.7-11	ALTERNATE TWO-TIER CONCEPT UTILIZING DEPLOYABLE TRUSS MODULES	54
3.8-1	TYPICAL TETRATRUS MODULE	57
3.8-2	PLANAR AREA EXPANSION	59
3.8-3	TETRATRUS PACKAGING CHARACTERISTICS	61
3.8-4	PACKAGING ARRANGEMENT FOR SEVEN-MODULE MISSION	62
3.8-5	MULTIPLE MODULE, UNIFORM DENSITY PAYLOAD	63
3.8-6	PRELIMINARY DESIGN, TETRATRUS SHT 2	65
3.8-7	PRELIMINARY DESIGN, TETRATRUS " 3	67
3.8-8	MULTI-MODULE PLANAR AREA EXPANSION	69
3.8-9	TWO-TIER SPACE PLATFORM CONCEPT	71
3.8-10	MULTI-RING TWO-TIER TETRAHEDRAL TRUSS	73
4.0-1	STRUT CONFIGURATIONS	74
4.2-1	ARTICULATED LATTICE TRUSS CONCEPT	76

# ILLUSTRATIONS (Continued)

<u>Figure No.</u>		<u>Page</u>
4.2-2	COLLAPSIBLE STRUT CONCEPT	77
4.2-3	CABLE-STAYED LATTICE COLUMN WITH TELESCOPIC CHORDS	78
6.1-1	CLUSTER FITTING WITH HINGED ELEMENTS	84
6.1-2	COMPOSITE STRUT APPLICATIONS	86
6.1-3	TELESCOPIC STRUT SECTION	87
6.1-4	LATTICE COLUMN CONCEPTS WITH GRAPHITE/EPOXY CHORDS	88
6.1-5	FOLDABLE LATTICE COLUMN CONCEPT	89
7.4-1	ORBITING LARGE SPACE STRUCTURE	97
7.4-2	TETRAHEDRAL TRUSS PRIME MODULE	98
7.4-3	TEMPERATURES, GEOSYNCHRONOUS ORBIT, MEMBERS 1,2,7,8	101
7.4-4	TEMPERATURES, GEOSYNCHRONOUS ORBIT, MEMBERS 3,9	102
7.4-5	TEMPERATURES, GEOSYNCHRONOUS ORBIT, MEMBER 4	103
7.4-6	TEMPERATURES, GEOSYNCHRONOUS ORBIT, MEMBER 5	103
7.4-7	TEMPERATURES, GEOSYNCHRONOUS ORBIT, MEMBER 6	104

## TABLES

<u>Number</u>		<u>Page</u>
3.2-1	PLANAR ARRAY CHARACTERISTICS	15
3.2-2	PLANAR ARRAY TETRATRUS CHARACTERISTICS-EQUAL AREA WITH VARIABLE NUMBER OF HEXAGONAL RINGS	20
3.2-3	PLANAR ARRAY CHARACTERISTICS-EQUAL AREA PLANFORM WITH FIXED STRUT WALL THICKNESS	21
3.6-1	TRUSS CHARACTERISTICS	32
3.7-1	COMPARISON OF RESULTS FROM ROD AND PLATE ELEMENT NASTRAN MODELS OF 14 RING ARRAY	47
4.2-1	STRUCTURAL CHARACTERISTICS OF STRUT ASSEMBLY	76
4.3-1	LATTICE COLUMN PACKAGING AND TOTAL DEVELOPED LENGTH	80

## 1.0 INTRODUCTION & SUMMARY

Ultra-large structures will be required to meet the requirements of future space projects which will enable man to further explore space and to extend his capability to bring about the industrialization of space. The "Outlook for Space"<sup>(1)</sup> study examined the potential space contributions to national needs. It identified goals, objectives, and themes for civilian use as well as the exploration of space during the remainder of this century. A recurring concept in this study was the utilization of large data gathering satellites transmitting information to low cost user terminals such as digital TV displays, hand-held computers with miniaturized microelectronic transceivers and ultimately a pocket or wrist configuration for information readout or communication applications.

The objective of this study was to establish structural concepts that could be used to build ultra-large structures in space. The selected concepts were to be scaleable or employ a building block approach which would utilize standard structural units. The study was to develop sufficient data to provide confidence that the selected concept could be utilized in a functional system, in space, in 1985. The completed structure will be used in low earth orbit less than 556 km (300 nm) or geosynchronous orbit approximately 37,040 km (20,000 nm) and will be transported from earth by the Space Shuttle.

A review of various future space projects including Space Solar Power Satellites, communication antennae, earth resource observation stations, and other "work platform" facilities indicated that a modular planar truss structure and a long slender boom concept would serve as building block approaches. Combinations of these two basic structures provide configuration flexibility which allows for a wide variety of mission objectives.

The cost of transportation to orbit, the amount of Extravehicular Activity (EVA), type of assembly equipment, and the mission timelines while in low earth orbit, are the major considerations that determine the relative efficiency of assembling a given structure. Previous studies of this fabrication/



assembly scenario investigated several options to build large structures, e.g., a mobile assembler delivered by Shuttle and supplied with deployable beam units,<sup>(2)</sup> a Shuttle construction base which uses the RMS to retrieve prefabricated elements from the payload bay and systematically form truss modules on holding fixture,<sup>(3)</sup> and a construction platform initially erected from multiple Shuttle flights and utilizing "beam building modules" supplied with raw materials to fabricate/assemble larger more complex structures in-situ.<sup>(4)</sup>

The normal industrial engineering trades conducted in this study that determined the "where and how to" fabricate the structure were biased somewhat by the desire to be functionally ready for space by the mid-nineteen eighties. Ground fabricated structures which can be characterized by an extensive cost and manufacturing data base appeared to be the best near-term option for fabrication. This led to the assembly option chosen for this study which was an earth assembled and packaged structure. This concept, as well as meeting the near term objective, has the desirable feature of element quality assurance/rejection prior to launch. The on-orbit productivity of this concept, in terms of constructing a given area of structure in the lowest amount of time, is unmatched by even the most optimistic estimates of on-orbit fabrication/assembly schemes.

The structural configurations chosen for the study were the tetrahedral planar truss and lattice column. These are concepts receiving a wide amount of usage by various study groups. Work performed in the configuration analysis area benefitted greatly from earlier studies performed by Boeing under Contract NAS1-13967<sup>(5)</sup> which identified the tetrahedral truss as having the lightest weight and the highest first mode frequency when compared to other generic trusses of equal depth and planform area.

This study addresses the problems associated with the assembly packaging of these efficient structural concepts. Articulating joints and collapsing details are defined to allow packaging densities to approach values that effectively utilize the payload mass capability of the Shuttle.

A deployable planar truss building block module is described in parametric form to allow a broad application base for this type of structure. For example, structural trade studies involving static and dynamic analyses of a single module were performed using mass and stiffness as parameters. The finite-element model used in the trades consisted of approximately 3900 degrees of freedom and 2600 structural elements. Multiple assembly of these building block modules provides rapid surface area expansion, but the cost of structural analysis using high fidelity single module models is prohibitive. Consequently, simplified modeling approaches for multi-module concepts are warranted and were defined as a part of the structural trade studies. In addition, rigid body deployment analysis techniques were developed to assess kinetics and kinematics of automatic deployment of the building block module. The deployment models provided preliminary evaluation of candidate deployment methods.

These trade studies showed that the fundamental frequency becomes quite low ( $<1$  Hz), as the planar area increases from  $10^2$  to  $10^3$  m<sup>2</sup> or more. A "two tier" concept is envisioned which utilizes the deployable modules as the payload interface or secondary structure and a deeper tetrahedral truss to provide the necessary strength or stiffness. The planar modules could thus provide a variable attachment spacing compatible with the particular payload or mission requirement. The deeper primary truss could be fabricated from deployable lattice members or if the spacecraft size warrants it a "beam builder" or erectable concept used.

A deployable lattice column is described that can be packaged to densities approaching the Shuttle mass limits. Parametric trades were made for this concept including a method to optimize the lattice elements for a simultaneous column/crippling failure.

## 2.0 STUDY APPROACH

The initial approach to establish a "building block" structural concept was to review proposed future space missions. Applications were identified ranging from antenna/reflector systems in the 100 to 300 meter diameter range to major elements of Space Solar Power Satellite concepts that have planar areas of several square kilometers and struts or columns as long as 100 to 1500 meters. The design requirements for the structural configuration for each of these missions evolves from a specified surface area and/or geometric restrictions of flatness or curvature. The Shuttle payload packaging and weight limitation (fore and aft CG variation) dictated a packaging density approaching  $100 \text{ kg/m}^3$  for a structure having very low deployed density in orbit. It was apparent that, while the various applications would have the size and packaging commonalities, they would also have other unique system or performance requirements. Therefore, a parametric approach was taken in order to present configuration data that might be utilized in a variety of applications. This would allow a payload configurator to do a rapid preliminary design to "ballpark" his approach.

The program was conducted in task form as outlined in Figure 2-1. The Task One effort examined future space mission requirements that would contribute to the design definition of the structural concepts. Design criteria were established in a very general form and are shown in Figure 2-2. Conceptual building-block designs were formulated which satisfied these criteria. Computer-aided analyses, packaging studies and typical joint designs were products of this task which lead to preliminary designs of a deployable planar truss module (tetratruss) and a building-block compression member (lattice column structure).

The Task Two effort indicated that in order to minimize program costs the performance or productivity of a given concept should be measured as a function of total surface area (with respect to the tetratruss) or deployed length (lattice column) delivered to low earth orbit in each STS launch. The emphasis then was to identify those concepts which have the highest deployed area or length per unit mass. The cost of the tetratruss in prelaunch configuration is discussed in Section 6.0.

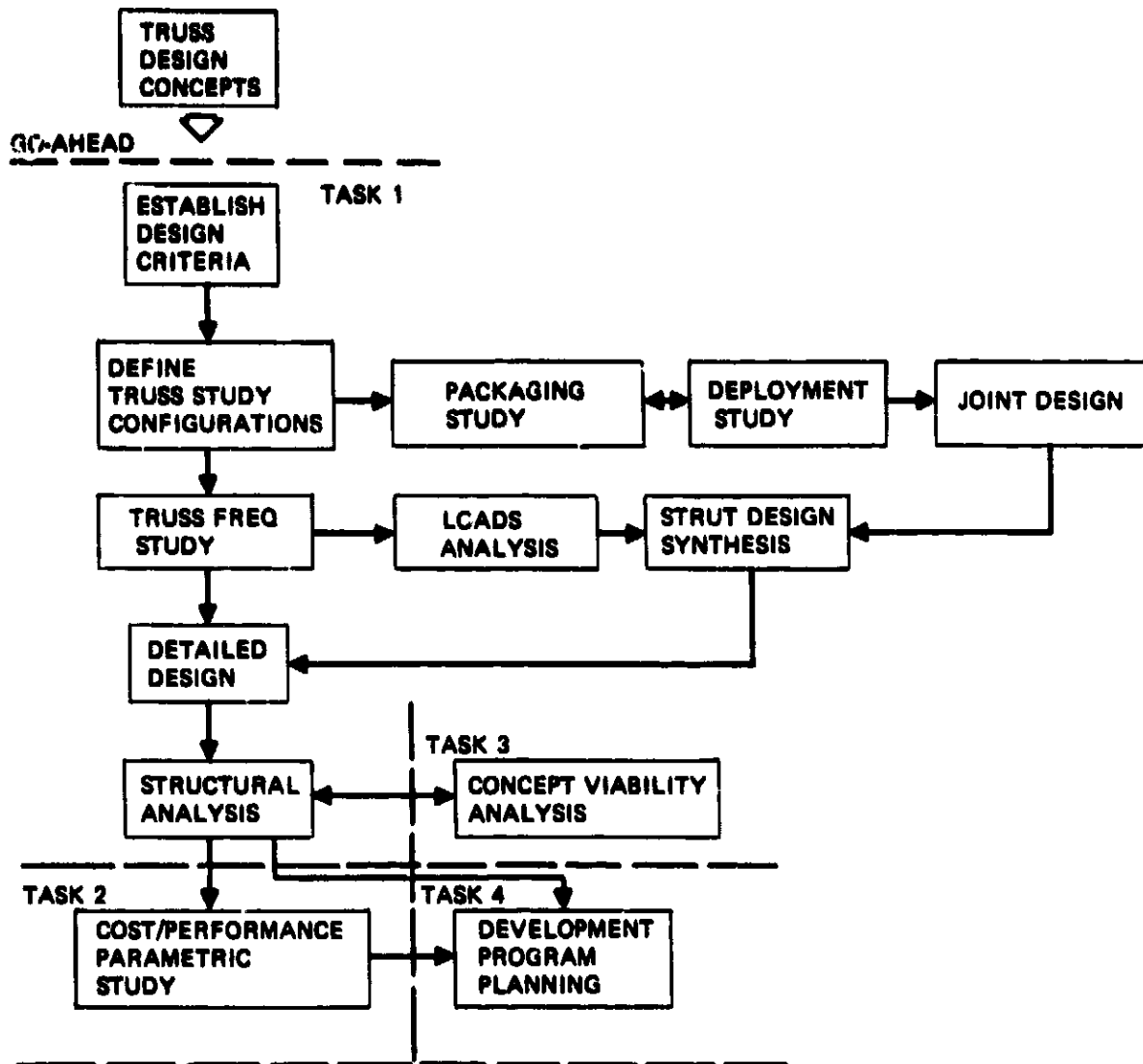


*Figure 2.0-1. Large Space Erectable Structures Program Plan*

Structural configuration	<ul style="list-style-type: none"> <li>• 10 to 1,000 m long</li> <li>• Planar surface area 100 m<sup>2</sup> to 1,000,000 m<sup>2</sup></li> <li>• High stiffness-to-weight ratio</li> <li>• Good attachment capability</li> <li>• Packaging compatible with weight and volume of shuttle</li> <li>• Column-critical elements <math>L/p \geq 200</math> <math>D/t \geq 100</math></li> </ul>
Mission requirement	<ul style="list-style-type: none"> <li>• Low Earth orbit deployment and assembly</li> <li>• Transfer to geosynchronous orbit</li> </ul>

**Figure 2.0-2. Building-Block Design Criteria**

The concept viability analysis conducted in Task Three influenced the design concepts by restricting them to those which had fabrication precedence. Hardware and test experience from previous developmental and in-house work were used to insure that concepts showed similarity in design and that no new technology would be required. Low cost manufacturing options were identified and high-rate production techniques such as injection molding of detail parts were baselined to keep the prelaunch configuration at the lowest possible cost.

A developmental plan, the final task, discusses a program to validate the design and analysis uncertainties. Elements tests including scaled 1-g deployment of a modular tetratruss unit are outlined. Tests to verify as-built tolerances which relate to joint friction and damping are viewed as a necessary input to accurately characterize the structural stiffness when deployed.

### 3.0 PLANAR ARRAY DEVELOPMENT

Planar structural concepts were examined from previous IR&D work in space erectable large area structures. Some of these concepts are shown below.

<u>Configuration</u>		<u>Distinguishing Features</u>
Unfurlable Segments	}	Flexible Membrane
Inflatable Membrane		
Stabilized Mesh		
Telescopic Modules	}	Rigid Elements
Hinged Panels		
Stiffened Gore Segments		
Expandable Trusses		

#### 3.1 TRUSS CONFIGURATIONS AND SELECTION

Only the configurations with "rigid elements" had the potential to be assembled in modular form into the very large areas required. The expandable truss configuration was therefore pursued as a planar area concept. Truss-type structures have excellent structural efficiency and are amenable to scaling through element sizing, length and depth changes.

Previous contract studies<sup>(5)</sup> had indicated that the tetrahedral truss was suitable for a wide variety of applications that required flat, single curvature or double curvature surface contours. The effective stiffness properties of a tetrahedral truss are of "isotropic" nature and are relatively high for a given truss mass. Torsional stiffness is notably high for this concept. The tetrahedral truss also has identical length column members which is important in minimizing cost.

A basic tetrahedral module is shown in Figure 3.0-1. This module consists of three repeating tetrahedrons joined at a common apex. The upper and lower surfaces are formed with the addition of three identical length members. The upper surface plane is hexagonal and the lower surface is triangular for this module. This basic module is used throughout the study and is referred to as

a one-"ring" module. A two-"ring" module is constructed by adding additional tetrahedons and connecting members to the perimeter of the single module. A two-ring module is shown in Figure 3.0-2. As indicated, the upper surface remains hexagonal and the lower surface has an irregular shape. This basic nomenclature is used to describe tetrahedral trusses of one to "n" number of rings.

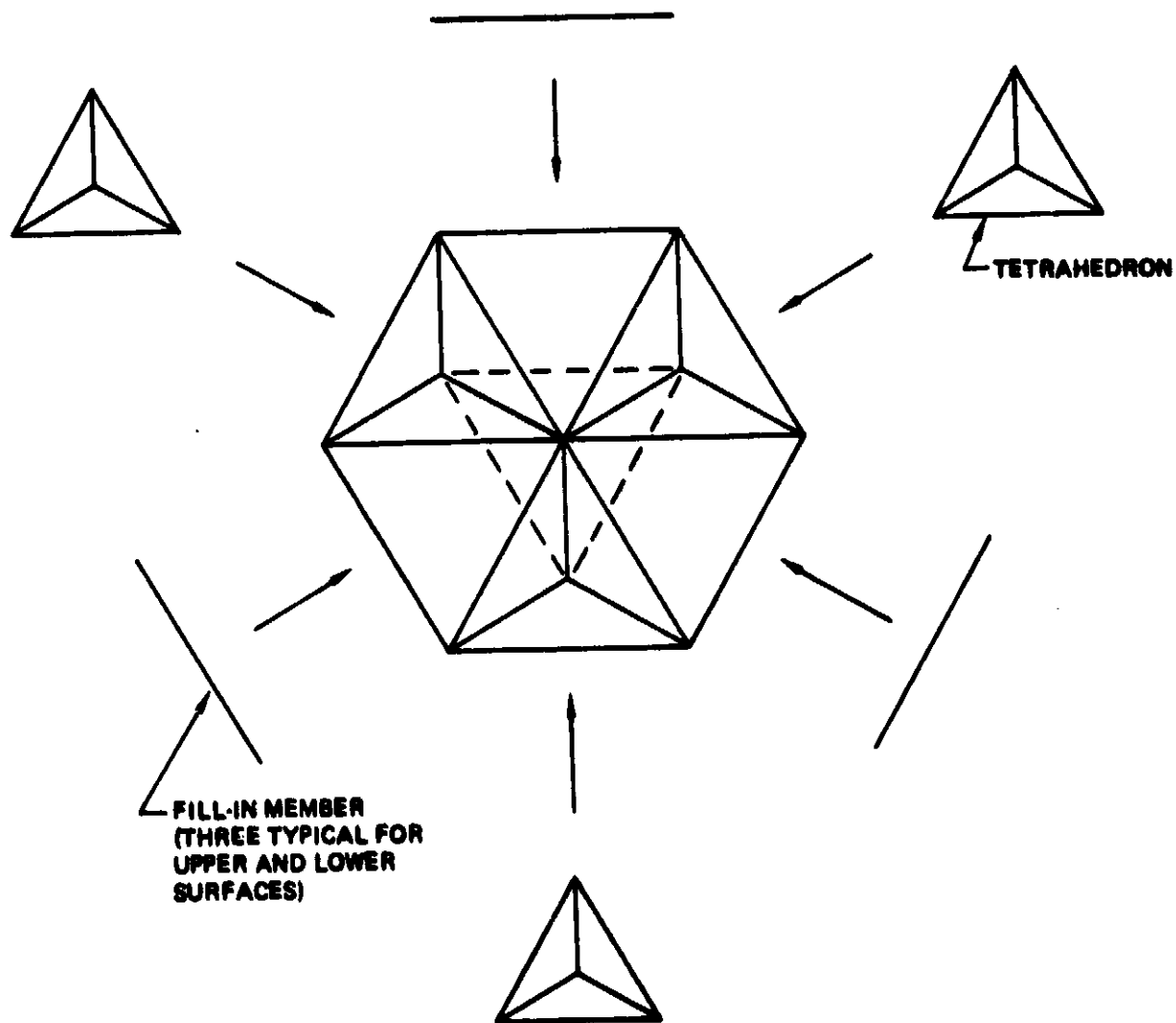
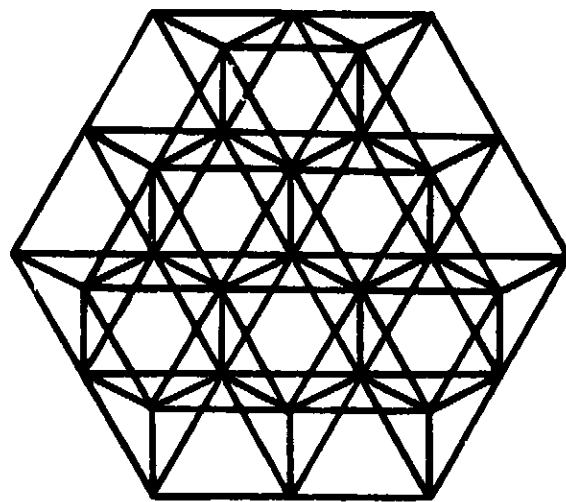
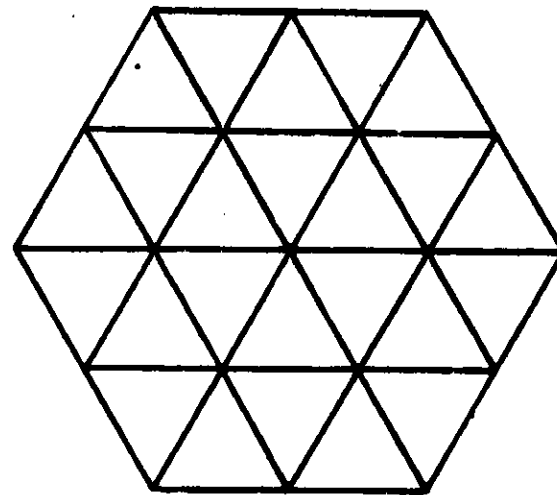


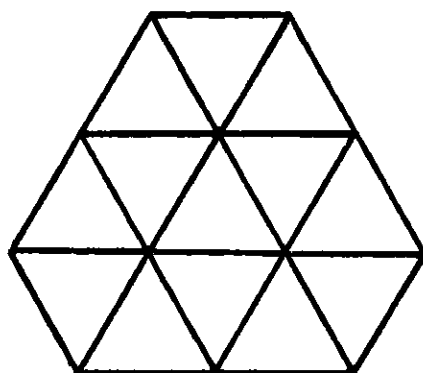
**Figure 3.0-1. Basic Tetrahedral Module**



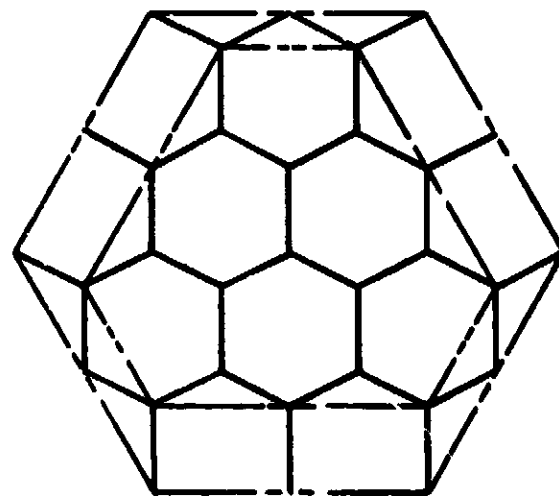
**ASSEMBLY**



**LOWER-SURFACE ELEMENTS**



**UPPER-SURFACE ELEMENTS**



**ELEMENTS BETWEEN  
SURFACES**

**Figure 3.0-2. Two-Ring Truss Array**

The open nature of tetrahedral truss causes a minimum of member shadowing and thus offers better thermal deformation control. It was also felt that a truss concept that featured basic repeating modules could be verified on the ground by 1-g and environmental simulation testing of single repeating units of the larger structure. In Section 7.0 is a discussion of a structural development plan which includes component development tests as well as tests for analytical model verification.



### 3.2

### PACKAGING STUDY

The packaging arrangement of the truss modules is governed by how tightly the individual members can be folded and articulated to form a compact array which would fit into the 4.57 m. x 18.29 m. payload bay. The Shuttle payload bay is shown in Figure 3.2-1. It was assumed for this study that the entire payload bay volume would be available to store the structure. It was determined in earlier studies that truss structures which deploy to areas as large as 100 meters in diameter could be packaged and accommodated in the bay. The packaging ground rules for this study were to (1) examine several variations of an articulated truss configuration to improve the packaging density shown in previous studies, and (2) to show the effect on deployed area by packaging multiple modules.

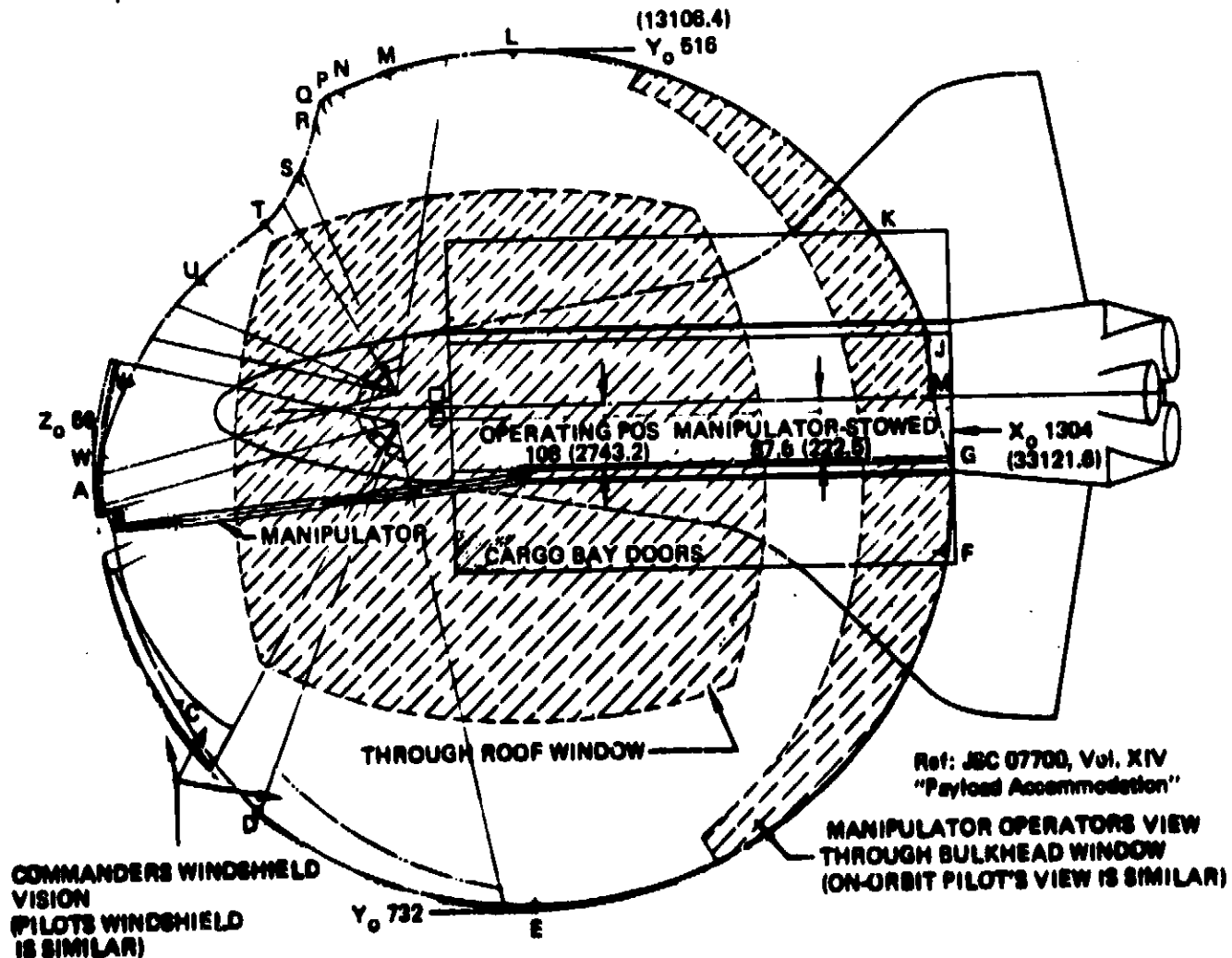


Figure 3.2-1. Cargo Bay and RMS Reach Envelope

The payload capability of the Space Transportation System (STS) to deliver a given payload to orbit is shown in Figure 3.2-2 which is taken from JSC Publication 07700, Vol. XIV, Rev. D, Space Shuttle System Payload Accommodations. As indicated, for circular orbits up to approximately 407 km (220 nm) at 28.5 degree inclination, 29,484 kg (65,000 lbs) can be delivered. If no fore and aft center of gravity limitation is imposed on the orbiter, the payload weight-to-volume ratio (packaging density) would be approximately  $97.7 \text{ kg/m}^3$  ( $6.1 \text{ lb/ft}^3$ ). The cargo CG limits are shown in Figure 3.2-3. Strict adherence to this curve to transport a 29,484 kg payload would indicate that, for a packaged module that fills the payload bay cross section, a maximum length of 14.7 m (48.2 ft) of payload could be packaged at a density of  $121.9 \text{ kg/m}^3$  ( $7.61 \text{ lb/ft}^3$ ). The total allowable mass, because of this cg limitation, is reduced to 12,977 kg (28,609 lbs) if a uniformly distributed payload is packaged to fill the bay. This latter case represents a packaging density of  $43.2 \text{ kg/m}^3$ .

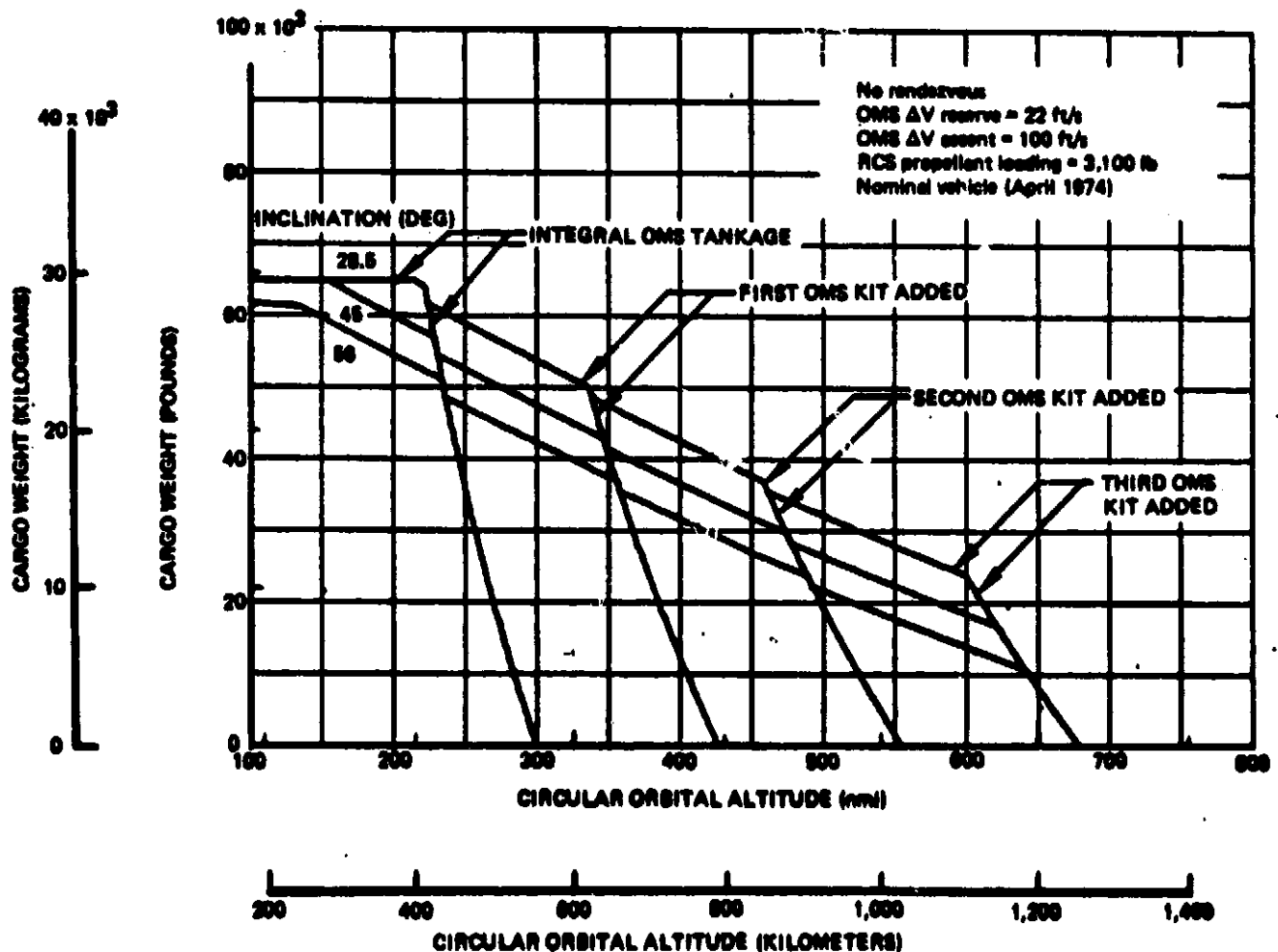
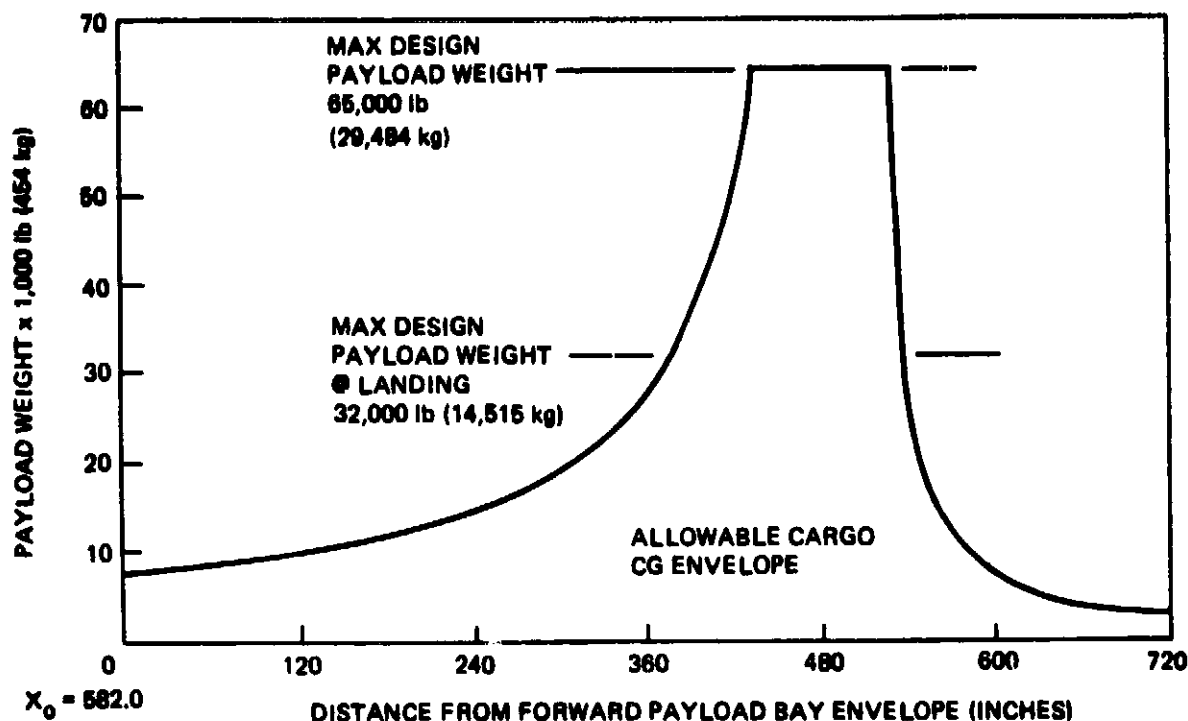


Figure 3.2-2. Cargo Weight Versus Circular Orbital Altitude (KSC Launch, Delivery Only)



**Figure 3.2-3. Cargo CG Limits (Along X Axis)**

(2.7 lb/ft<sup>3</sup>). It was determined that a packaging arrangement that permitted a variation in packaging density would be suitable for the largest variety of applications. This is also true if an entire STS payload would be used to transport only structure to revisit a construction site in low earth orbit.

An articulating scheme for folding a tetrahedral truss is shown in Figure 3.2-4. As reported in LaRC Contract NAS1-13967, the truss surface members are hinged at either end to a cluster fitting and each has a hinge joint at mid-span. The diagonal members are hinged to the cluster fittings and thus are allowed to rotate. The packaging of the module then is achieved by folding the surface members, in half, away from the diagonals. The diagonals will rotate until the entire cluster forms a columnated bundle or package as shown. The packaged cross section is determined by how closely the individual members can nest together. For this configuration it appears that adjacent cluster fittings can be positioned a distance of 3 times the basic member diameter. This would then indicate that the packaged dimension for a one-"ring" array would be 6 diameters. As additional hexagonal "rings" are packaged they also form a hexagonal cross section. The packaged length for this scheme is twice the individual member length.


$$n = \frac{42.7 \text{ mm}}{6 \times .51 \text{ mm}} = 13.95 \approx 14 \text{ rings}$$

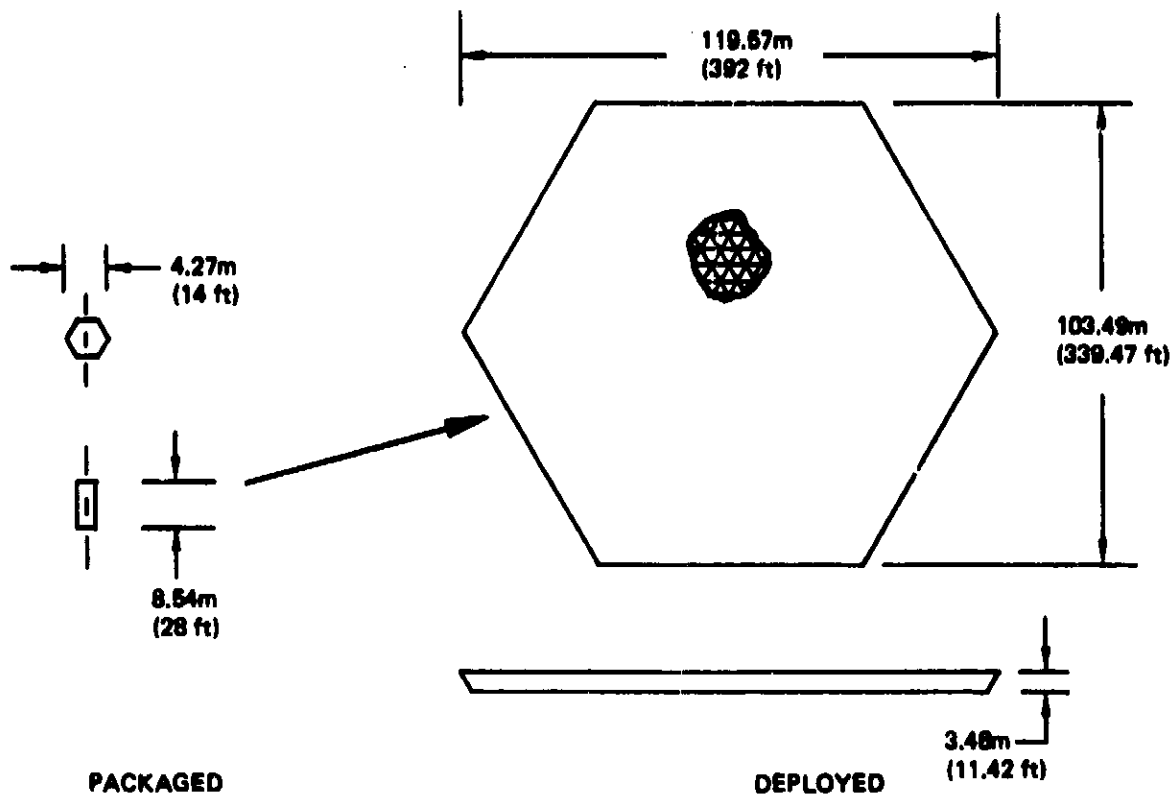


**Figure 3.2-5. Packaged and Deployed Characteristics of Tetratruss Module**

The developed planar area can be calculated from the expression given in Table 3.2-1. The packaging density for this concept is  $36.8 \text{ kg/m}^3$  ( $2.3 \text{ lb/ft}^3$ ). The volume, area and deployed mass per unit area are shown in Table 3.2-1. Also shown in this table are data for a fourteen-ring truss of equal area comprised of aluminum elements. The packaging densities of both concepts are shown. Two units of the graphite/epoxy truss could be carried to the low earth orbit specified. However, this payload would represent only 25% of the mass delivery capability.

Additional packaging data were generated to cover other tetratruss (tetrahedral truss) configurations. Figure 3.2-6 shows the relationship of member diameter to the number of packaged hexagonal rings. This represents the maximum member diameter as the number of hexagonal rings increases from five to fourteen.

**Table 3.2-1. Planar Array Characteristics**

Strut members			Array characteristics	
	Aluminum	Gr/Ep	Number of elements	
Length, m (in)	4.27 (168)	4.27 (168)	Upper surface	1,680
Diameter, m (in)	0.061 (2.00)	0.061 (2.00)	Lower surface	1,808
Wall thickness, m (in)	0.00061 (0.020)	0.00061 (0.024)	Diagonals	1,764
Weight, kg (lb)	0.95 (2.09)	0.84 (1.40)		
Joint factor	1.1	1.1		
Material density, kg/m <sup>3</sup> (lb/in)	2.768 x 10 <sup>3</sup> (0.1)	1.550 x 10 <sup>3</sup> (0.056)		
Packaged data			Deployed data	
Volume	101 m <sup>3</sup> (3,585 ft <sup>3</sup> )		Area	9,273 m <sup>2</sup> (99,808 ft <sup>2</sup> )*
Weight			Density/area	
Gr/Ep	3,667 kg (8,065 lb)		Gr/Ep	0.40 kg/m <sup>2</sup> (0.081 lb/ft <sup>2</sup> )
Aluminum	5,475 kg (12,070 lb)		Aluminum	0.59 kg/m <sup>2</sup> (0.121 lb/ft <sup>2</sup> )
Packaged density			* $A_p = 2.596076 \text{ m}^2 L_s^2$	
Gr/Ep	36.4 kg/m <sup>3</sup> (2.27 lb/ft <sup>3</sup> )		where $A_p$ = planar area, $m$ = no. of rings;	
Aluminum	54.2 kg/m <sup>3</sup> (3.39 lb/ft <sup>3</sup> )		$L_s$ = length of strut members	

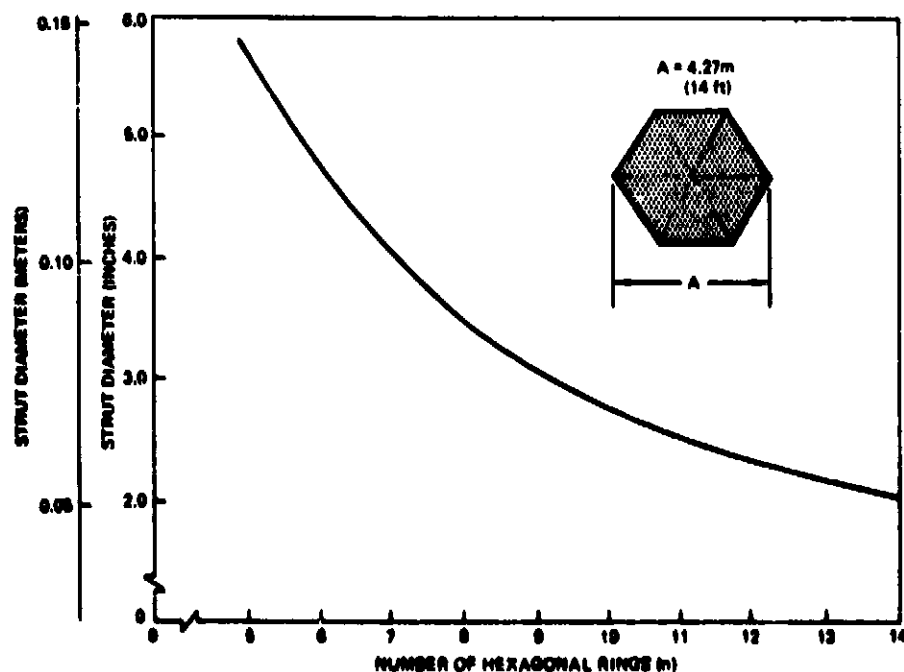


**Figure 3.2-6. Strut Diameter Versus Number of Hexagonal Rings for Packaged Truss**

Each point on the curve represents a full packaged section as shown ("A" = 4.27 m (168 in)). Using this data and Figure 3.2-7 a strut length or distance between hard points can be established as a function of element slenderness ratios. This data would be helpful in determining the buckling resistance for a range of strut materials. For example, if a payload required a structural tie-down or hard point at say 200 in. intervals, Fig 3.2-7 would be used to determine the number of hexagonal rings to be packaged. Using an  $L/\rho$  of 200, Figure 3.2-7 indicates that 9 hexagonal rings would be required. Figure 3.2-6 would then indicate that the strut diameter would be slightly greater than .076 m (3.0 in.).

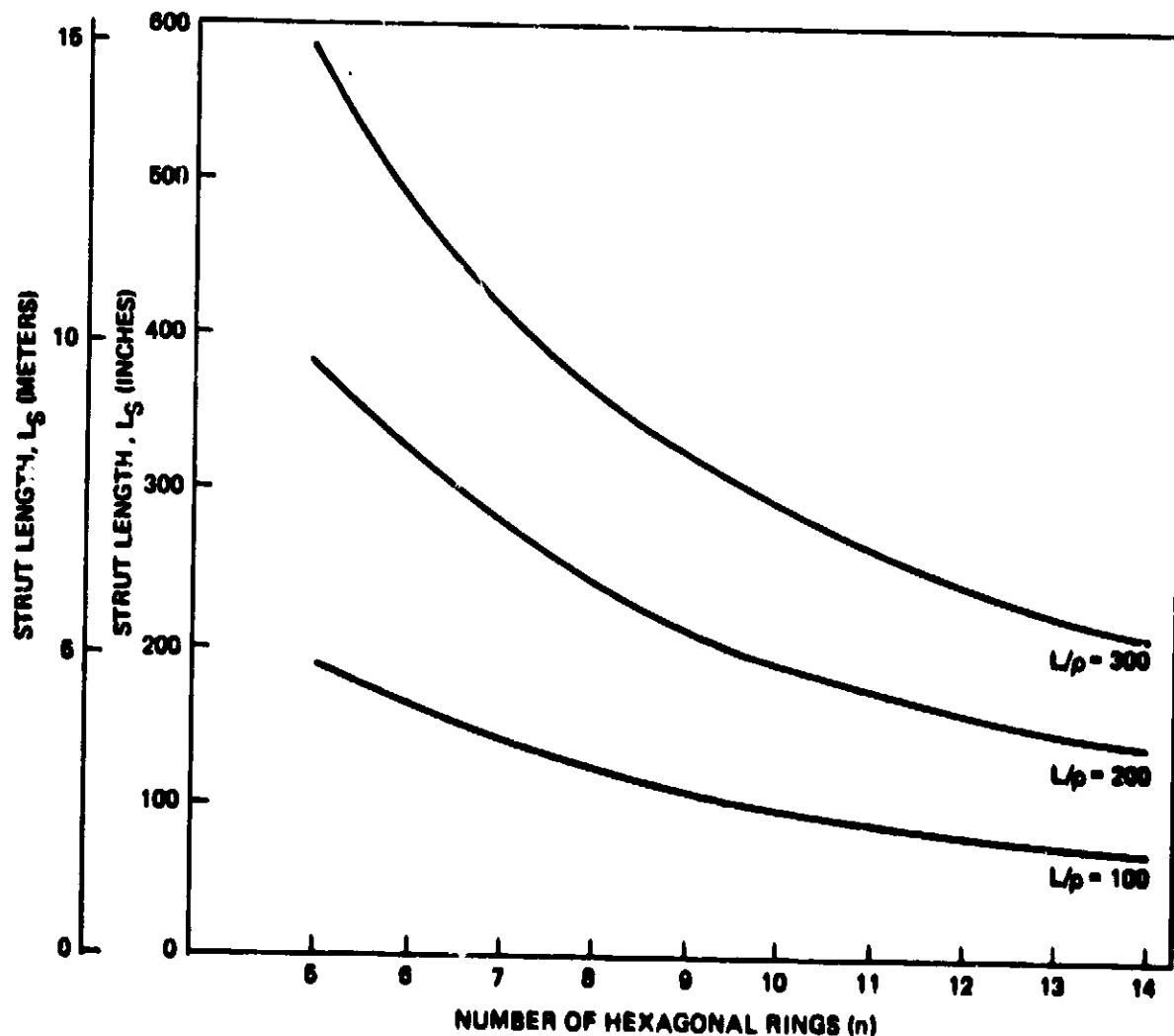


Figure 3.2-7. Strut Length Versus Number of Hexagonal Rings for Variable  $L/\rho$

If a given planar area is desired, Figure 3.2-7 can be entered and various combinations of strut lengths and number of rings, for a constant  $L/\rho$ , will generate the same planar area. It is well to note, however, that the number of individual elements as a function of ring number increases dramatically as shown by the curve in Figure 3.2-8. There is an obvious incentive to choose the longest member length, consistent with attachment requirements, to minimize the number of hexagonal rings to develop a given planar area.

The surface nodes or attachment points can be determined from the following expressions:

$$N_{SU} = 3n(n + 1) + 1$$

and  $N_{SL} = 3n^2$

where "n" = Number of hexagonal rings

$N_{SU}$  = Number of Upper Surface Nodes

$N_{SL}$  = Number of Lower Surface Nodes

These relationships are plotted in Figure 3.2-9. The lower surface will always have fewer attachment points than the upper surface due to the "irregular" shape. This irregularity is minimized as the number of hexagonal rings increases. This data applies to "regular" tetratruss modules which have equal length members for both top and bottom surfaces and the diagonals.

A possible method of achieving a variable or tapered planar array would be to arrange perimeter "rings" of hexagonal modules and vary the length of the diagonal or core members. This would allow the nodal spacing on both top and bottom surfaces to remain the same while accomplishing the depth variations.



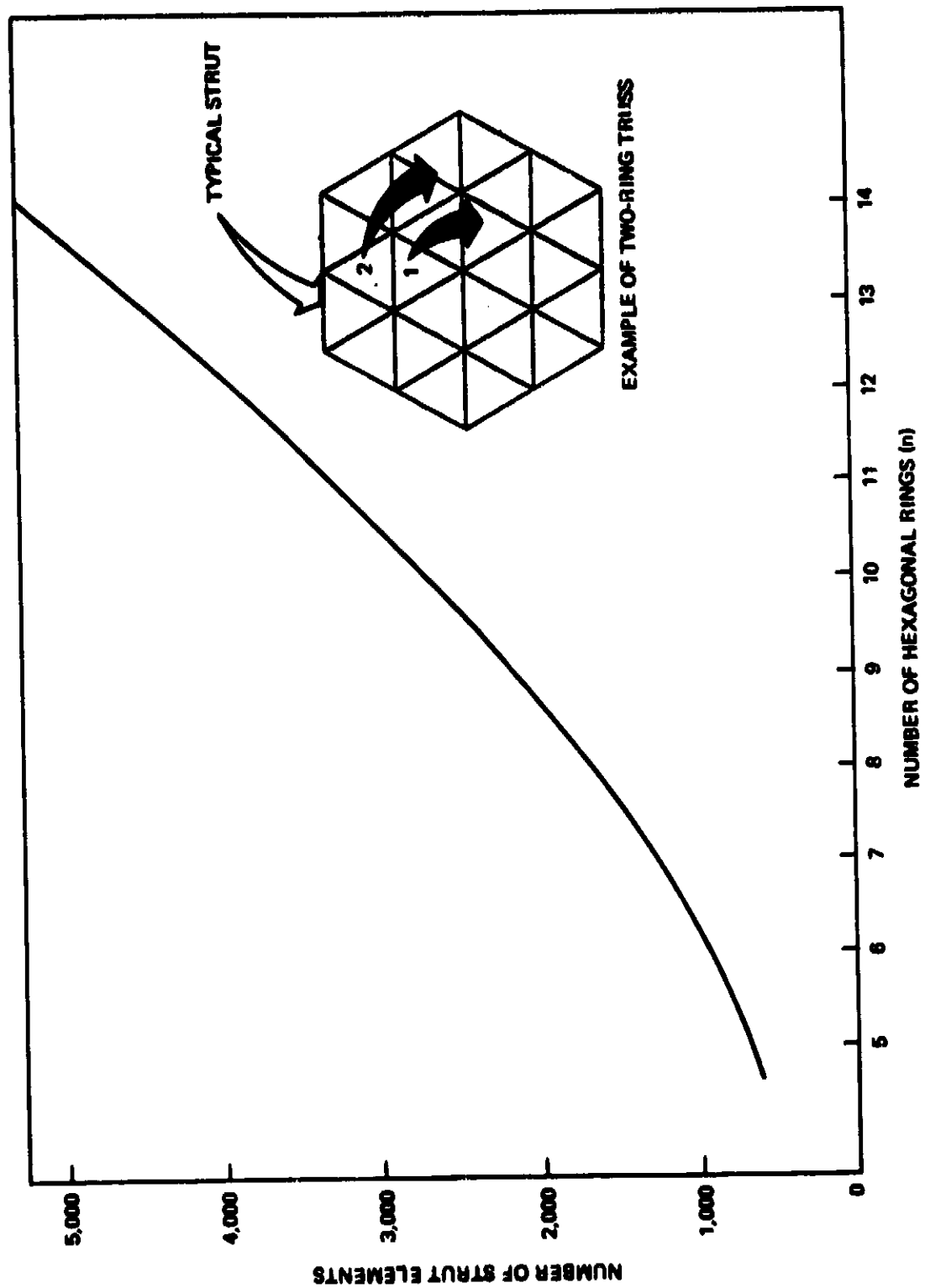


Figure 3.2-8. Number of Truss Elements (Struts) Versus Number of Hexagonal Rings

Tables 3.2-2 and 3.2-3 show characteristics of the tetratruss planar array. The truss strut diameter is chosen as the maximum diameter, as a function of the number of hexagonal rings, that provides a packaged cross section of 168 in. If the strut D/t is held constant at one hundred, which is the usual cut-off point for circular cross sections, and if the strut length is set by establishing the L/ $\rho$  at two hundred, the array weight as shown in Table 3.2-2 changes from 2737 kg (6035 lbs) to 7554 kg (16,654 lbs). Each of these arrays would have an identical platform area. Figure 3.2-3 illustrates an interesting feature of the tetratruss. If the strut wall thickness is held at a constant gage, say .51 mm (.020 in), and again holding L/ $\rho$  at two hundred, the weight of the array essentially becomes constant. This permits a high degree of versatility when utilizing these arrays as "building blocks." The configurator has a choice of attachment spacing and location even if he is constrained to a minimum gage situation. The D/t varies from one hundred to two hundred eighty, and thus the individual member compression capability varies from approximately 3380 N (760 lbs) to 9608 N (2160 lbs) when the .051 m (2.0 in.) diameter strut is increased to .14 m (5.60 in.).

It was felt that, while a typical Shuttle-type payload would be a combination of an orbital transfer vehicle or system combined with a packaged spacecraft module, attempts should be made to densify the structural module. A technique to achieve a "variable" packaging density is shown in Figure 3.2-10 which consists of segmenting the individual truss elements and allowing them to telescope into a more compact unit. The telescoped elements would have locking features (discussed in Section 3.4) to prevent linear and rotational motion when the members are fully extended. The packaging density of the 14-ring truss shown in Figure 3.2-10 is estimated to be 124 kg/m<sup>3</sup> (7.76 lb/ft<sup>3</sup>) if made from graphite epoxy materials. Thus a range of packaging densities is available, depending on the initial tetratruss sizing (number of rings and member gages) and the degree of telescoping incorporated. The added complexity and cost incurred by the additional segments and joints is offset by the ability to customize the structural module to more closely match the fore and aft center of gravity restrictions. This capability should provide weight-limited rather than volume-limited cargoes to low earth orbit. Structural area scale-up utilizing telescoped tetratruss modules is discussed in Section 3.8.

Table 3.2-2. Planar Array Tetrahedron Characteristics (Equal Area With Variable Number of Hexagonal Rings)

No. of hex rings (n)	Strut dia m (in) 1	Wall thickness m (in) 2	Strut area m <sup>2</sup> (in <sup>2</sup> )	Strut length, L <sub>3</sub> m (in) 3	Strut weight kg (lb) 4	No. of struts	Array weight kg (lb)
14	0.061 (2.000)	0.00051 (0.0200)	0.000080 (0.1244)	3.56 (140.0)	0.474 (1.0450)	5,250	2,737.5 (6,035)
13	0.055 (2.150)	0.00055 (0.0215)	0.000093 (0.1438)	3.81 (150.0)	0.585 (1.2980)	4,524	2,929.8 (6,459)
12	0.050 (2.330)	0.00059 (0.0233)	0.000109 (0.1688)	4.14 (163.0)	0.750 (1.6530)	3,852	3,177.0 (7,004)
11	0.065 (2.550)	0.00065 (0.0255)	0.000130 (0.2022)	4.53 (178.4)	0.982 (2.1643)	3,234	3,492.3 (7,699)
10	0.071 (2.800)	0.00071 (0.0280)	0.000157 (0.2438)	4.98 (196.0)	1.300 (2.8670)	2,670	3,819.3 (8,420)
9	0.079 (3.110)	0.00079 (0.0311)	0.000194 (0.3008)	5.53 (217.8)	1.776 (3.9164)	2,160	4,220.8 (9,305)
8	0.089 (3.500)	0.00089 (0.0350)	0.000246 (0.3810)	6.22 (245.0)	2.541 (5.6010)	1,704	4,762.4 (10,499)
7	0.102 (4.000)	0.00102 (0.0400)	0.000321 (0.4976)	7.11 (280.0)	3.792 (8.3597)	1,302	5,431.0 (11,973)
6	0.119 (4.670)	0.00119 (0.0467)	0.000408 (0.6783)	8.31 (327.0)	6.037 (13.3082)	954	6,435.0 (13,966)
5	0.142 (5.600)	0.00142 (0.0560)	0.000629 (0.9754)	9.96 (392.0)	10.406 (22.9410)	660	7,554.3 (16,654)

1 Maximum diameter for packaging in Shuttle bay

2 Assumes D/+ = CONST = 100

3 Assumes L/p = CONST = 200

4 Assumes Gr/Ep @ 1.661 x 10<sup>3</sup> kg/m<sup>3</sup> (0.080 lb/in<sup>3</sup>)

Note: Area = CONST = 2.588076 n<sup>2</sup> L<sub>3</sub><sup>2</sup>  
A = 6,439 m<sup>2</sup> (69,311 ft<sup>2</sup>)

Table 3.2-3. Planar Array Tetrahedral Truss Characteristics (Equal Area Planform With Fixed Strut Wall Thickness)

No. of hex rings (n)	Strut dia m (in)	Wall thickness m (in)	Strut area m <sup>2</sup> (in <sup>2</sup> )	Strut length, L <sub>s</sub> m (in)	Strut weight kg (lb)	No. of struts	Array weight kg (lb)
14	0.061 (2.00)	0.00051 (0.020)	0.000080 (0.1244)	3.56 (140.0)	0.474 (1.0450)	5,250	2,737.5 (6,035)
13	0.055 (2.15)	0.00051 (0.020)	0.000086 (0.1338)	3.83 (150.6)	0.548 (1.2090)	4,524	2,728.9 (6,016)
12	0.059 (2.33)	0.00051 (0.020)	0.000094 (0.1451)	4.15 (163.4)	0.645 (1.4225)	3,852	2,734.3 (6,028)
11	0.055 (2.55)	0.00051 (0.020)	0.000103 (0.1580)	4.54 (178.9)	0.774 (1.7067)	3,234	2,753.8 (6,071)
10	0.071 (2.80)	0.00051 (0.020)	0.000113 (0.1747)	4.99 (196.6)	0.935 (2.0808)	2,670	2,745.2 (6,062)
9	0.079 (3.11)	0.00051 (0.020)	0.000125 (0.1942)	5.56 (218.5)	1.155 (2.5460)	2,180	2,743.8 (6,049)
8	0.089 (3.50)	0.00051 (0.020)	0.000141 (0.2187)	6.26 (246.1)	1.465 (3.2293)	1,704	2,745.6 (6,063)
7	0.102 (4.00)	0.00051 (0.020)	0.000161 (0.2501)	7.15 (281.4)	1.916 (4.2233)	1,302	2,743.8 (6,049)
6	0.119 (4.67)	0.00051 (0.020)	0.000189 (0.2922)	8.35 (328.8)	2.615 (5.7545)	954	2,743.8 (6,049)
5	0.142 (5.60)	0.00051 (0.020)	0.000226 (0.3506)	10.02 (394.6)	3.765 (8.3008)	680	2,733.4 (6,026)

1 Maximum diameter for packaging in Shuttle bay

2 Assumes L/p = CONST = 200

3 Assumes Gr/Ep @ 1.661 x 10<sup>-3</sup> kg/m<sup>3</sup> (0.060 lb/in<sup>3</sup>)

Note: Area = CONST = 2.588076 n<sup>2</sup> L<sub>s</sub><sup>2</sup> = 5,439m (69,311 ft<sup>2</sup>)

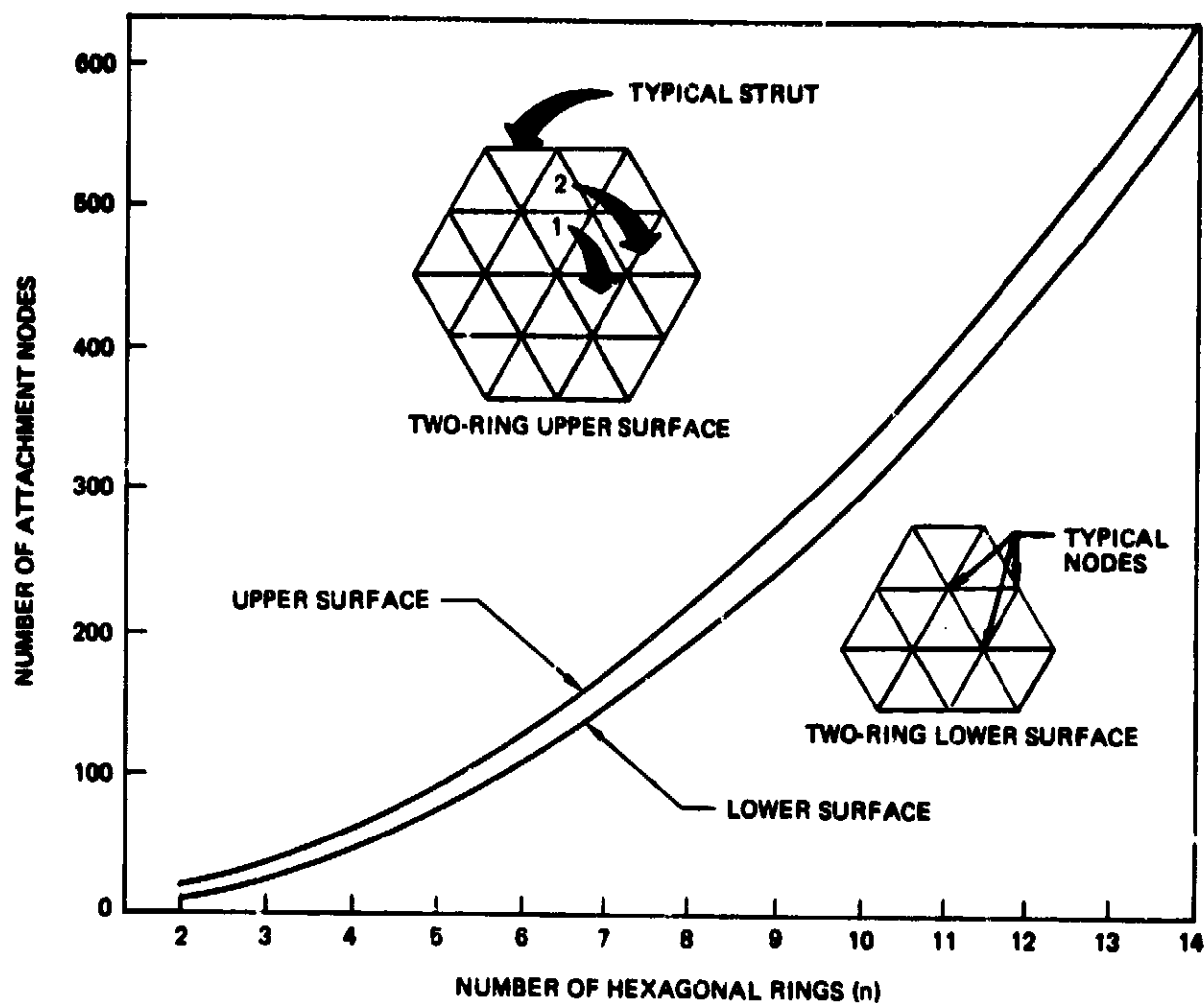


Figure 3.2-9. Number of Attachment Points Versus Number of Hexagonal Rings

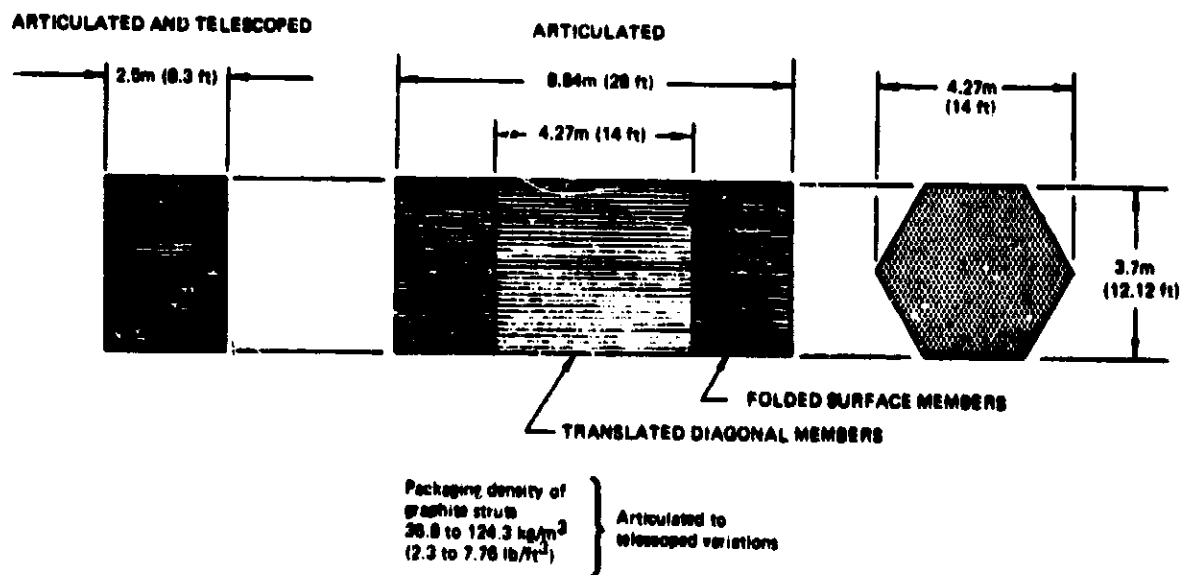


Figure 3.2-10. Packaging Geometry of 14-Ring Tetrahedral Truss

### 3.3 MATERIAL SELECTION AND MEMBER CONFIGURATION

The material selection for a given structural application on any large area spacecraft will be determined more by elastic response (stiffness) and thermo-physical characteristics than by strength considerations. Large structures in both L.E.O. and G.E.O. will be in a rather benign naturally occurring load environment. Orbital transfer will be strongly influenced by the acceleration tolerance of the configuration being moved. Analysis of a typical tetratruss module (see Section 3.7) under .05g acceleration indicated only local resizing would be required. Surface control of flatness or shape is a desired feature for most applications examined for this study. Thermal gradients, whether caused by the particular orbit/inclination or waste heat from spacecraft systems can best be handled by a material system having a low coefficient of thermal expansion. For these reasons, graphite/epoxy (Gr/Ep) and graphite/thermosplastics (Gr/Tp) are recommended as prime material candidates. These particular composite materials have the highest stiffness and strength to density ratios compared to metallics and other composite systems. Graphite composites have use temperatures from -250 to 450°F so should not be limited in their application. Long-term physical property retention should be addressed and accelerated environmental testing is recommended as discussed in Section 7.0.

To insure efficient "compression critical" elements, tubular members were selected. The cross-sectional local crippling strength can be more closely tied to overall column behavior than can open-section members which have another possible failure mode. The torsional-rolling mode, coupling with local elastic buckling, requires close attention to detail design and analysis. Further confidence can be had in closed tubular members in terms of thermal expansion response. Laminate orientations to achieve "zero expansion" characteristics often require ply orientations at differing angles. This can be done in tubes (eliminating free-edge problems) as was demonstrated in the Space Telescope Metering Truss Contract (NAS8-29825)<sup>(6)</sup>. Tubular truss components were tested in this developmental contract and exhibited an average expansion coefficient of  $7.2 \times 10^{-8}$  cm/cm/°C ( $4 \times 10^{-8}$  in/in/°F). From an

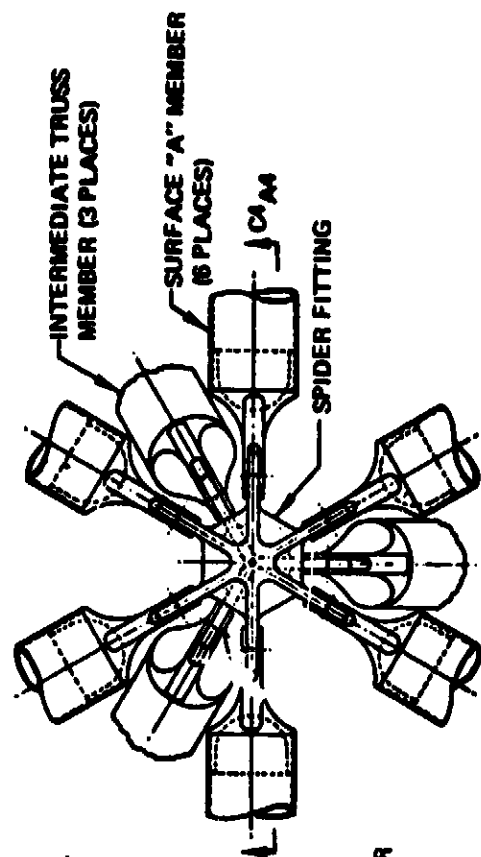
assembly standpoint, it was determined that joint eccentricity problems could also be minimized, e.g., the difficulty in passing the shear centers of intersecting members through the centroid of the cluster joints.

### 3.4 JOINT INVESTIGATIONS

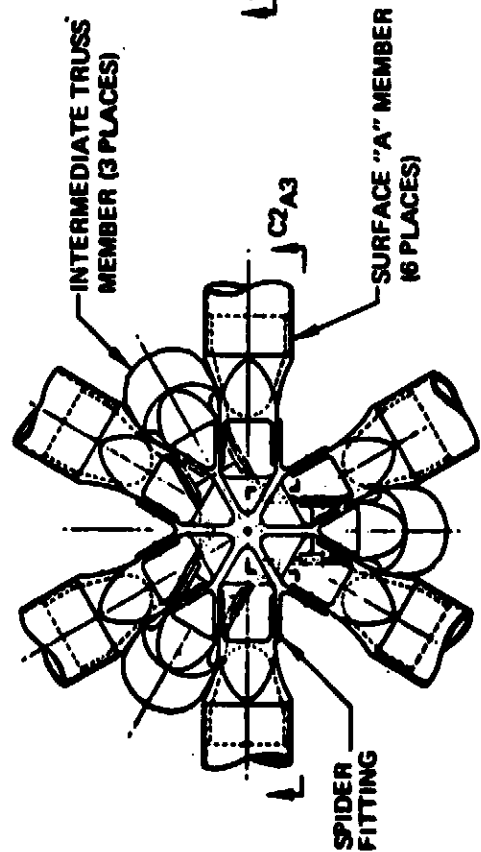
The preassembled tetratruss module will require joints and hinge fittings that allow the truss members to fold and articulate for dense packaging. In addition, the modules must be capable of deployment by either self-erecting devices or man-assisted-by-machine techniques into a rigid (no joint play) structure. The goal of this part of the study was to identify fittings and joints that would add a minimum amount of weight to the structure and to provide schemes that rigidize the joints when they are in deployed position.

Preliminary designs were prepared of the joints and hinge fittings for the tetratruss module including locking concepts for the telescopic members. Cluster fitting arrangements were prepared that would allow the close nesting of tubular members assumed in the packaging studies. Two cluster design concepts are shown in Figure 3.4-1; each provides for attachment and hinging of six surface elements and three diagonal elements. A wide-clevis design is shown as well as a single lug version. Payload attachment fittings or stand-offs can be attached at the center of these clusters. The choice between these concepts and others will depend on joint stiffness requirements and the cost of fabrication. Each truss element will terminate in a clevis fitting as shown in Figure 3.4-1. These fittings will be adhesively bonded to the tubular members.

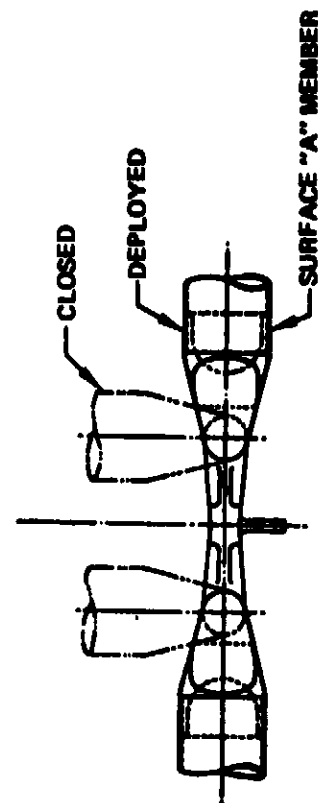
A hinge fitting concept, which will allow the surface members to fold in half for packaging is shown in Figure 3.4-2. If the tetratruss module is designed to be "self-erecting," torque springs can be installed in this hinge to provide stored energy. This hinge concept is also envisioned as having a ball-and-socket engagement which would provide initial locking when in the deployed position. The "socket" side of the hinge has a capsule, containing an adhesive, that would be ruptured, allowing the material to cure and firmly hold the ball



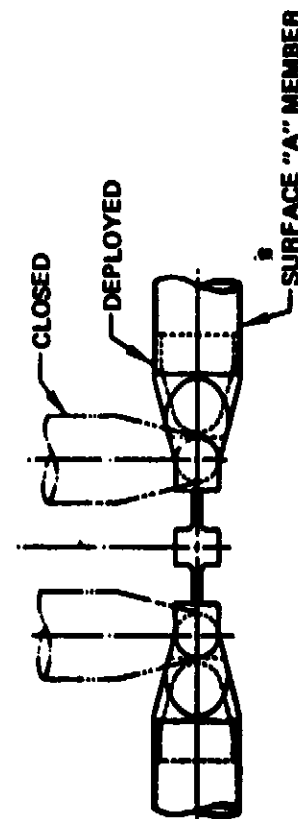
SINGLE LUG



WIDE CLEVIS



SECTION C4  
SCALE: 1/1



SECTION C2  
SCALE: 1/1

Figure 3.4-1. Cluster Fitting Joint Concepts



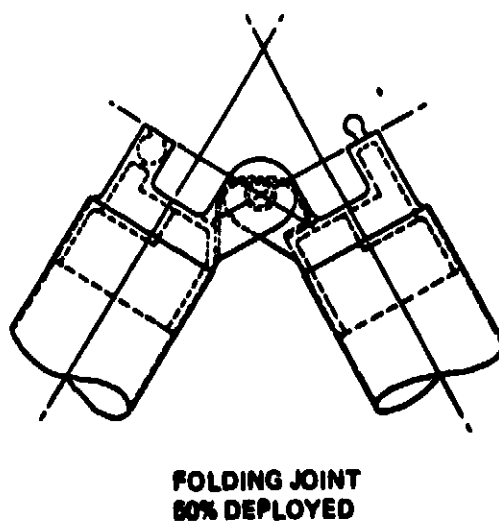
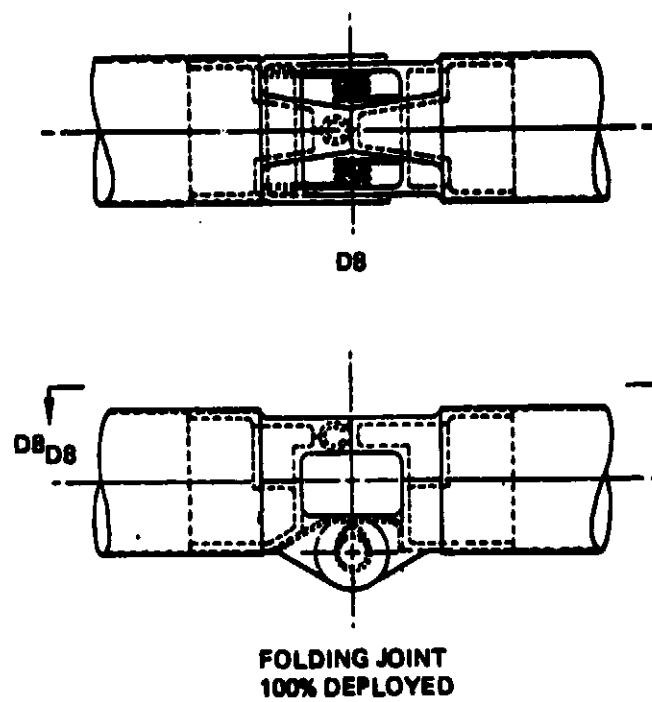


**Figure 3.4-2. Folding Hinge Joint Concept**

in final position. This concept can also provide active damping of the inertia loading near the end of the deployment cycle, as the closing pressure would cause a small amount of rigidizing material to bleed through a vent hole.

This type of joint chemical-rigidization could also be applied to the clevis lug interfaces to lock up the pinned connections to prevent structural deadband resulting from loose tolerances. A "zero slop" total assembly would be highly desirable to enable accurate dynamic assessments to be made and to predict damping effects. Figure 3.4-3 shows a concept to rigidize pinned lug-clevis interfaces. A serrated spacer or washer is added at the interface which contains rigidizing material which is activated during the last few degrees of deployment rotation to provide an adhesive bond. The telescopic members will require locking features such as those shown in Figure 3.4-4 to prevent linear and translational motion when the segments are at the fully extended position.

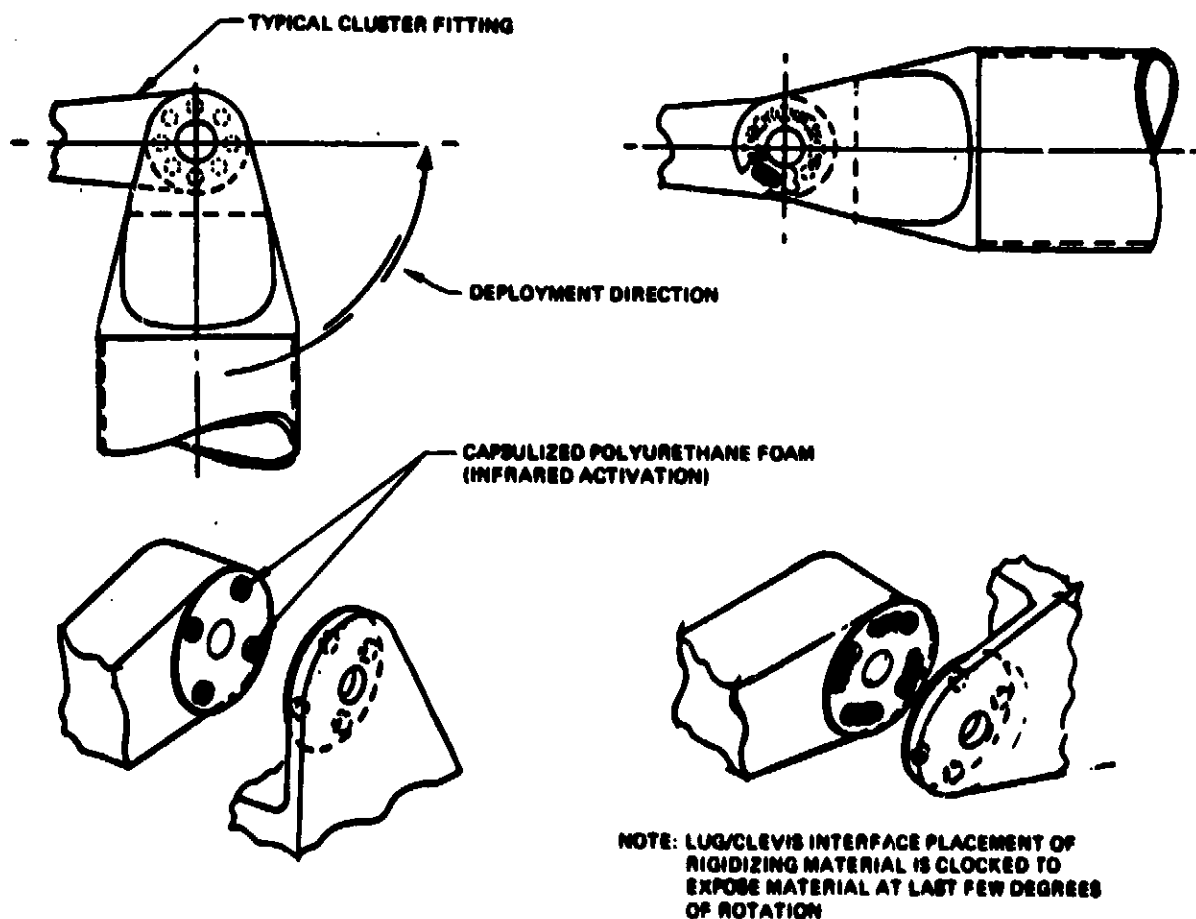


Figure 3.4-3: Rigidizing Concept for Clevis-Lug Interface

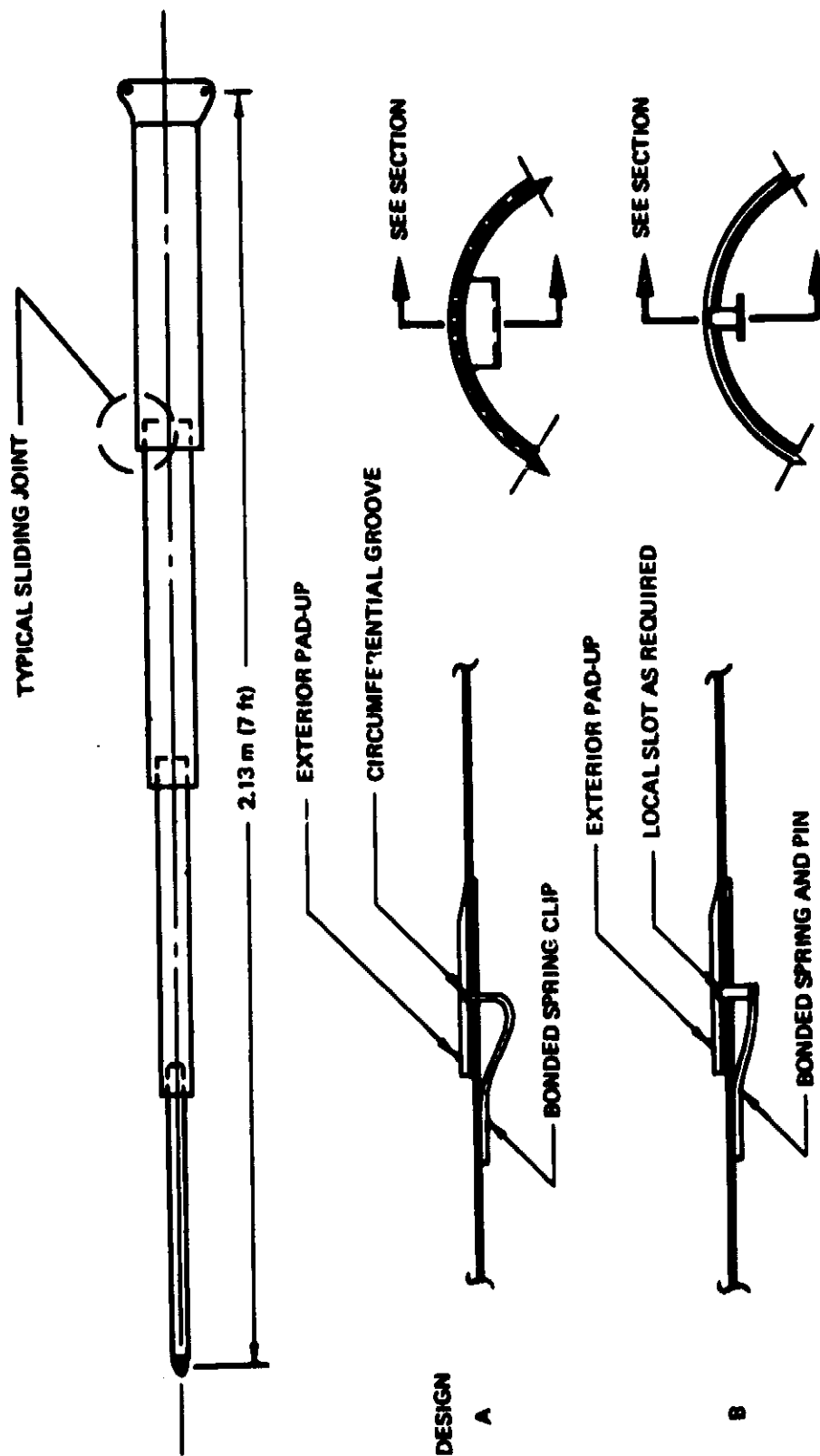


Figure 3.4-4. Locking Concepts for Telescoping Struts

### 3.5 WEIGHT ESTIMATES

A method of quickly assessing the weight of a tetratruss module of "N" hexagonal rings is discussed below. First of all, the quantity of individual components in the module is determined by the following expressions:

<u>ELEMENT LOCATION</u>	<u>QUANTITY</u>	
Top Surface Struts	$9N^2 + 3N$	
Bottom Surface Struts	$9N^2 - 6N$	where N = number
Core Perimeter Struts	$9N - 3$	of hexagonal rings
Total Truss Struts	$27N^2 - 3N$	
Top Cluster Fittings	$3N^2 + 3N + 1$	
Bottom Cluster Fittings	$3N^2$	
Strut Clevis Fittings	$54N^2 - 6N$	
Surface Hinge Fittings	$18N^2 - 3N$	

The weight of a typical component is calculated and multiplied by the quantity in that location. For example, the top and bottom surface may require sizing differing from the core of diagonal members. The interior rings of a given design might also require different sizes than the outer rings to vary the stiffness or strength characteristics. This can be accounted for by a summation of the quantity expressions for the members in the hexagonal rings affected.

For preliminary design purposes, the tetratruss struts would all have equal length and sizing. A joint factor could be applied to the total weight of the struts, say 10 to 20%, to arrive at a total structure weight.

### 3.6 DEPLOYMENT ANALYSIS

A computer program called KAATS was developed to analyze the dynamics of deployment of a twenty-four member tetrahedral truss as shown in Figure 3.6-1. The truss was idealized as a system of rigid body links, springs and dampers. Three degrees of freedom are permitted; the three generalized coordinates are the angular rotation in the plane of the lower surface, the angle  $\psi$  in Figure 3.6-1 and vertical motion (Z-direction) of the entire truss from an inertial

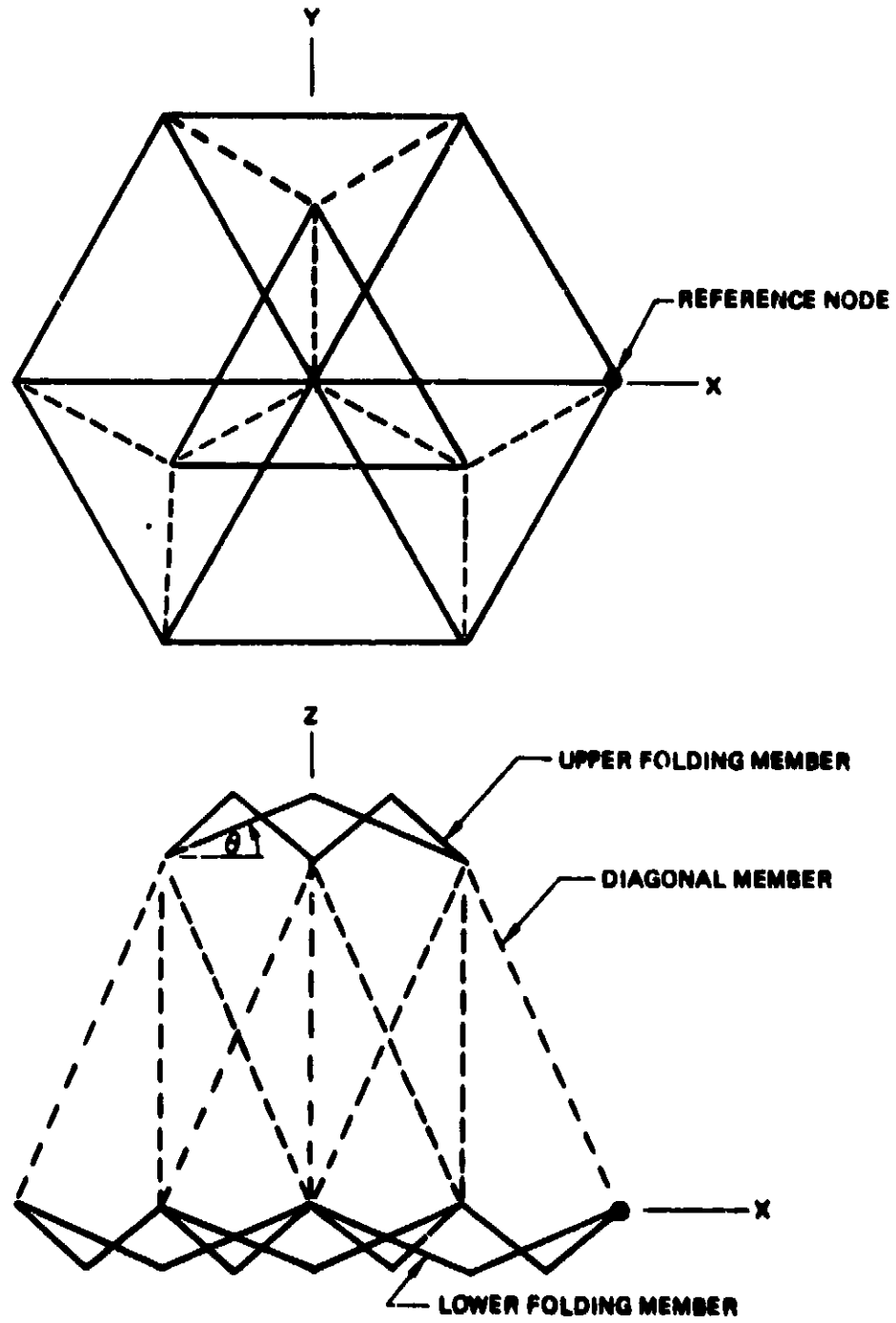


**Figure 3.6-1. Partially Deployed Inner Ring of Tetrahedral Truss**

reference plane. The equations of motion are numerically integrated to obtain histories of positions, velocities, and accelerations of truss members. KAATS was derived from the Prometheus<sup>(7)</sup> computer program.

### 3.6.1 Kinematic Analysis Model

In order to study deployment characteristics of the tetrahedral truss, a digital computer program for kinematic analysis was developed. The program, KAATS (Kinematic Analysis of Articulated Truss Structures), provides a rigid body analysis of deployment of the twenty-four member tetrahedral truss shown in Figure 3.6-1.

The program provides options for various deployment modes such as deployment springs located at selected hinges and the use of rotation about the Z-axis. Energy dissipation for controlled deployment is defined as constant or variable joint friction and viscous damping. Input data include dimensions of truss members and mass properties of members and hinge clusters. Program output consists of translational and rotational histories of position, velocity and acceleration of truss members and hinge clusters. Histories of system kinetic energy and total energy are also provided. It should be noted that while the model describes the inner ring of a tetrahedral truss, the output data can be used to predict the rigid body kinematics of a tetrahedral array of n-number of rings.

### 3.6.2 Analysis Results

Several demonstration problems were studied with the KAATS program. These problems provide some insight into the more complex analysis of kinetic as well as kinematic characteristics of deployment of an elastic structure.

Basically, the problems consisted of deployments of an undamped rigid body truss using either springs located at the mid-hinge of folding members or the spin-deployment option. During this study, it was noted that the program provides rapid convergence to suitable results. Each problem required approximately 10 seconds CPU time on an IBM 370 system; each problem solution carried the deployment from fully folded to full open position.

Program parameters used in the spring deployment mode are shown in Table 3.6-1. Figures 3.6-2, -3, and -4 show, respectively, the variation in time for complete deployment, maximum radial velocity, and radial acceleration at full deployment as functions of spring constant. The acceleration vs. spring rate plot is shown for the configuration just prior to full deployment when the deployment angle  $\theta$  is approximately 0. radian. The radial acceleration is negative at this time and results in tensile forces in upper and lower folding members.

**Table 3.6-1. Truss Characteristics**

- Material density:  $2.768 \times 10^3 \text{ kg/m}^3$  ( $0.1 \text{ lb/in}^3$ )
- Members: Tubes  $4.27\text{m} \times 0.051\text{m}$  o.d.  $\times 0.00051\text{m}$  wall ( $168 \text{ in} \times 2.0 \text{ in o.d.} \times 0.02 \text{ in wall}$ )
- Joints: No friction; weight is 10% total weight.
- Deployment springs: Located at midhinge of folding members. Spring torque constant during deployment.
- Truss assumed made of rigid members deployed in zero-g with no initial rotation or translation and no internal structural damping.

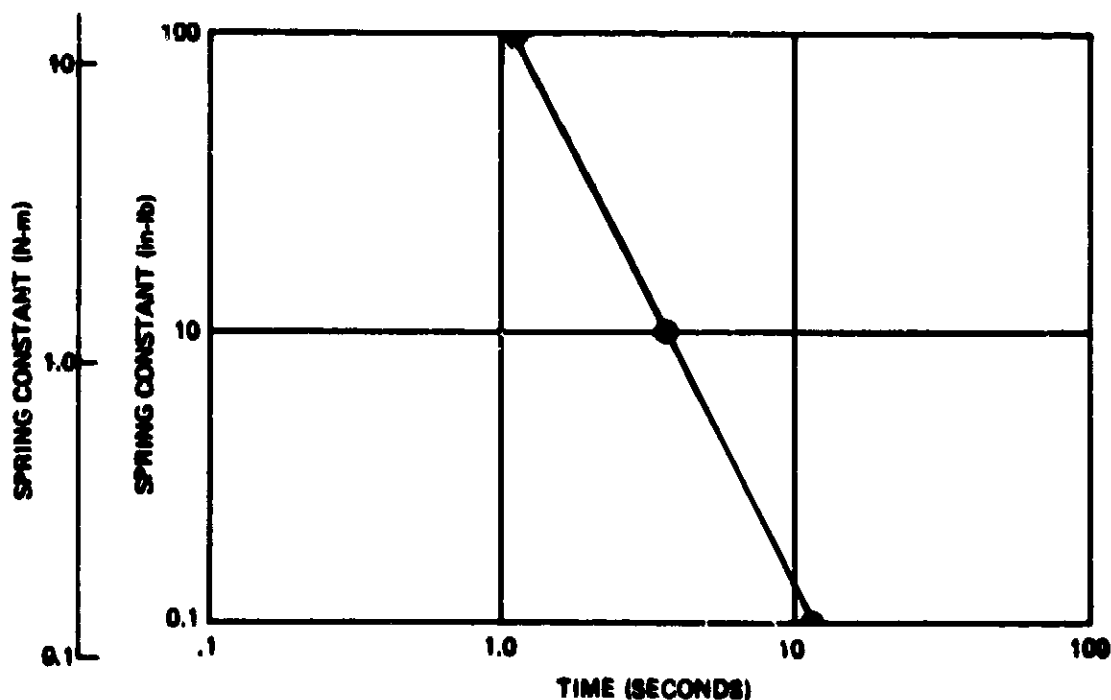


**Figure 3.6-2. Rigid Body Deployment Time Versus Spring Constant With Springs at Midhinge of Folding Members**

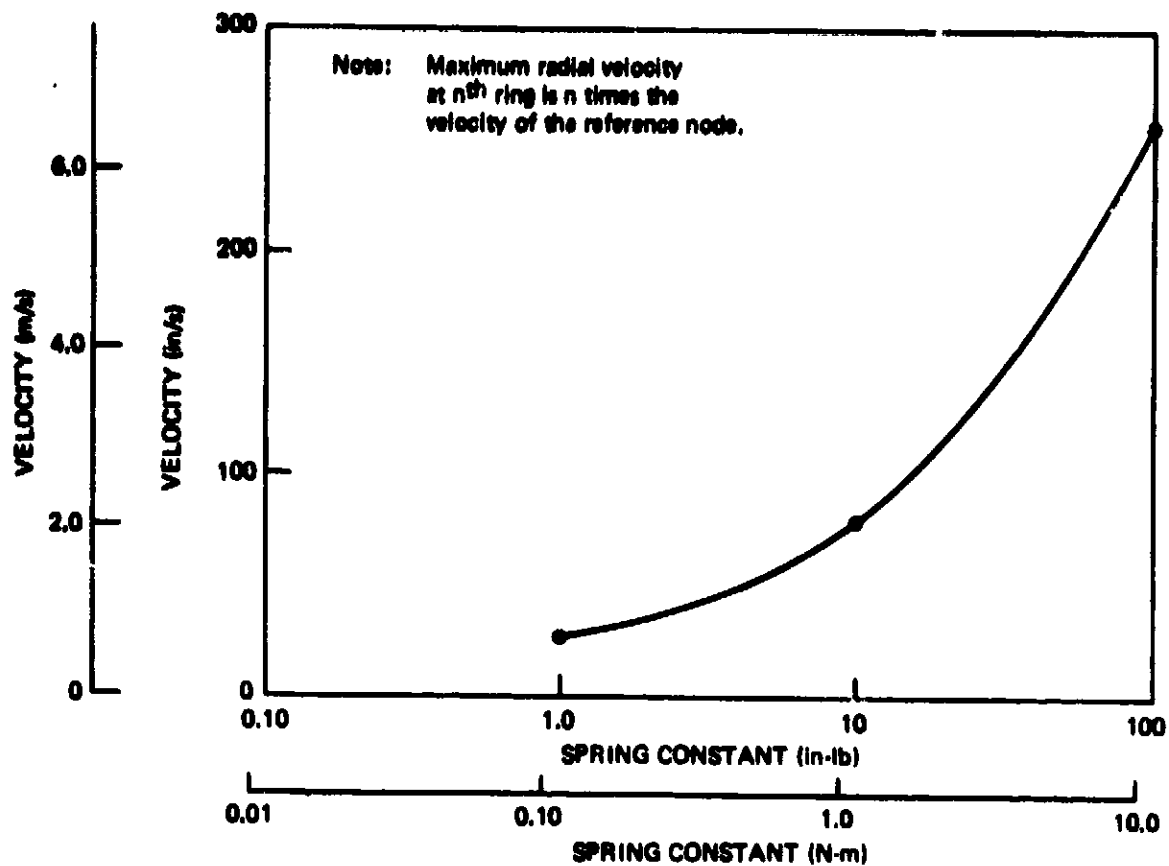


Figure 3.6-3. Maximum Radial Velocity of Reference Node Versus Spring Constant

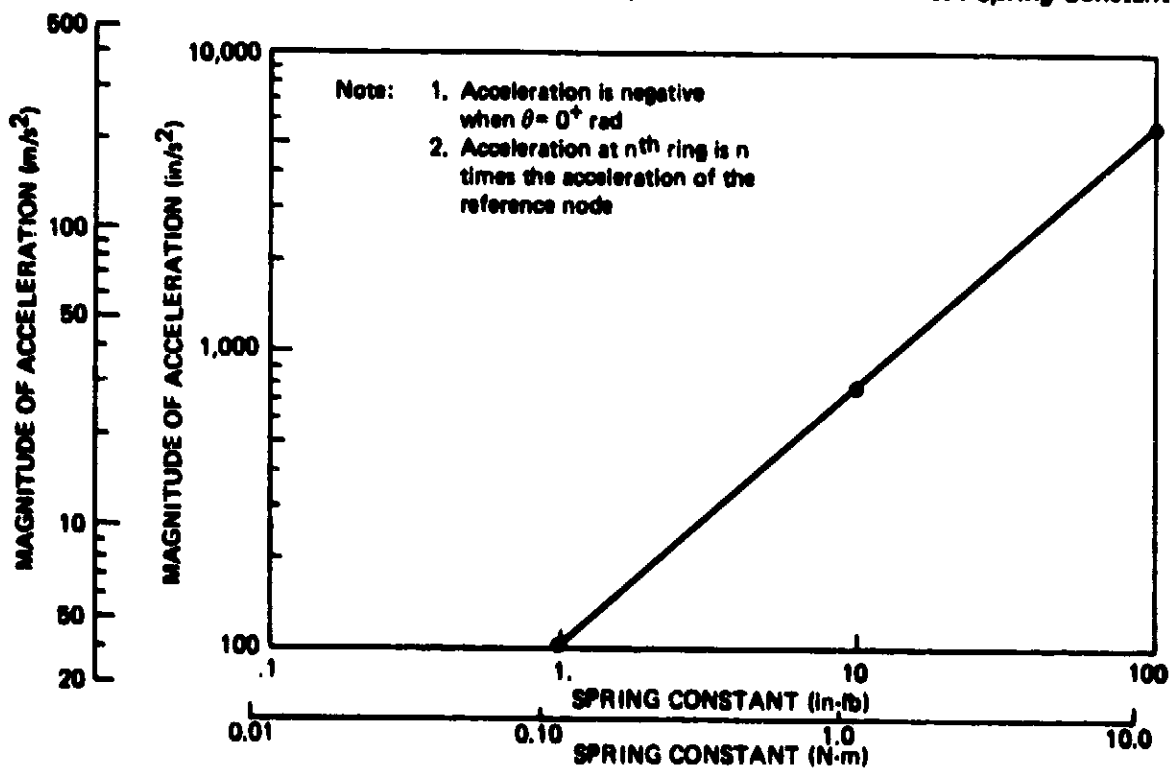


Figure 3.6-4. Magnitude of Radial Acceleration of Reference Node Versus Spring Constant When Deployment Angle  $\theta = 0^{\circ}$  rad.



Typical plots of the motion of the truss with 1.13 Nm (10 inch-pound) deployment springs are shown in Figures 3.6-5, -6, -7, and -8. These data show a relatively uniform motion throughout the first 3.30 seconds of deployment, at which time the radial velocity reaches a maximum and deployment is 83% complete.

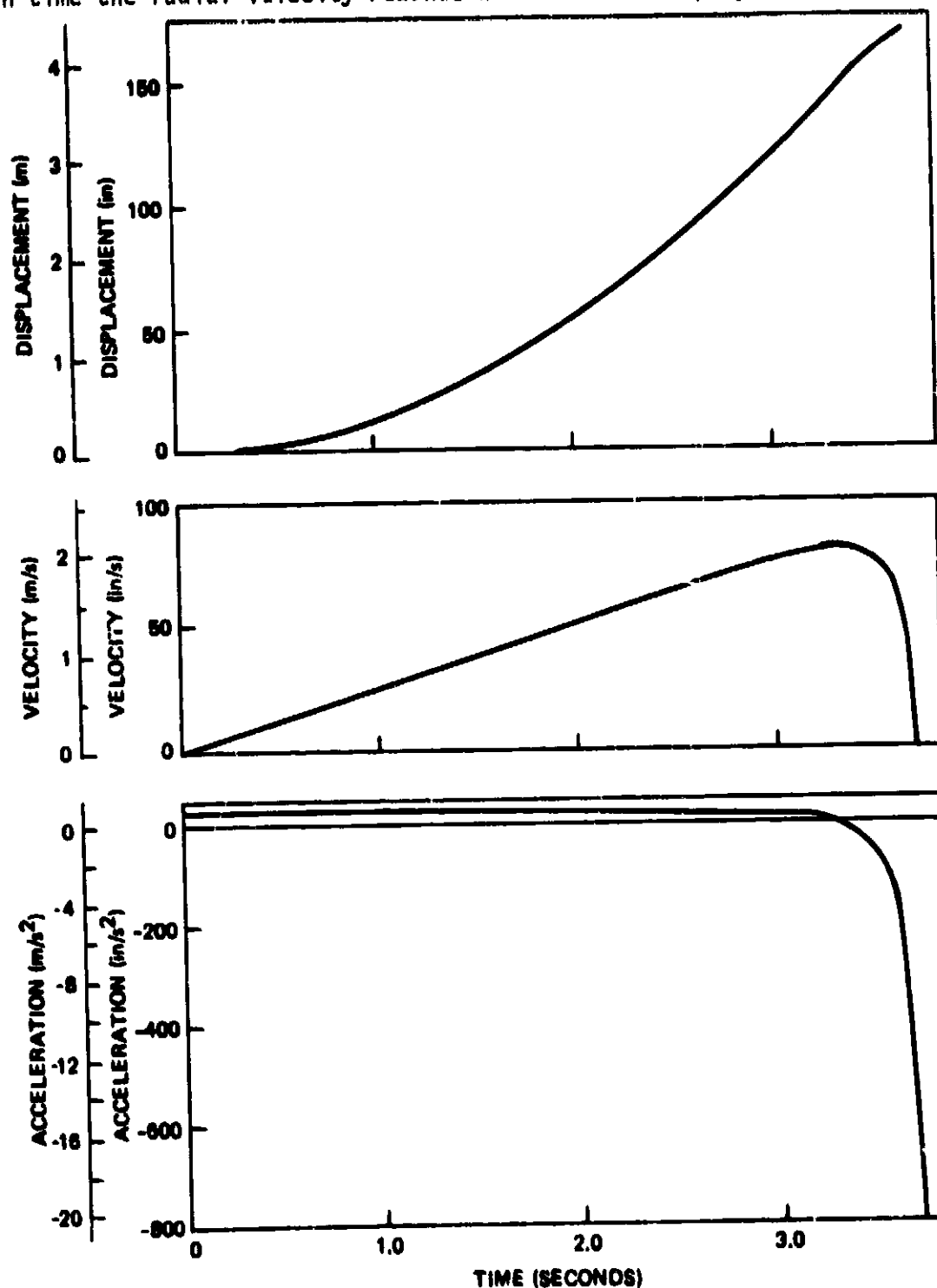
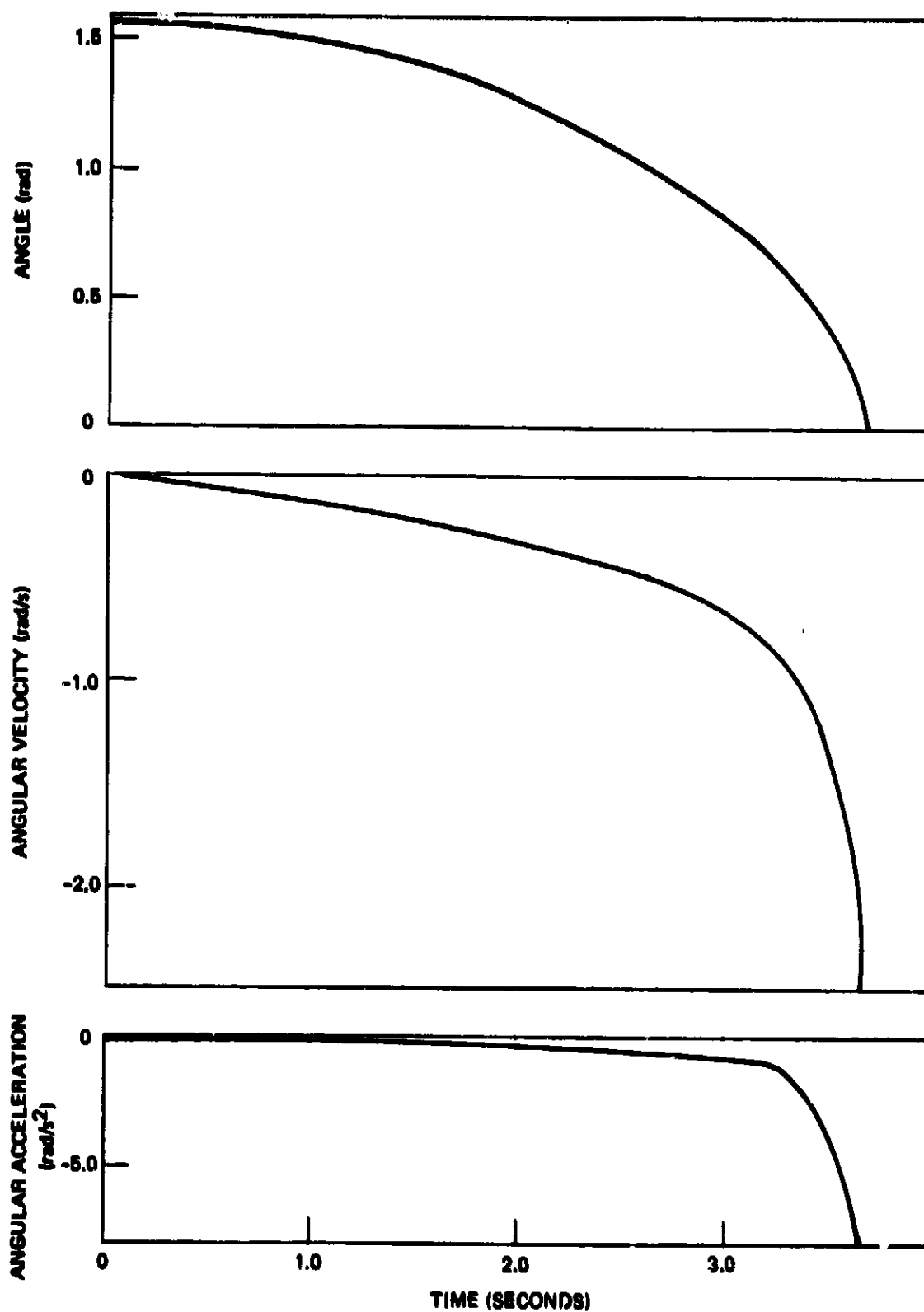


Figure 3.6-5. Rigid Body Radial Displacement, Velocity, and Acceleration of Reference Node



**Figure 3.6-6. Rigid Body Rotation of Upper Surface Folding Members About Member CG (Angles and Rates Are the Same for Upper and Lower Surface Members, but Signs are Opposite.)**

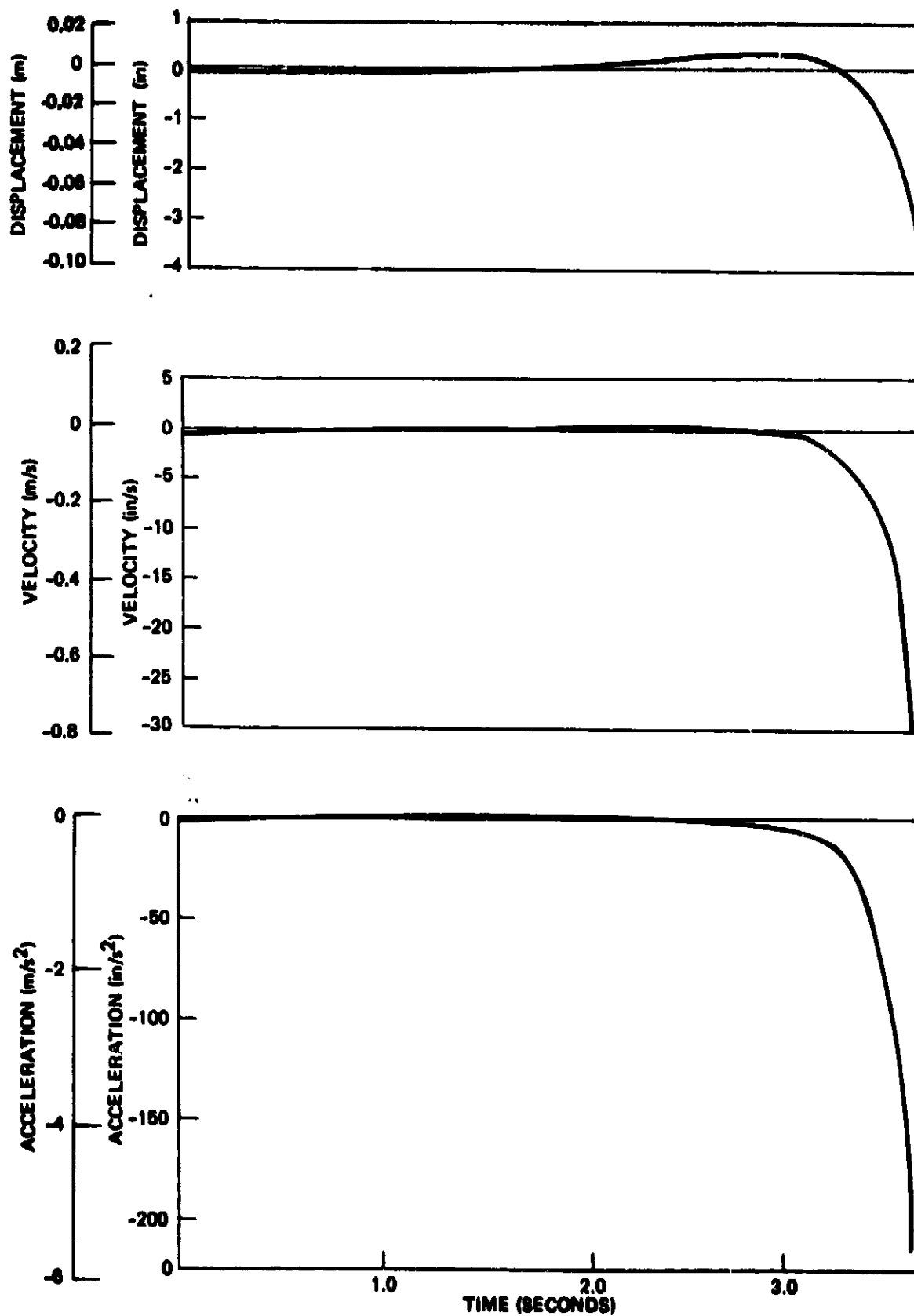
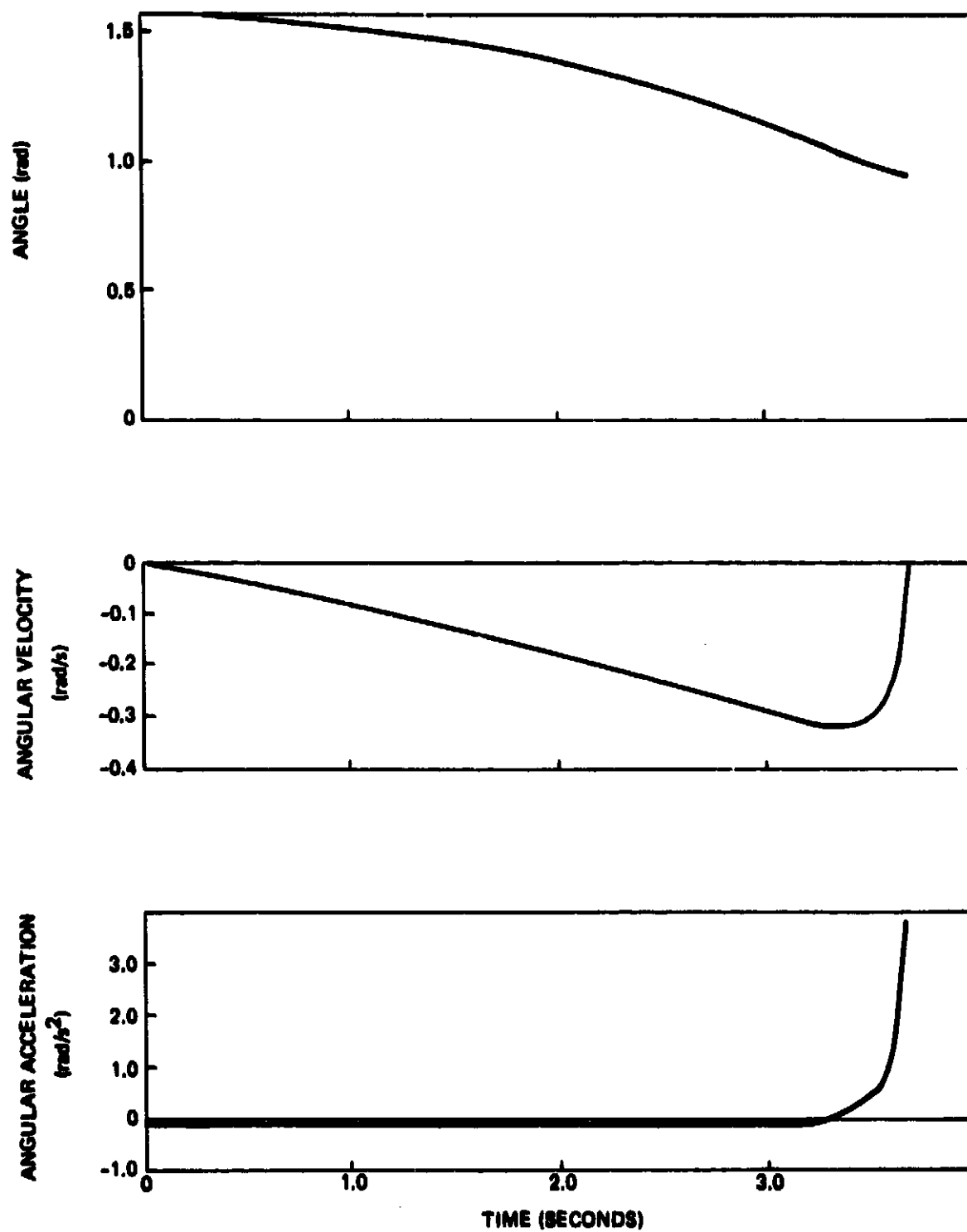


Figure 3.6-7. Rigid Body Motion of Truss in Z-Direction With 1.13 N-m (10-in-lb) Spring Constant at Mid-Hinge of Folding Members



**Figure 3.6-8. Rigid Body Rotation of Diagonal Members About Member CG**

Deployment is complete at 3.69 seconds; thus the deployment rates show large changes during the final 0.39 second of motion.

Data derived from the spring deployment analysis were used to compute rigid body forces in a 14-ring aluminum truss. The data shown in Figure 3.6-9 are the forces in the radial truss members of Figure 3.6-10. The force plot is for the undamped aluminum truss configuration with 1.13 Nm deployment springs at the mid-hinges of the folding members. These radial forces occur just prior to full deployment when the deployment angle  $\theta$  is approximately zero. The radial acceleration is directed toward the center of the truss and results in tensile forces in the deployed members.

The forces were computed by lumping the effective mass at each hinge location and applying the rigid body radial acceleration at that point. The inertial loads were distributed along load paths as shown in Figure 3.6-10. This distribution causes the 6 radial struts (running from the center to each vertex) to be the most heavily loaded members. The maximum tensile force for the specified condition is 9345 N (2100 pounds) in the innermost elements (ring #1). The 9345 N force results in a direct tensile stress of  $400 \times 10^6$  (58 Pa) KSI in these elements. This represents an upper limit of the deployment induced stresses.

The rigid body force distribution does not account for transients such as impact loading when the hinges close and lock at complete deployment. Analysis of the transient conditions must await future development of the KAATS computer program as discussed in Section 7.0 Structure Development Planning.

Force distribution curves for deployment spring constants other than 1.13 Nm may be obtained by applying accelerations obtained from Figure 3.6-4. For example, the forces in the radial elements of an aluminum truss deployed with 0.113 Nm (1.0 inch-pound) springs are 1/8 the values shown in Figure 3.6-9; the reference node accelerations for 0.113 and 1.13 Nm spring constants are shown as  $-2.54$  and  $-20.32 \text{ M/sec}^2$  ( $-100$  and  $-800 \text{ inch/sec}^2$ ), respectively.

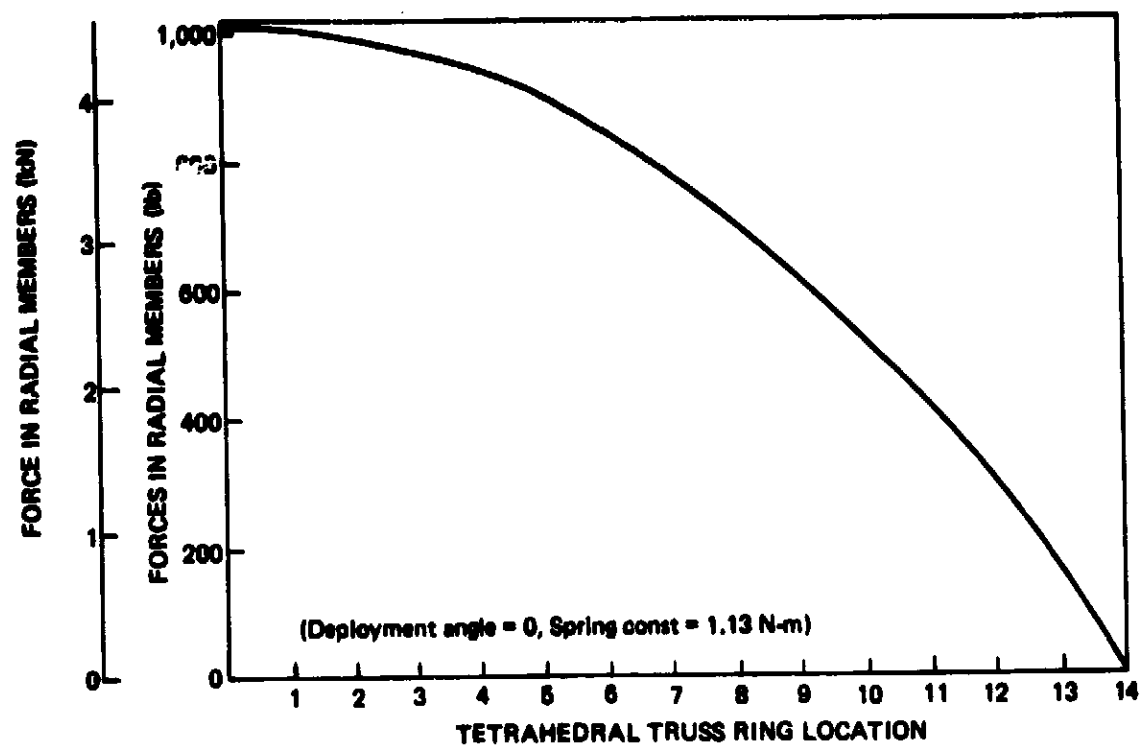


Figure 3.6-9. Load Distribution in Radial Truss Members

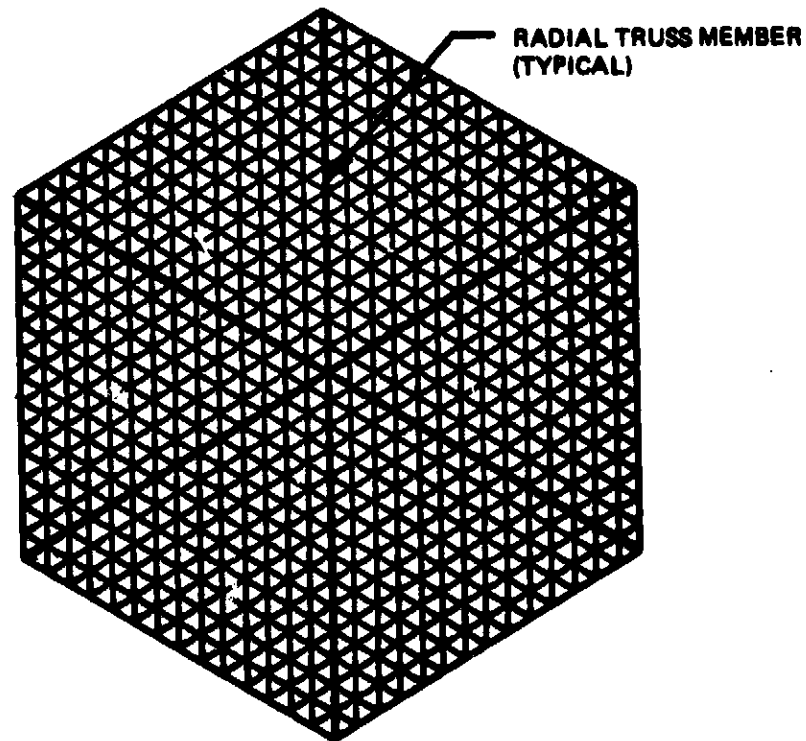


Figure 3.6-10. Lower Surface Member of 14-Ring Tetrahedral Truss

Analyses using the spin deployment option in KAATS were performed on the undamped aluminum truss. Initial spin rates varying from 10.0 to 50.0 radian/second about the truss Z-axis were applied to a model with lumped masses which simulated the rigid body mass moment of inertia of the 14-ring array. Typical results of spin deployment analyses are shown in Figures 3.6-11, -12, and -13.

Figure 3.6-11 is a plot of kinetic energy of rotation of the undamped 14-ring truss at the beginning and end of deployment. For example, the initial kinetic energy of the truss is approximately  $1.13 \times 10^5$  Nm ( $1 \times 10^6$  inch-pounds) for an initial spin rate of 10 radian/second. As deployment proceeds, the spin rate decreases because of conservation of angular momentum until a final rate of approximately 0.0048 radian/second is achieved at the end of the deployment. The final kinetic energy of rotation for this example is approximately 113 Nm (1000 inch-pounds).

Figure 3.6-12 is a plot of the maximum average coulomb torque permitted in each hinge if there is to be enough energy in the system to achieve complete spin deployment. This average friction torque was determined by equating the energy at end of deployment to the sum of energy dissipated at each hinge of the 14-ring array. The coulomb torque was assumed constant during deployment. The maximum allowable average coulomb torque varies from  $4.52 \times 10^{-3}$  to  $9.04 \times 10^{-2}$  Nm (0.04 to 0.08 inch-pounds) over the range of initial spin rates of 10.0 to 50.0 radian/second. Low friction hinges will be a necessity if spinup is to be a candidate deployment mode.

Figure 3.6-13 shows rigid body deployment time as a function of initial spin rate. The deployment times varied from approximately 4.2 to 0.3 seconds over the investigated range of initial spin rates.

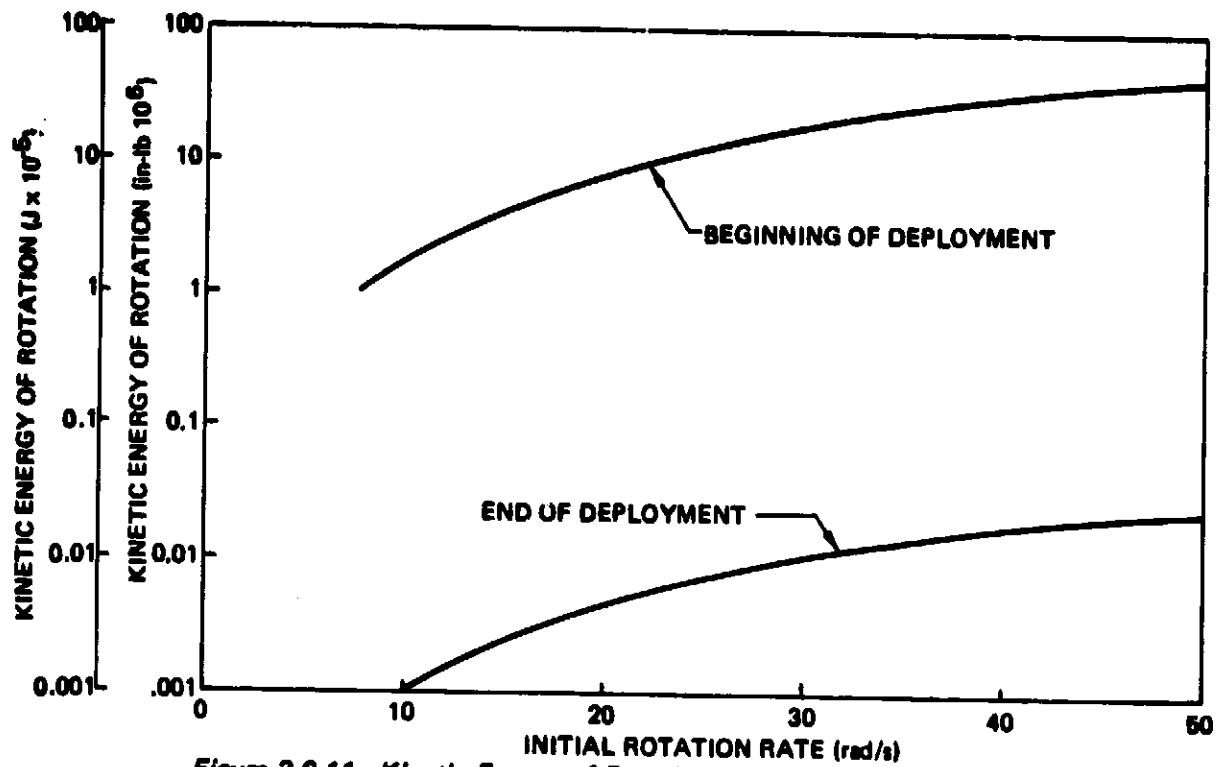


Figure 3.6-11. Kinetic Energy of Rotation of 14-Ring Truss With No Hinge Friction

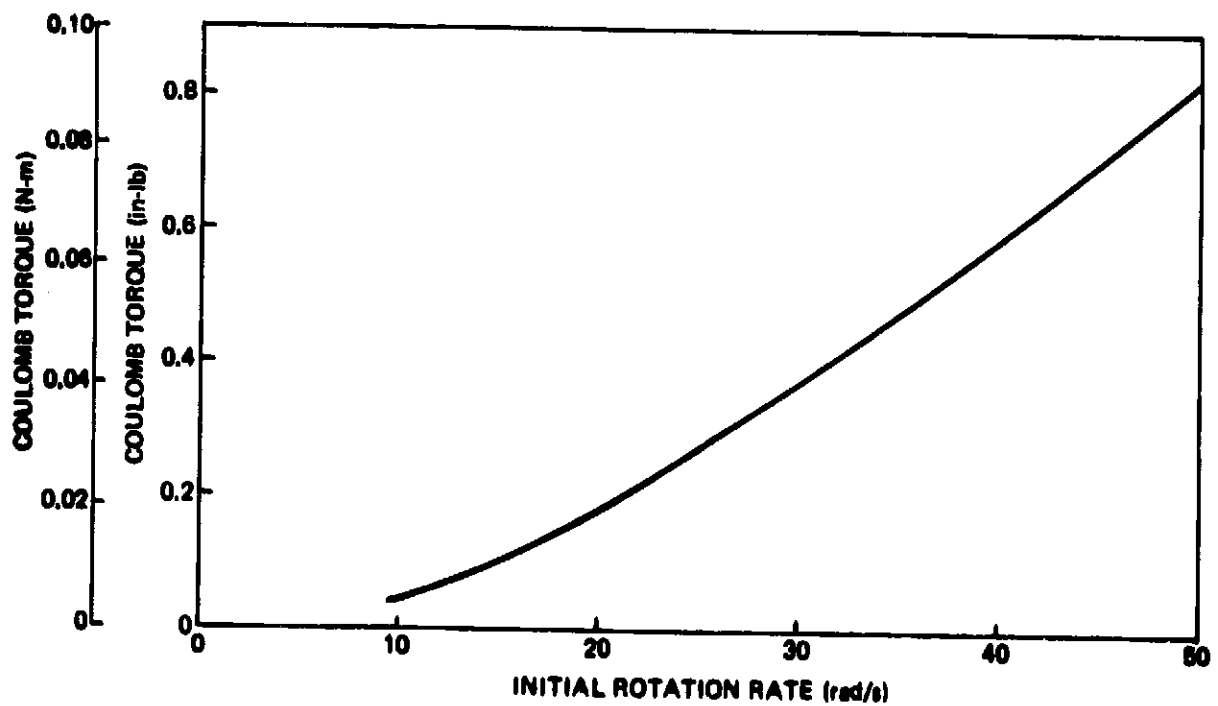
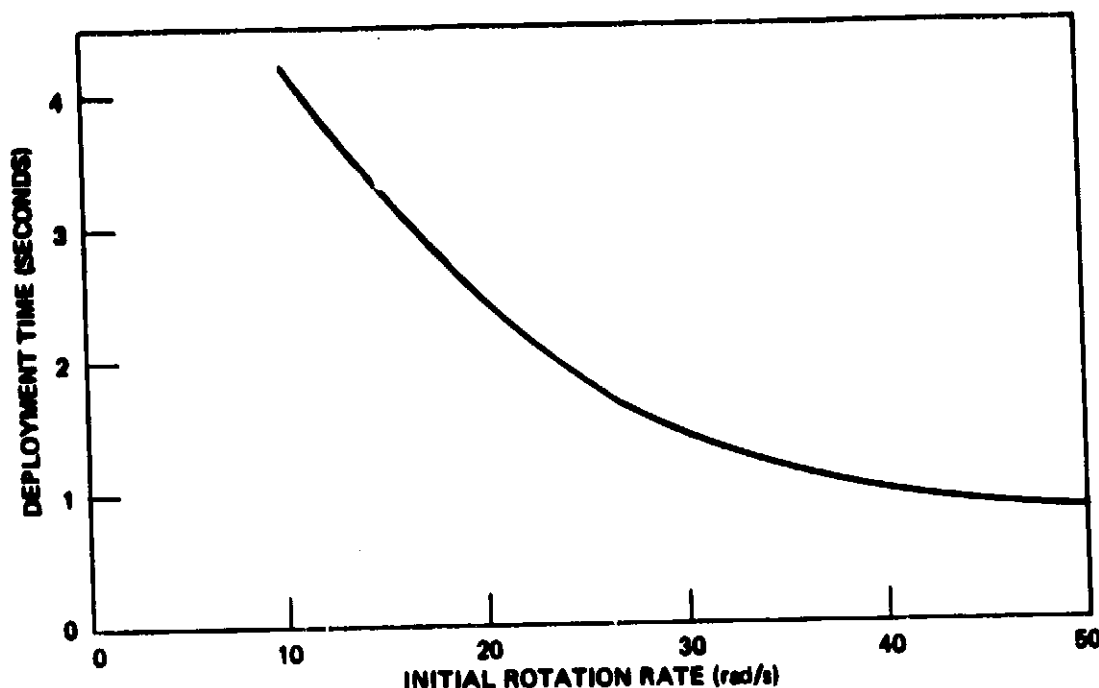


Figure 3.6-12. Maximum Average Coulomb Torque Per Hinge to Achieve Spin Deployment of 14-Ring Array Truss





**Figure 3.6-13. Deployment Time Versus Initial Rotation Rate for Deployment of 14-Ring Truss With No Hinge Friction**

### 3.7 FREQUENCY AND STRENGTH ANALYSIS

Computer analyses of various tetrahedral arrays were performed to evaluate their strength and stiffness characteristics. These analyses were conducted with the NASTRAN computer program for undamped models of arrays of five to fourteen rings of either aluminum or graphite-composite materials. Trades were also conducted to evaluate the variation in fundamental frequency with mass and depth of the truss. These analyses were generally performed with detailed models wherein all structural members were represented by appropriate finite elements (either rods or bars) available in NASTRAN. A simplified NASTRAN model using plate elements with fewer degrees of freedom was also developed for modal analyses of multi-module arrays.

#### 3.7.1 Fourteen-Ring Truss vs. Equivalent Plate

A NASTRAN model of a 14-ring tetrahedral truss was developed for static loads and modal analyses. The model, shown in Figure 3.7-1, consisted of one-half the structure and utilized symmetry along the Y-axis to reduce the program input and computation requirements. The half-model consisted of 651 grids, 3906 degrees of freedom and 2646 elements.

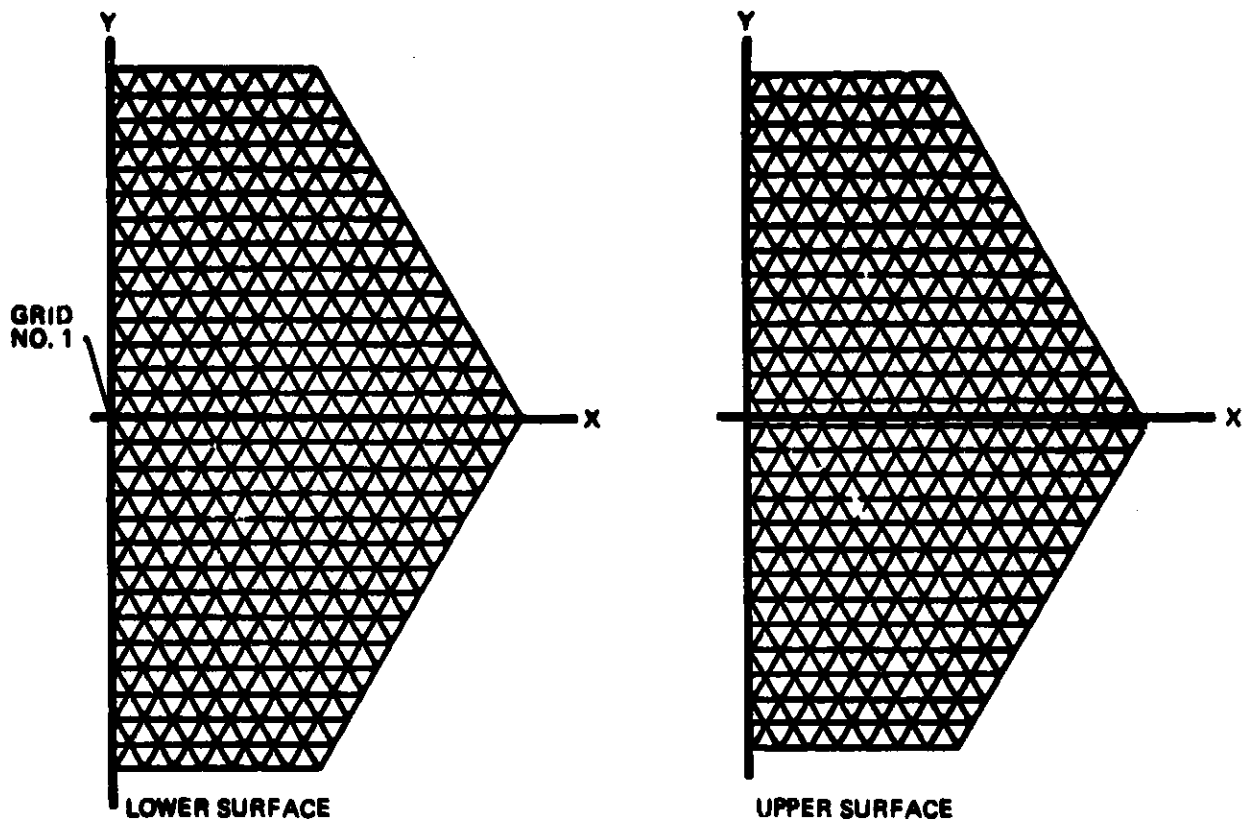


*Figure 3.7-1: NASTRAN Model of 14-Ring Array*

The truss structure consisted of equal length aluminum tubes. Mass was uniformly distributed to all grid points and a joint weight factor of 10% was applied. The total weight of the half model was 2740 kg (6035 pounds).

A force of 445 N (100 pounds) was applied at grid #1 in a direction normal to the x-y plane to study load distribution and static deflection of the truss under a uniform acceleration. The static loads analysis with inertia relief in NASTRAN was used for this portion of the problem which simulated a possible orbit transfer mode for the deployed truss. The thrust, reacted by the uniformly distributed mass of the truss, resulted in a uniform acceleration of  $0.1626 \text{ m/sec}^2$  (0.01657 g) in the Z-direction.

The most heavily loaded truss members of the total array are the three diagonal members connecting node #1 to the upper surface. The compression load was 363 N (81.6 lbs) in each of these members for the 0.01657g acceleration. All truss members were aluminum tubes with the following characteristics:

Tube Length	4.27 m	(168 in)
Tube Diameter	5.08 cm	(2 in)
Wall Thickness	.0508 cm	(0.02 in)
Modulus of Elasticity	$7.3 \times 10^{10}$ Pa	( $10.4 \times 10^6$ psi)
Euler Buckling Load	1006 N	(226 lb)

The compressive load in the critical members for accelerations or total array weights other than the analyzed condition can be obtained from the following equation:

$$p = 4 a M$$

where

p = compressive force in Newtons

a = uniform acceleration in  $\text{m/sec}^2$

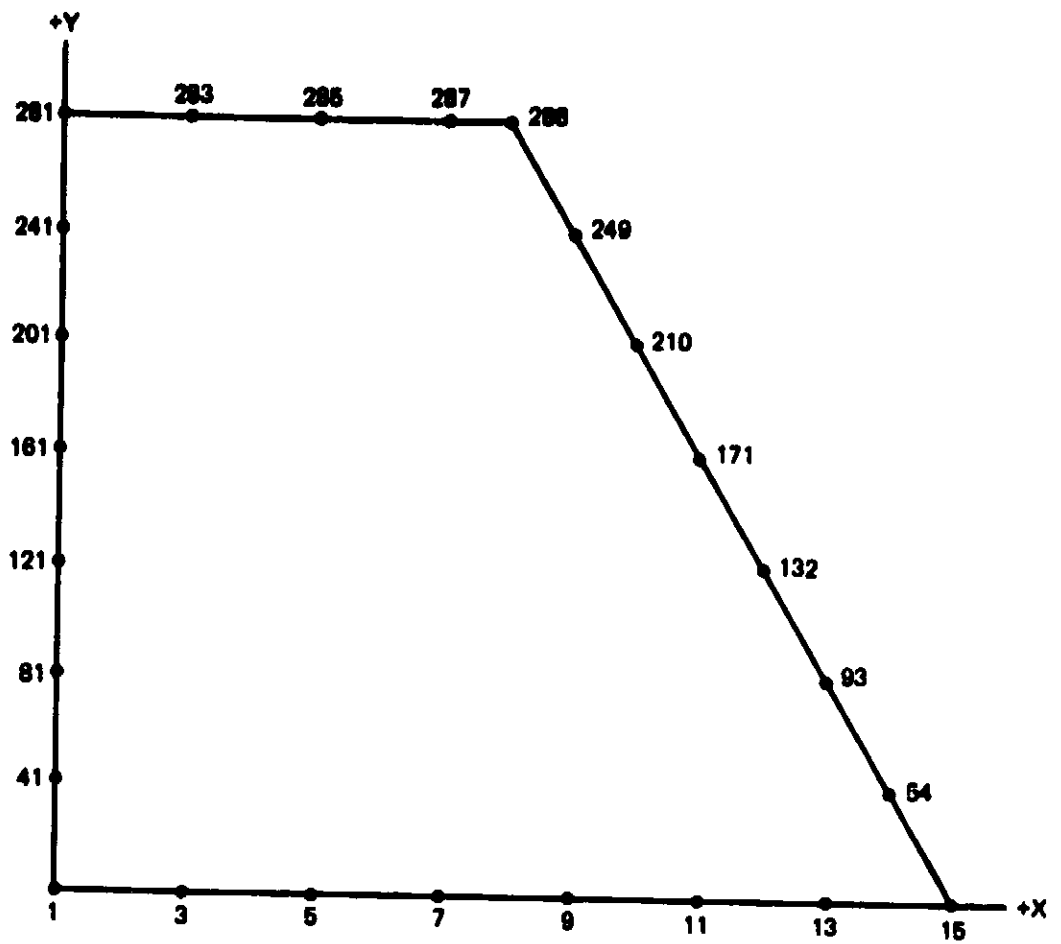
M = total mass in kilograms (assumed to be uniformly distributed)

Thus, a uniform acceleration of approximately  $.49 \text{ m/sec}^2$  (0.05g) resulting from a normal force at node #1 would load the critical members to the buckling capability for the total truss weight of 5480 kg (12,070 lbs).

Figure 3.7-2 shows the relative displacements of one quadrant due to  $.49 \text{ m/sec}^2$  acceleration in the +z direction. If a uniformly distributed equipment weight over the truss structure is considered along with the acceleration of  $.49 \text{ m/sec}^2$  the critical members will require beef-up to withstand the steady-state loading case.

A normal modes analysis was also conducted with the 14-ring model. The natural frequencies and nodal lines are shown in Figure 3.7-3. For these solutions, the structural mass was lumped at 110 grids on the lower surface.

A second dynamic analysis of the 14-ring module was performed using a NASTRAN plate-element model. The plate model was developed to provide simplified modal analyses of planar arrays. The results of the investigation, summarized in



*Edge Nodes of One Quadrant of Lower Surface of 14-Ring Array*

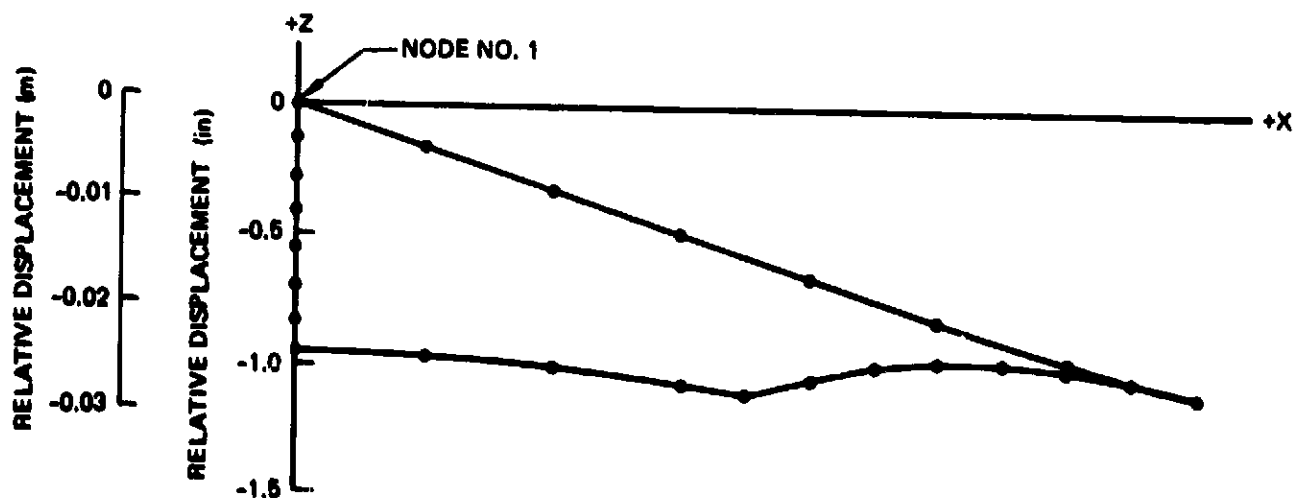


*Figure 3.7-2. Relative Displacement of One Quadrant of 14-Ring Array. Thrust Force of 2688N (604 lb) Applied at Node 1 of Total Array to Obtain Uniform Acceleration of  $0.49 \text{ m/s}^2$  ( $0.05g$ ) In +Z Direction*

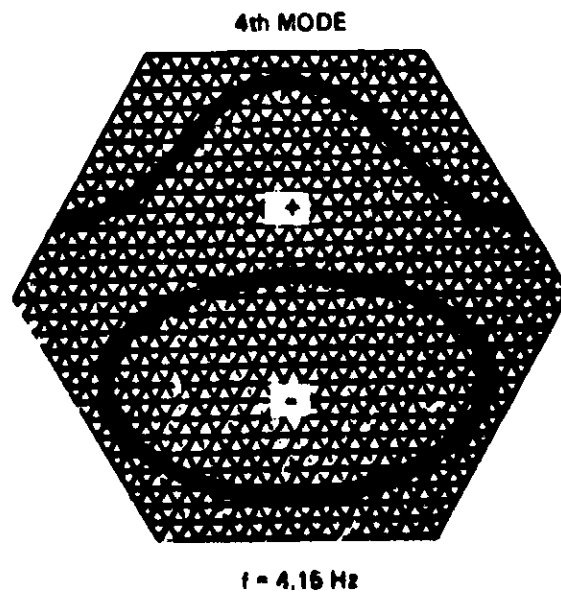
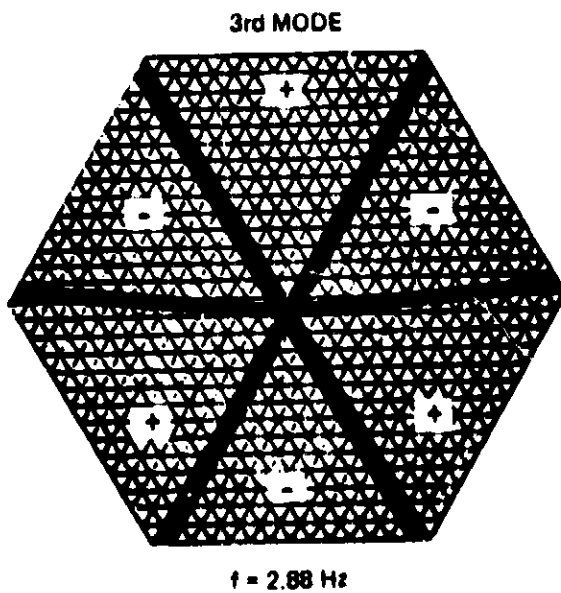
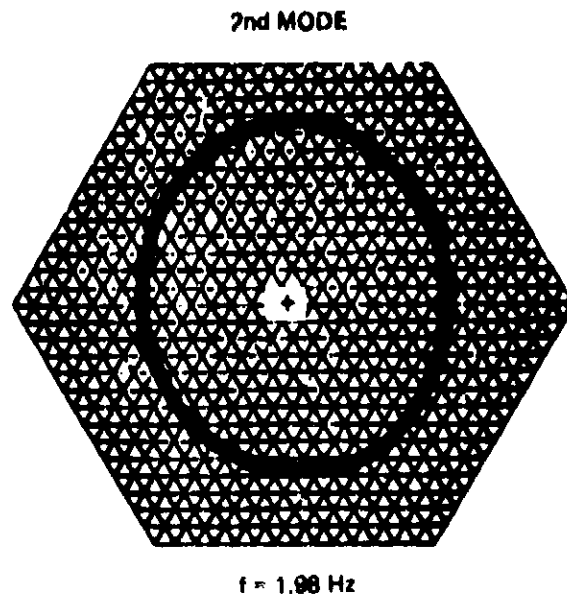
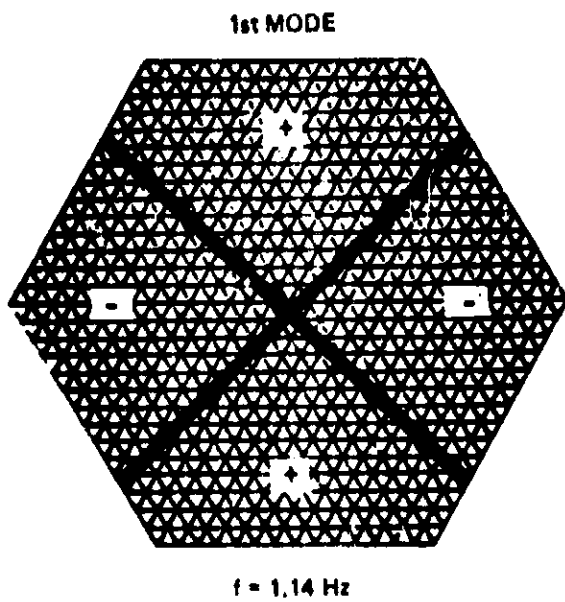


*Figure 3.7-3: Natural Frequencies and Nodal Lines of 14-Ring Truss*

Figure 3.7-4 and Table 3.7-1, show that the simplified model correlates well with the detailed model for the 1st and 2nd modes, but the plate mesh is too coarse for higher modes. The most significant result is the saving in computer time achieved with the plate model; average run timer per eigenvalue was six percent of the time required for the detailed model. The NASTRAN plate model provides a feasible technique for modal analyses of multi-module arrays.

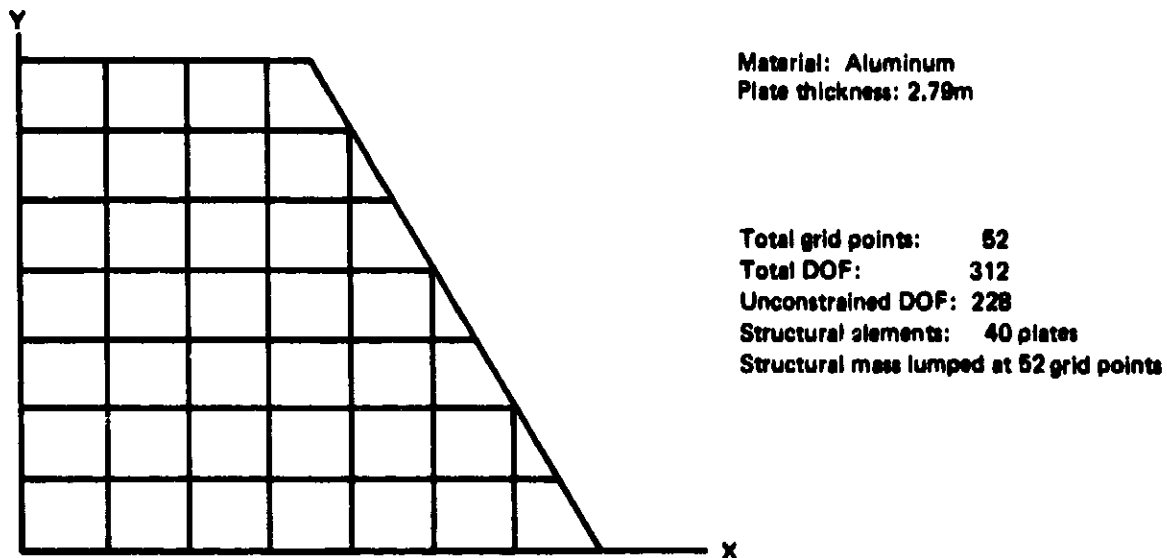


Plate thickness sized to give fundamental frequency of 1.14 Hz for free vibration of circular plate.  $t \approx (fr^2/8)\sqrt{\rho/E}$  where  $t$  = plate thickness  
 $r = 61m$ ,  $E = 6.9 \times 10^{10} Pa$ ,  $\rho = 2.77 \times 10^3 kg/m^3$

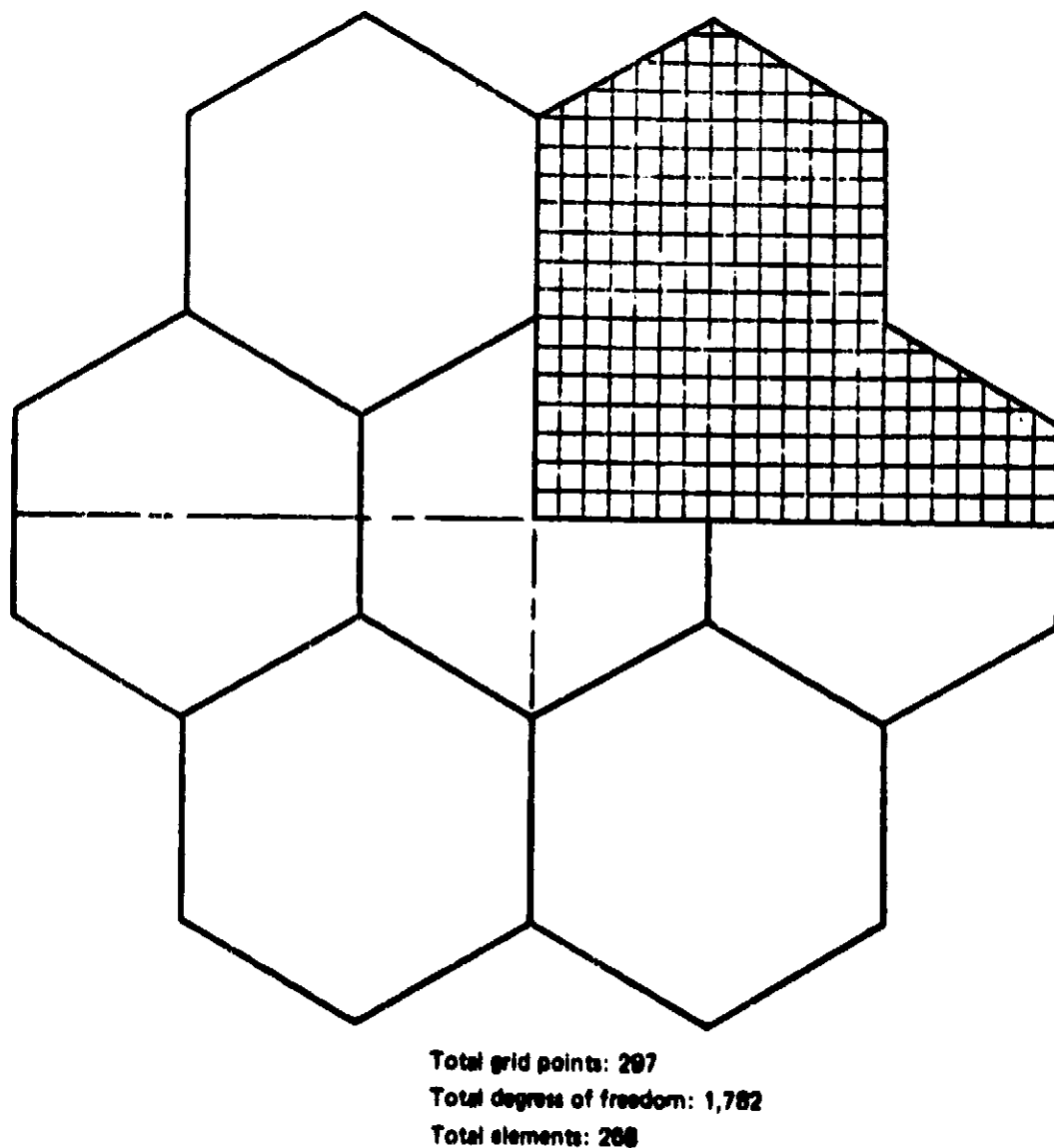
Figure 3.7-4: NASTRAN Plate Model of 14-Ring Array

Table 3.7-1. Comparison of Results From Rod-and-Plate Element (NASTRAN Models of 14-Ring Array)

Model	Frequency (Hz)				Avg CPU time per eigenvalue (min)
	1st Mode	2nd Mode	3rd Mode	4th Mode	
Rod element	1.14	1.98	2.98	4.16	6.3
Plate element	1.13	1.87	4.46	7.20	0.4
Note: Plate mesh appears to be too coarse to evaluate the natural frequencies and modes higher than the 2nd mode. No attempt was made to optimize the plate-element model for performance and efficiency.					

The plate model was then used to determine modal characteristics of multi-module arrays of the 14- ring tetrahedral truss module. The analyses were of truss structure alone with zero damping and symmetric boundary conditions on a one-quarter model of each multi-module array. The arrays that were analyzed consisted of 7- and 19- modules of the 14-ring truss.

The 7- module model and predicted frequencies, modes, and average IBM 370 CPU time per eigenvalue are shown in Figures 3.7-5 and -6. The results indicate that the NASTRAN plate-element models provide efficient tools for preliminary modal surveys of large space erectable structures.



**Figure 3.7-5. NASTRAN Plate-Element Model of Seven-Module Planar Array**

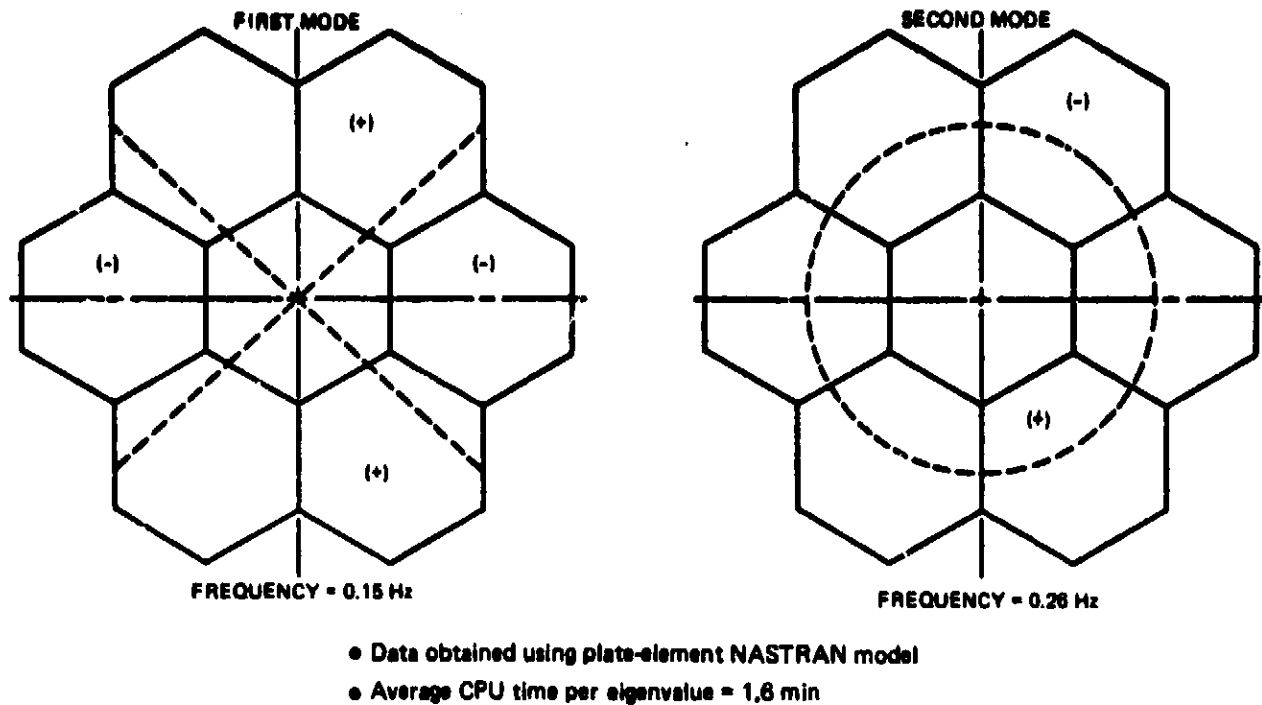


**Figure 3.7-6: Natural Frequencies and Nodal Lines for First and Second Modes of Seven-Module Planar Array**

A curve is also included in Figure 3.7-7 to show variation of the undamped fundamental frequency with planform area of the aluminum truss planar array. The calculated frequencies tend toward a straight line on a logarithmic plot; these data were fitted by the curve

$$f_1 = 7730/A^{.98}$$

where  $f_1$  = fundamental frequency ( $H_z$ )

$A$  = planform area ( $m^2$ )

### 3.7.2 Two-Tier Truss

The two-tier truss concept wherein the general strength and stiffness requirements for attitude control and orbital transfer are met by a primary truss structure overlayed with a secondary truss for equipment mounting was analyzed. Only the stiffness of the primary truss was considered in the analysis of a 5-ring primary structure shown in Figure 3.7-8.



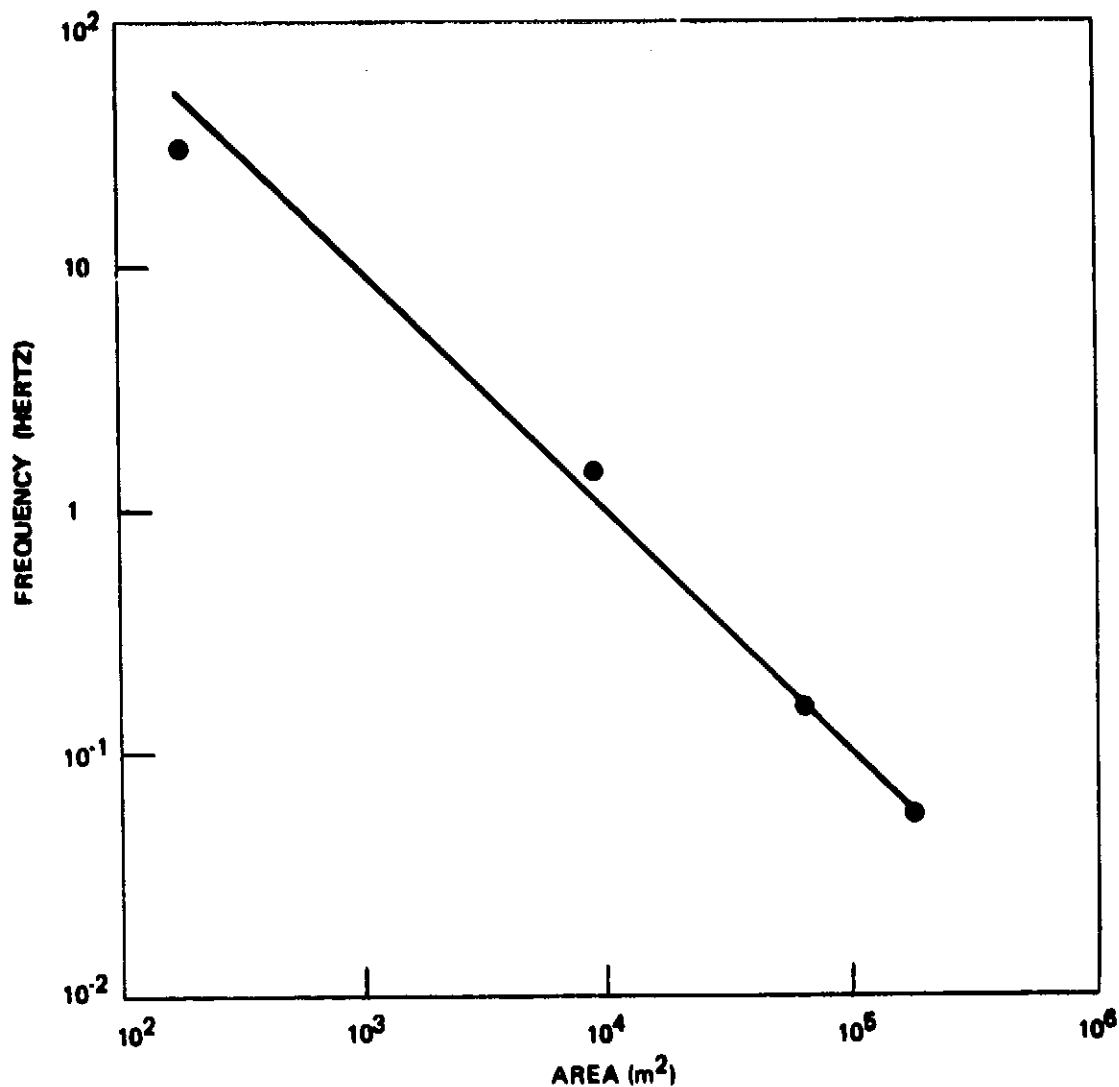


**Figure 3.7-7. Undamped Fundamental Frequency Versus Planform Area of Aluminum Truss Planar Array**

A parametric study was conducted to evaluate the effects of variation in system mass and depth of primary structure on the fundamental frequency. The baseline configuration of the antenna primary structure was comprised of 660 aluminum members connected to form the 5-ring tetrahedral planar truss.

The primary members of the baseline configuration were all 130 m long, and the distance between the faces of the baseline truss was 106 m. The length of the interplane members was changed to vary the depth of the primary truss from 106 m to 212 m. Corresponding structural masses were estimated to be approximately  $90 \times 10^3$  kg and  $113 \times 10^3$  kg and varied linearly between these points.

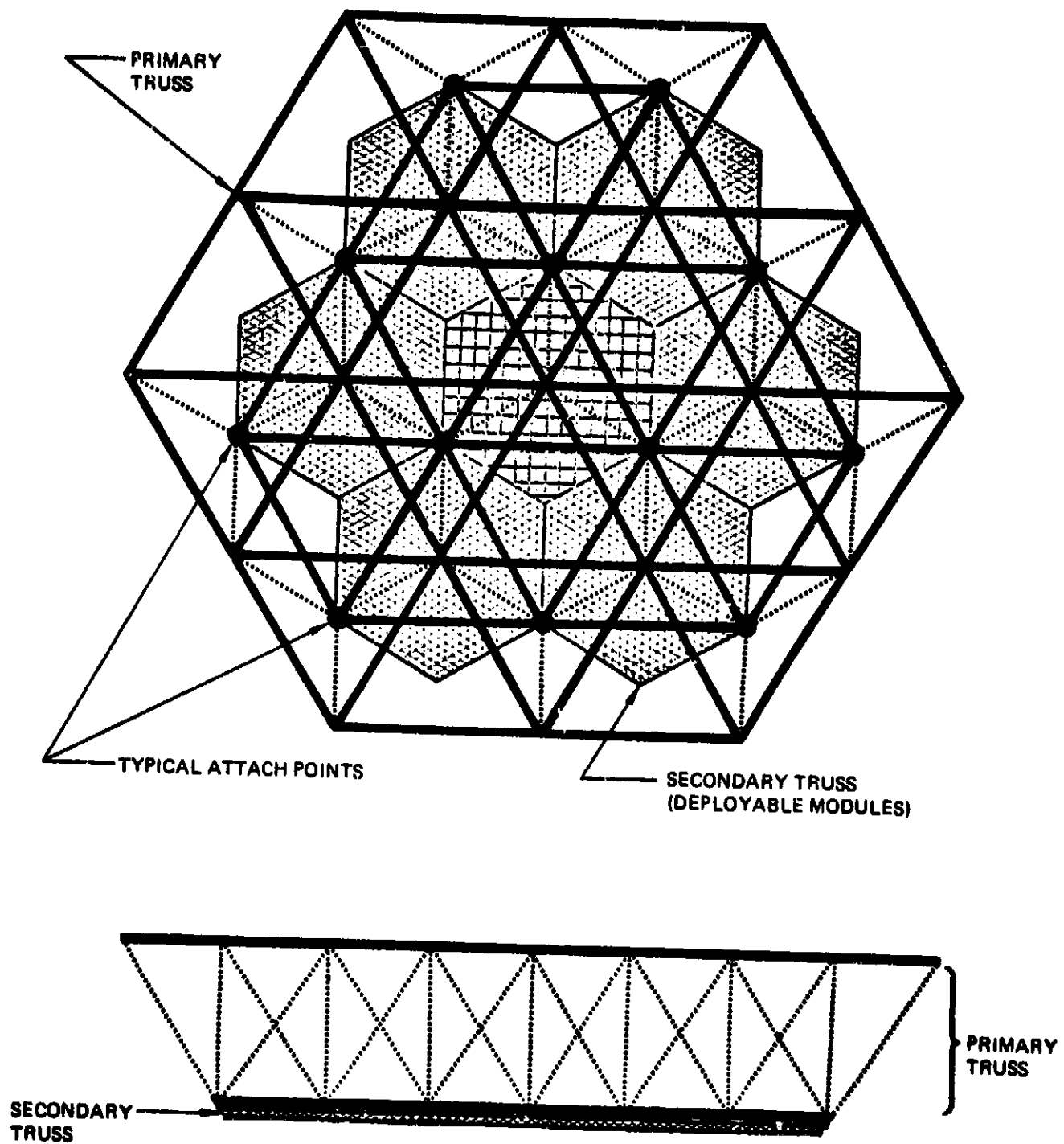
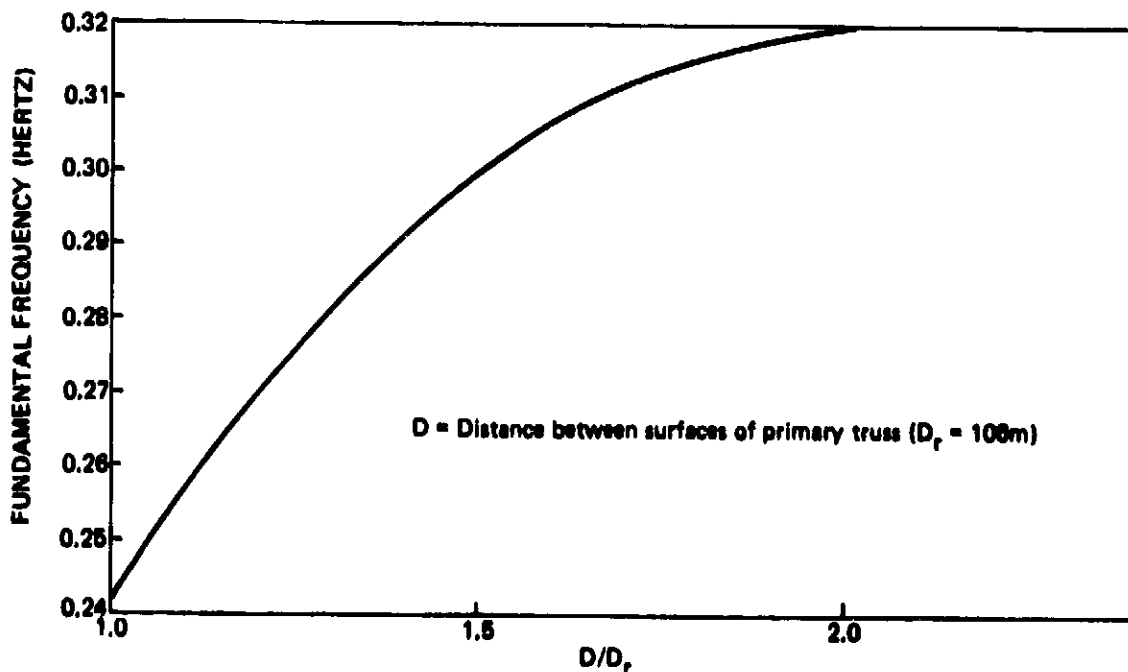


Figure 3.7-8. Two-Tier Tetratruss Concept Utilizing Deployable Truss Modules

A normal modes analysis of the primary truss was performed with the NASTRAN computer program. A structural model composed of rod elements was constructed to represent the 5-ring truss. Masses were lumped at the appropriate surface grids to represent the mass of the structure and an attached antenna system. The model was undamped and accounted only for stiffness of the primary structure. The frequency of the primary truss is shown in Figure 3.7-9. Fundamental frequencies of the truss with a range of system mass are shown in Figure 3.7-10. This mass range is an estimate of the requirements for a microwave antenna of this size taken from Reference 7.



**Figure 3.7-9: Effect of Structural Depth on Fundamental Frequency of 1,300m-Diameter (5-Ring) Primary**

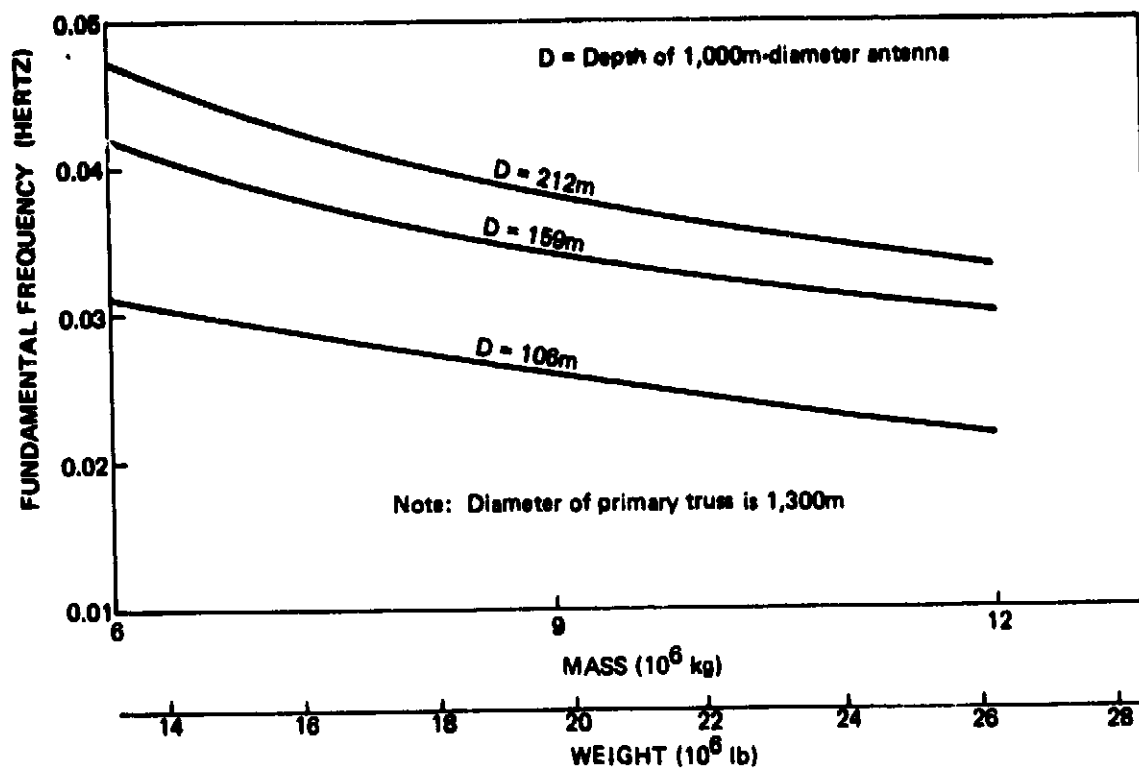


Figure 3.7-10: Effect of Mass and Structural Depth on Fundamental Frequency of 1,000m-Diameter Planar Antenna

A second NASTRAN model was developed to study the effect of removing the outer ring and connecting diagonal elements on the regular hexagonal surface (back face) of the primary truss. This modification, which is characterized in Figure 3.7-11, resulted in only 4 rings of elements on the back face and reduced the mass of the baseline truss by approximately  $17 \times 10^3$  kg. The fundamental frequency of the modified truss was computed to be 0.27 Hz. Thus, elimination of the extraneous ring of elements on the back face of the truss resulted in a 12.5% increase in fundamental frequency and a 19% decrease in mass of the primary structure.

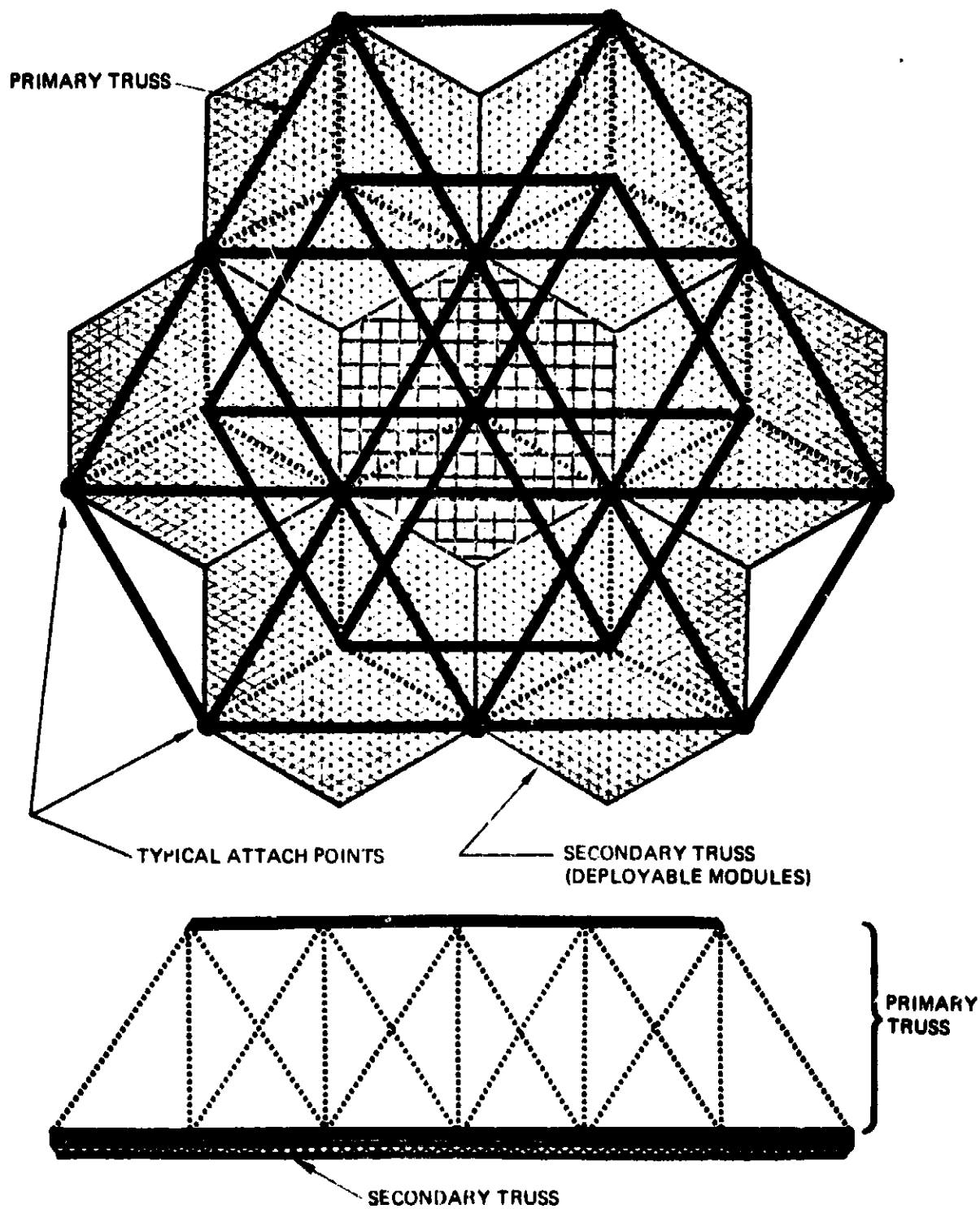


Figure 3.7-11: Alternate Two-Tier Concept Utilizing Tetratruss Modules

### 3.8 AREA SCALE-UP AND CONCEPT DRAWINGS

A typical tetratruss module is shown in Figure 3.8-1 with respect to the orbiter vehicle. An investigation was made to determine how the tetratruss building block modules might be scaled up into a larger structural assembly. Figure 3.8-2 shows how a single module would interface with six additional hexagonal modules. The packaging of seven modules was thus selected as an STS payload study model.

#### 3.8.1 Multiple Modules

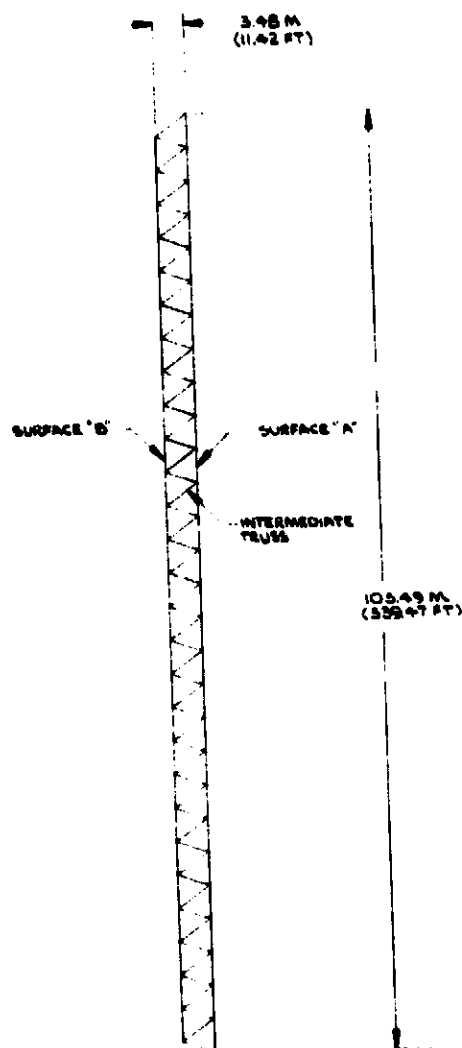
A fourteen-hexagonal ring tetratruss constructed from Gr/Ep struts was selected as the baseline configuration. Figure 3.8-3 shows the basic member characteristics. Packaged weight and geometry are given for an articulated version as well as two additional versions that had telescoping ratios of 3.4 and 4.6 (articulated packaged length divided by telescoped package length). The "B" and "C" versions represented denser packaging and were used as an exemplary way to control the payload center-of-gravity (C.G.) location. Figure 3.8-4 shows a packaging arrangement for "B" and "C" modules. As shown, approximately 16.4 m (54 ft) of payload bay is utilized and the payload weight is 22,997 kg (50,702.5 lbs). Other combinations of packaging density and placement are possible with the telescoping tetratruss modules including a uniform payload of seven modules as shown in Figure 3.8-5. In this manner, the structural area delivered to L.E.O. by one S.T.S. launch would be  $65,000 \text{ m}^2$  ( $698,000 \text{ ft}^2$ ). Figures 3.8-6 and -7 show additional features of a fourteen-ring tetratruss module. These preliminary design drawings were prepared to aid in the packaging, weight, cost and structural analyses.

#### 3.8.2 Area and Frequency Analysis of Multiple Modules

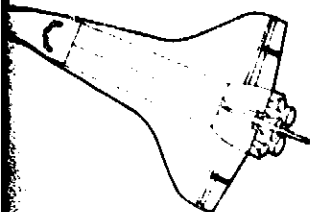
If the planar area is expanded by the addition of perimeter modules the developed area and first resonant frequency would be as shown in Figure 3.8-8. The tetrahedral truss could also be packaged into a rectangular planform or other geometrical shape. This study has used the hexagonal shape which closely approximates a circle which was a desired planar configuration for most identified applications.

180-20203

FOLDOUT FRAME



**FOLD-DOOR FRAME**



0 20 40 60  
SCALE - FEET

[illegible]

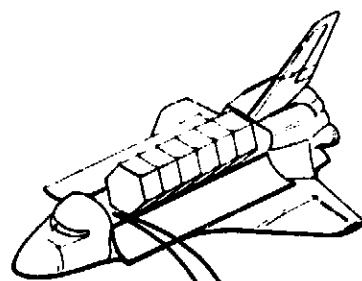
180-56563

**Figure 3.8-1. Typical Tetratruss Module**



180-20220311

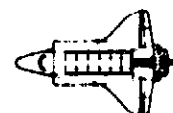
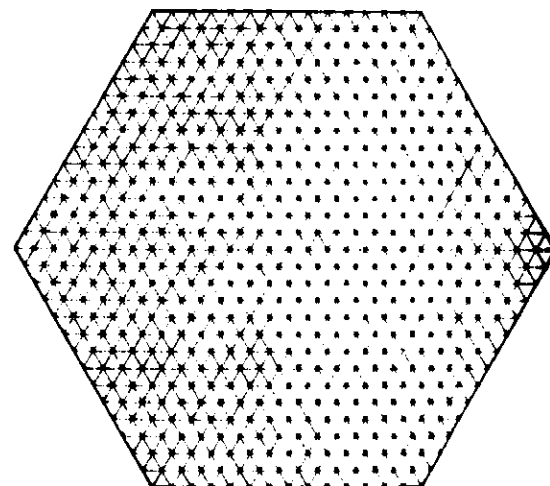
FOLDOUT FRAME



REMOVE



EXTEND



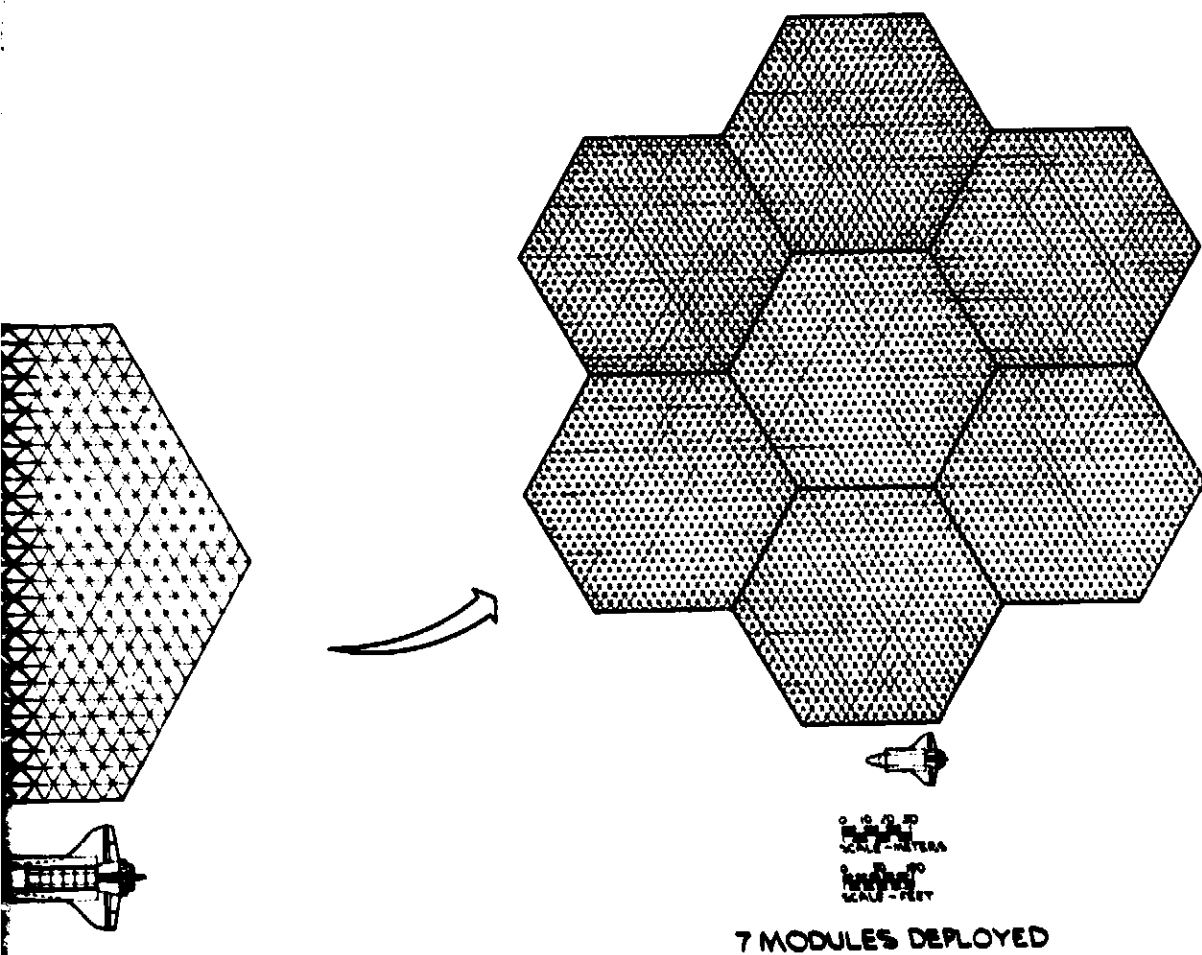
0 10 20  
SCALE - METERS  
0 10 20  
SCALE - FEET

1 MODULE DEPLOYED

7 MODULES IN LEO

FOLDOUT FRAME: 2

\*\*\*\*\* PAGE BLANK NOT FILMED \*\*\*\*\*

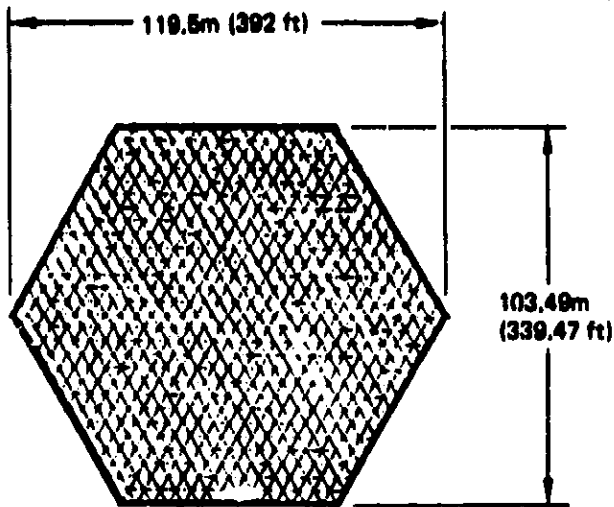


**7 MODULES DEPLOYED**

NAME SURNAME & INITIAL		DATE OF BIRTH		THE <b>ARMED</b> COMPANY	
FAMILY		NAME & ADDRESS		BATTLE ORIGINATED IN	
MILITARY UNIT		MILITARY UNIT		<b>TETRAHEDRON MODULE</b>	
				<b>SCALE-UP</b>	
PROFESSIONAL QUALIFICATION		PROFESSIONAL QUALIFICATION		DATE OF BIRTH	
				J <b>180-56567</b>	

**Figure 3.8-2. Planar Area Expansion**

**"PRECEDING PAGE BLANK NOT FILMED"**



● **STRUT MEMBERS**

LENGTH:	4.27m (168 in)
DIAMETER:	0.051m (2.00 in)
WALL THICKNESS:	0.00051m (0.020 in)
WEIGHT/STRUCT:	0.542 kg (1.185 lb)
JOINT FACTOR:	1.20
MATERIAL DENSITY:	$1.55 \times 10^3$ (0.056)

● **14-RING TETRATRUS**

● **PACKAGED WEIGHT**

● **PACKAGED GEOMETRY**

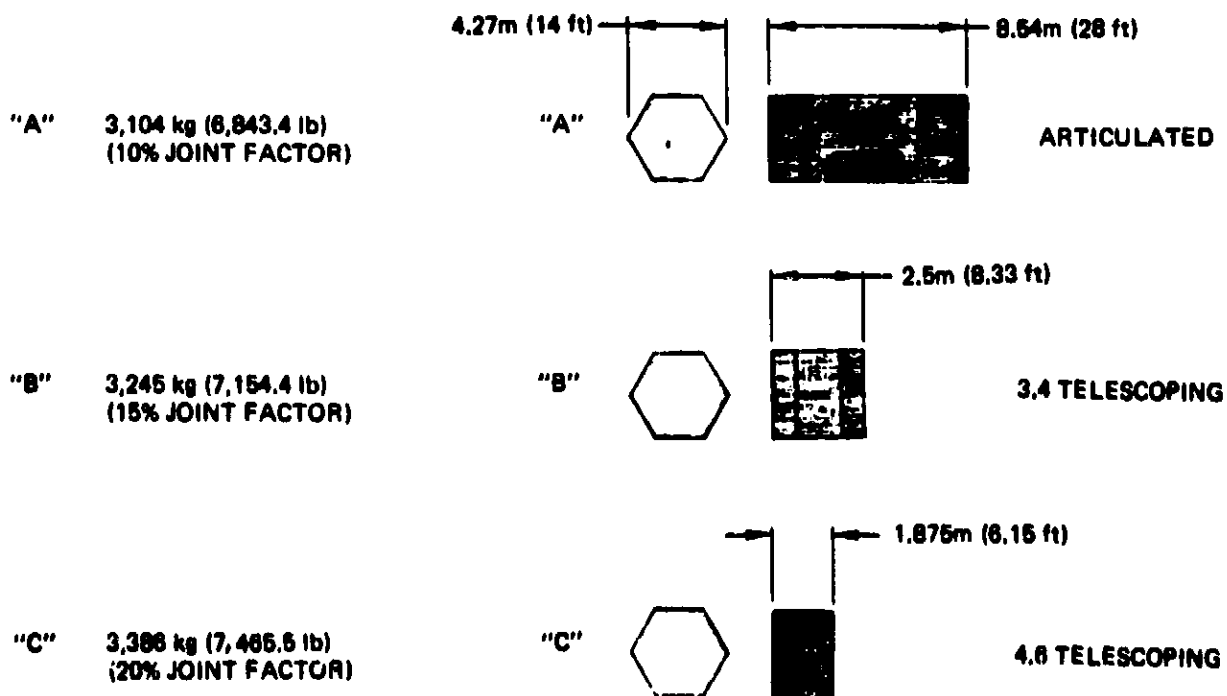
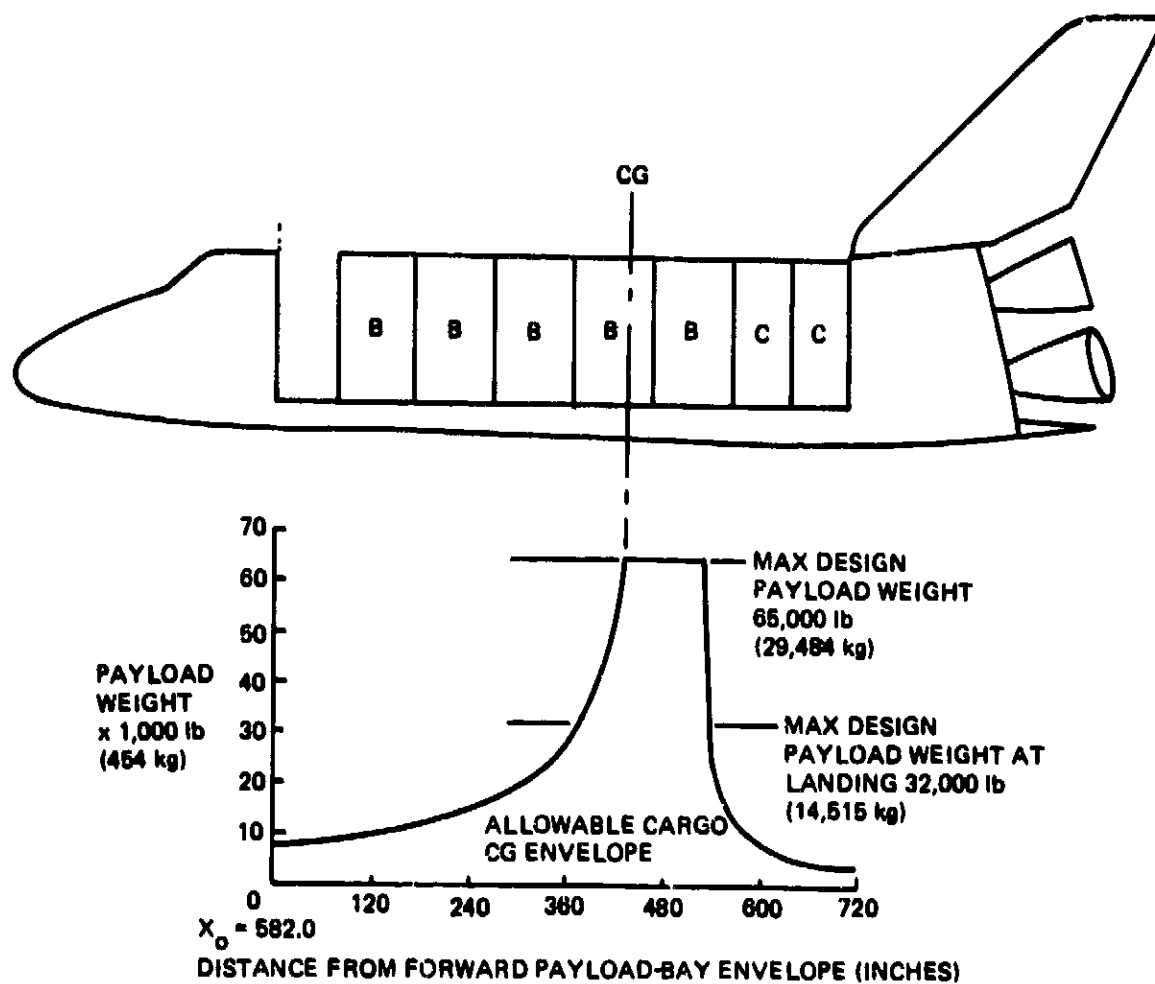


**Figure 3.8-3. Tetratruss Packaging Characteristics**



Total weight = 5 "B" modules + 2 "C" modules = 22,987 kg (50,702.5 lb)

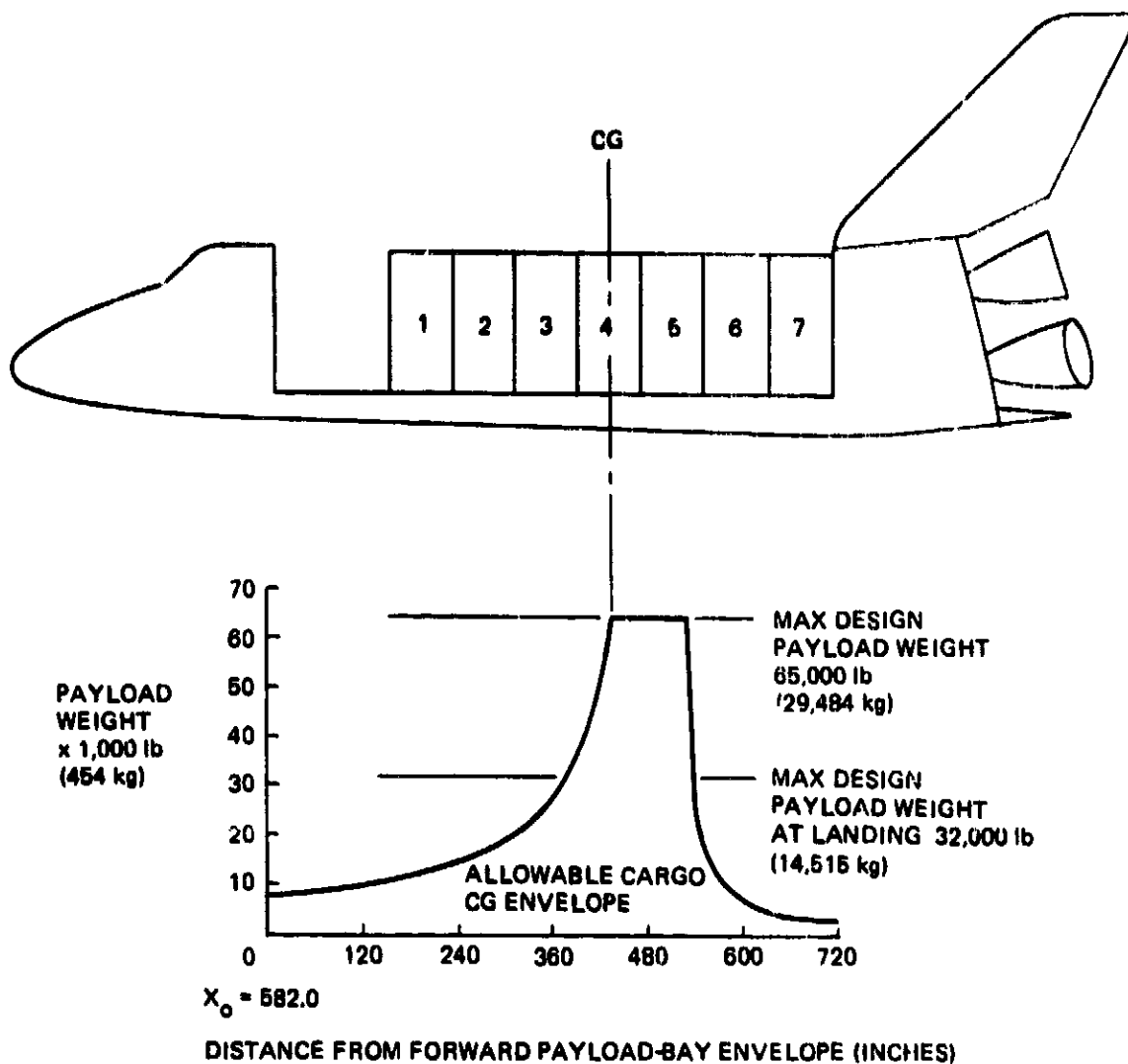
Total payload length = 16.42m (53.85 ft)

Average package density = 118 kg/m<sup>3</sup> (7.4 lb/ft<sup>3</sup>)

Center-of-gravity location from forward  
payload-bay bulkhead = 131.06m (430 in)\*

\* Location good for maximum payload = 29,484 kg (65,000 lb)

**Figure 3.8-4. Packaging Arrangement for Seven-Module Mission**



Total weight = 27,584.5 kg (60,812.4 lb)

Total payload length = 14.63m (48 ft)

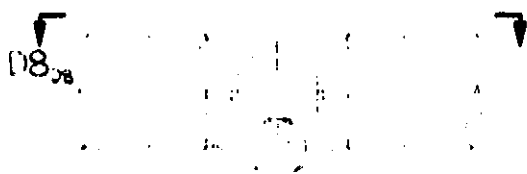
Average packaging density =  $159 \text{ kg/m}^3$  (9.96 lb/ft<sup>3</sup>)

Center-of-gravity location from  
forward-bay bulkhead = 131.06m (430 in)

**Figure 3.8-5. Multiple-Module, Uniform-Density Payload**



D8



D8

FOLDING JOINT  
50% DEPLOYED



B5

FOLDING JOINT  
50% DEPLOYED

1 2 3 4 5

SCALE - CENT METERS

SCALE - INCHES

370M  
(12.12 FT)

254M  
(8.33 FT)

SIDE VIEW  
TELESCOPED

8.33  
(2.82)

FOLDOUT FRAME

6

5

4

4.27M  
(14.00FT)

3.70M  
(12.12FT)

PLAN VIEW  
CLOSED

PLAN VIEW  
50% DEPLOYED

2.54M  
(8.33FT)

8.53M  
(28.00FT)

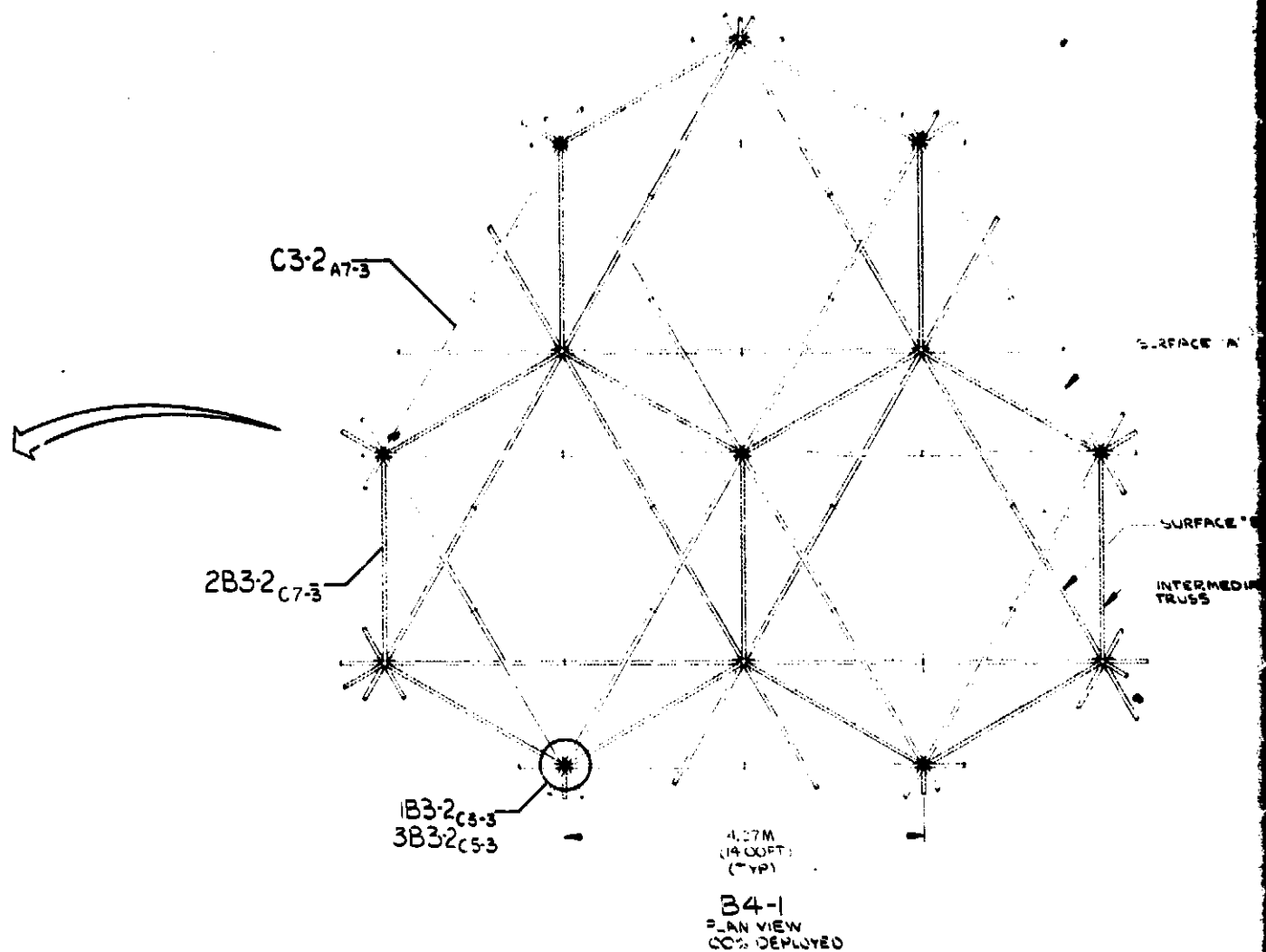
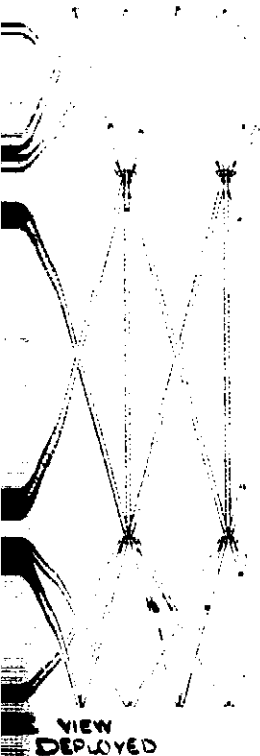
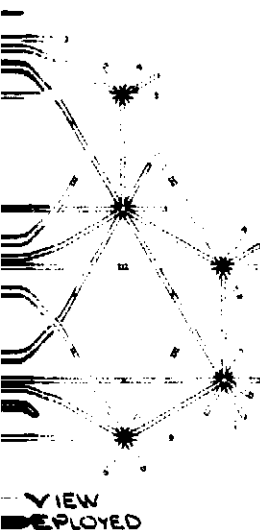
B5C7

SIDE VIEW  
EXTENDED

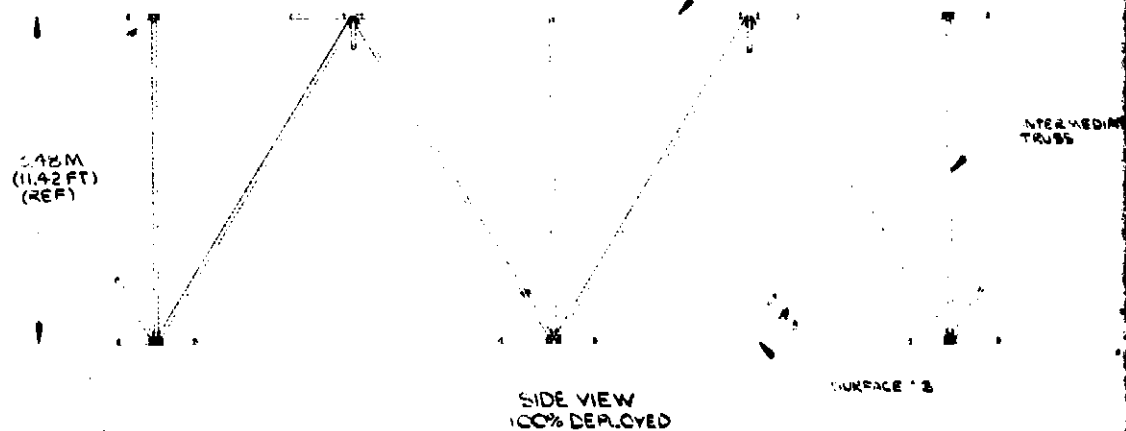
SIDE VIEW  
50% DEPLOYED

YOUTH FRAME

180 56563 2



5.48M  
(18.00FT)  
(REF)



DOOT FRG 3

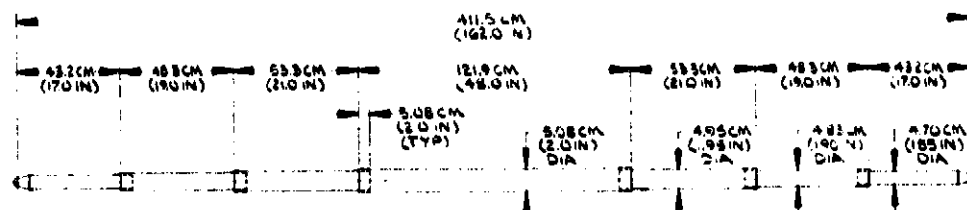
PRECEDING PAGE BLANK NOT FILLED



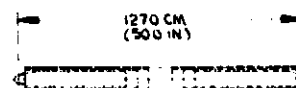


180-202033

# FOLDOUT FRAME



-DEPLOYED-

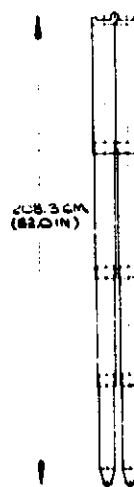


-TELESCOPED-

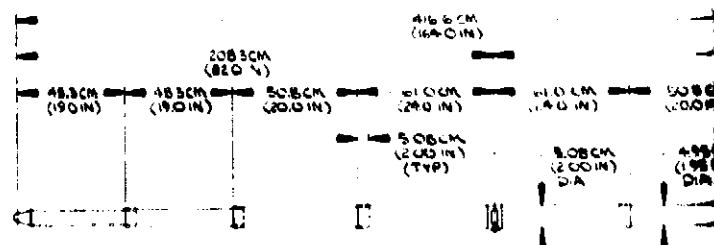
2B3-2  
INTERMEDIATE TRUSS MEMBER  
NO SCALE



TELESCOPED



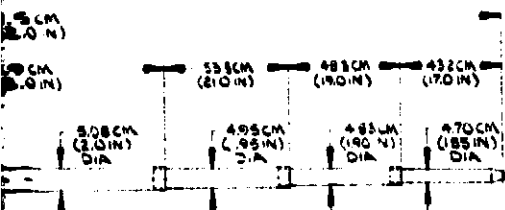
FOLDED



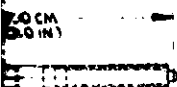
DEPLOYED

C3-2  
SURFACE MEMBER  
NO SCALE

# FOLDOUT FRAME 2

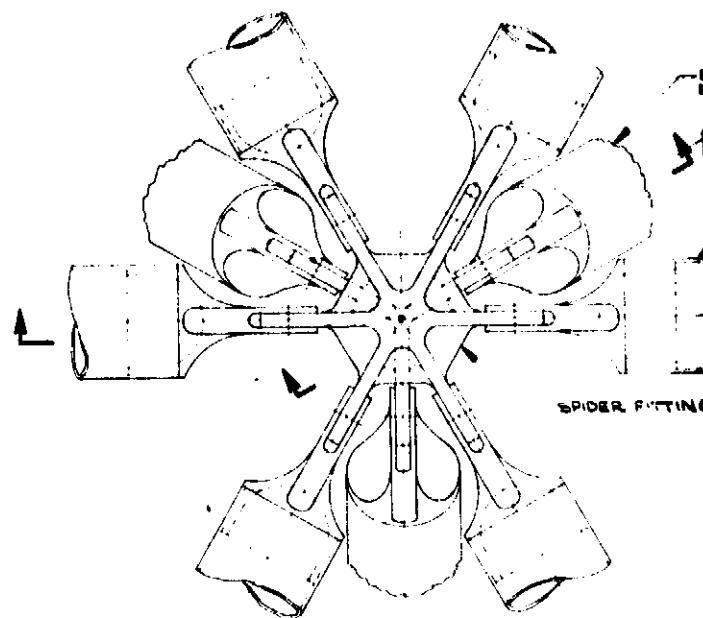


DEPLOYED -

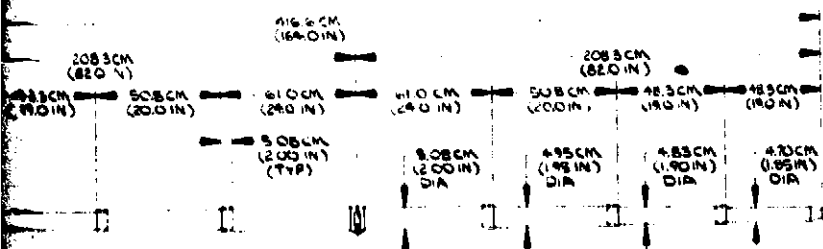


DEPLOYED -

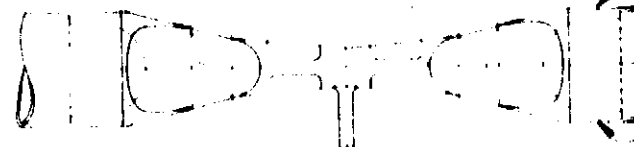
3B3-2  
TRUSS MEMBER  
SCALE



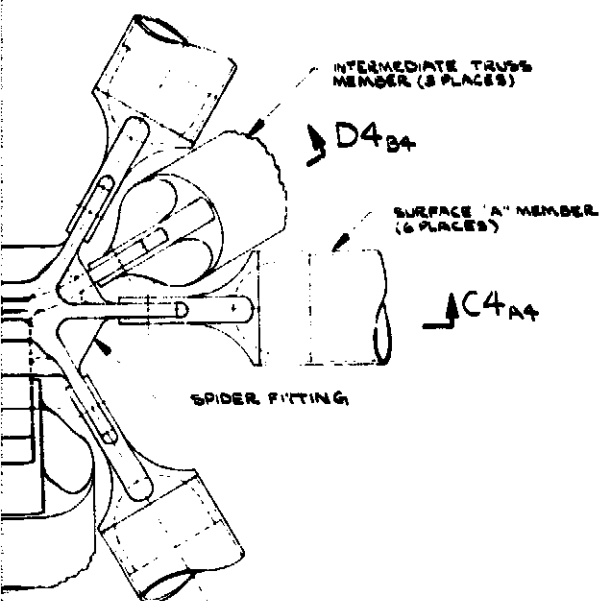
3B3-2  
PLAN VIEW  
PIN JOINT SPIDER FITTING  
SCALE: 1/1



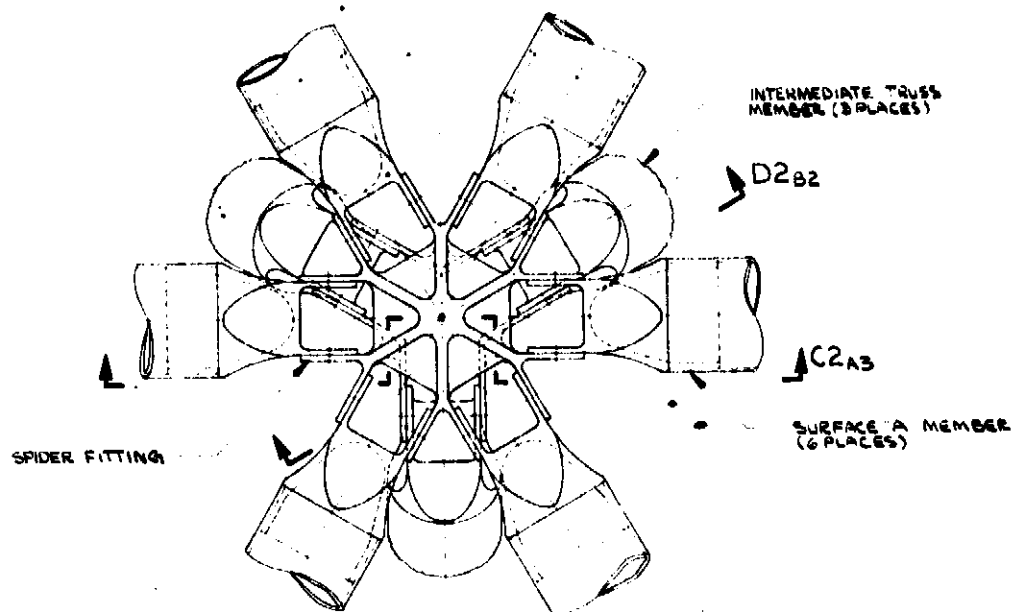
DEPLOYED



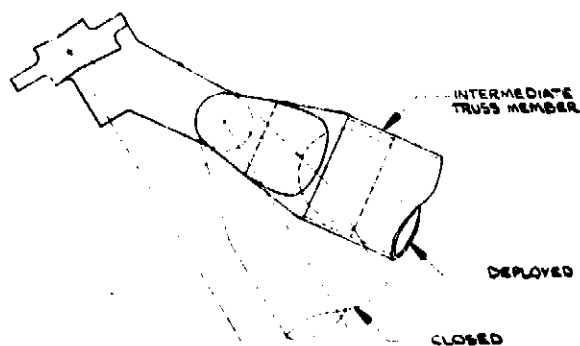
SECTION C4  
SCALE: 1/1



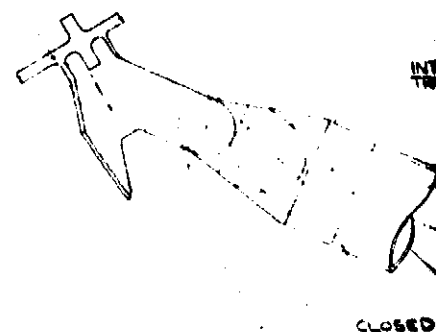
3-2  
VIEW  
SPIDER FITTING  
SCALE: 1/1



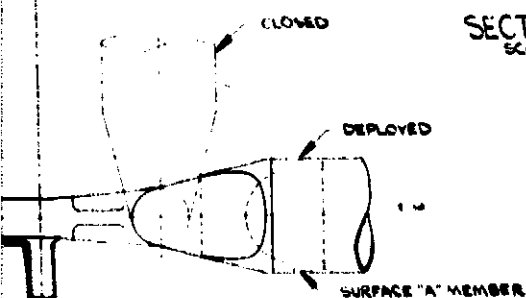
1B3-2  
PLAN VIEW  
WIDE MOUTH SPIDER FITTING  
(SCALE: 1/1)



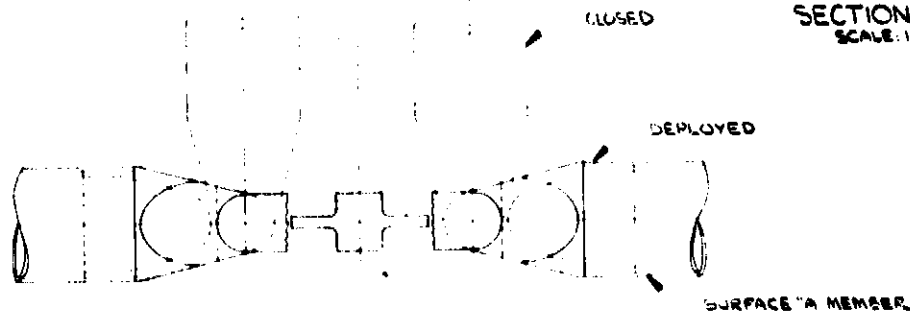
SECTION D4  
SCALE: 1/1



SECTION D2  
SCALE: 1/1



SECTION C4  
SCALE: 1/1



SECTION C2  
SCALE: 1/1

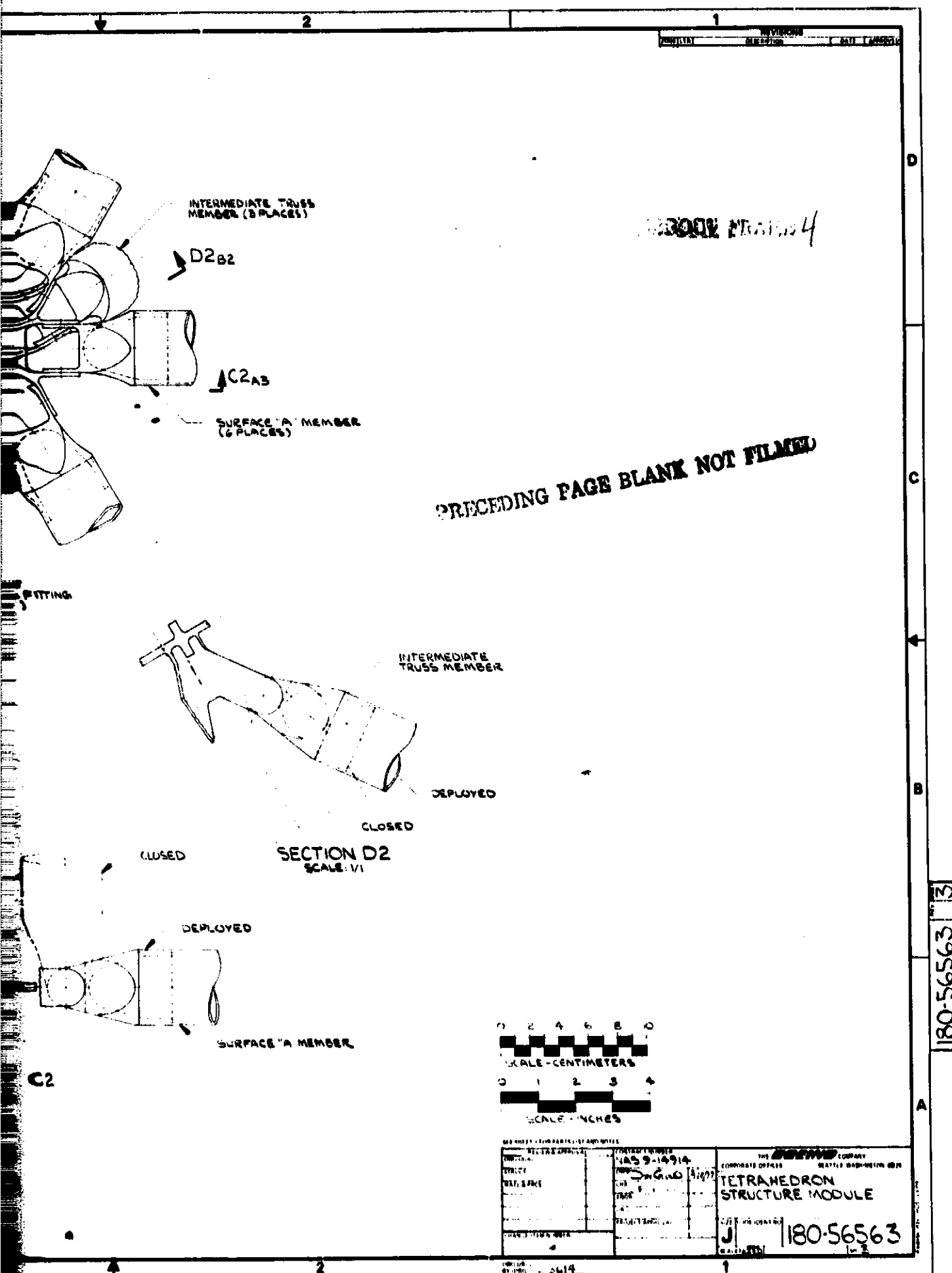
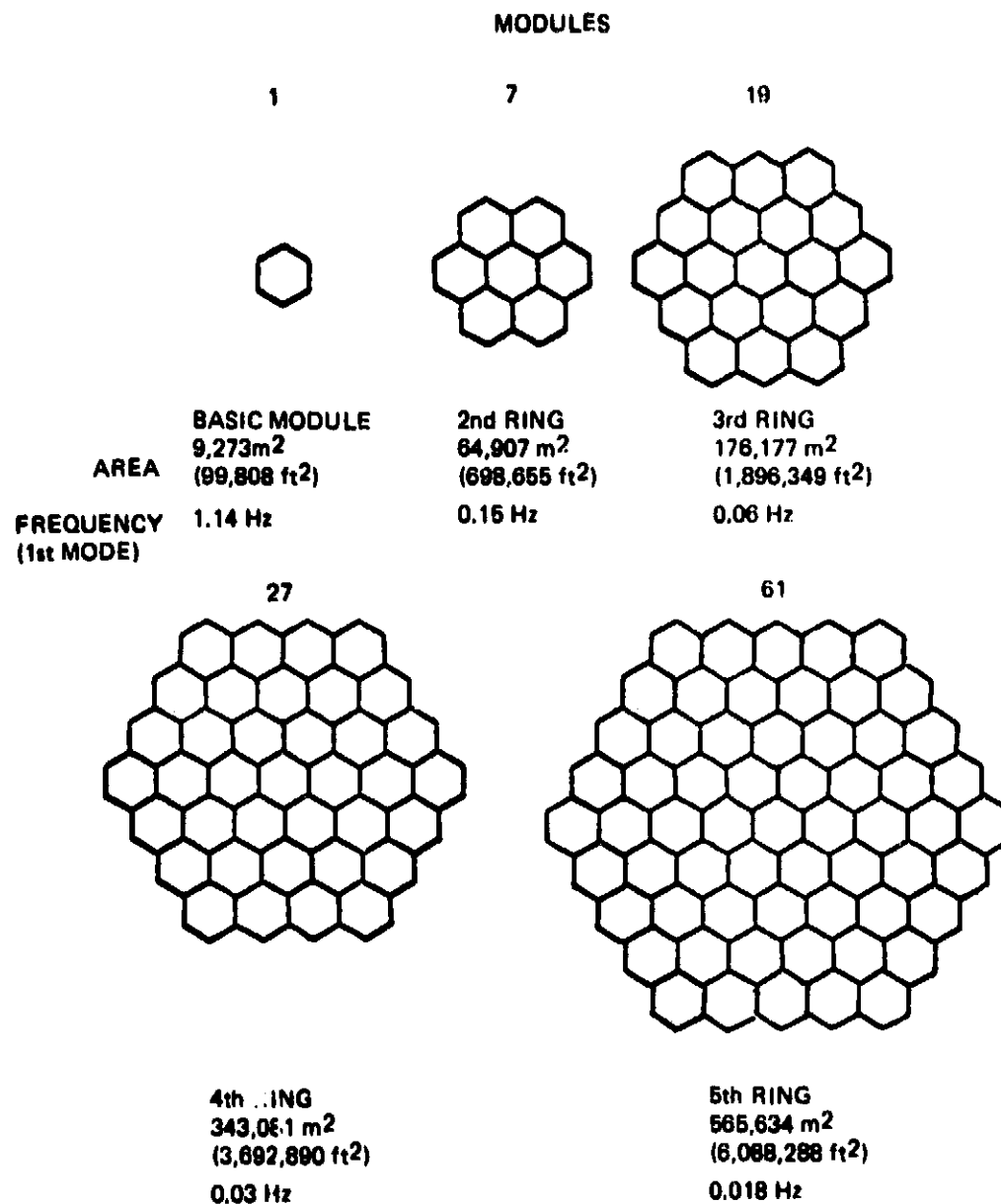


Figure 3.8-7. Preliminary Design, Tetratruss, Sheet 3 67



### 3.8.3 Two-Tier Tetrahedral Truss

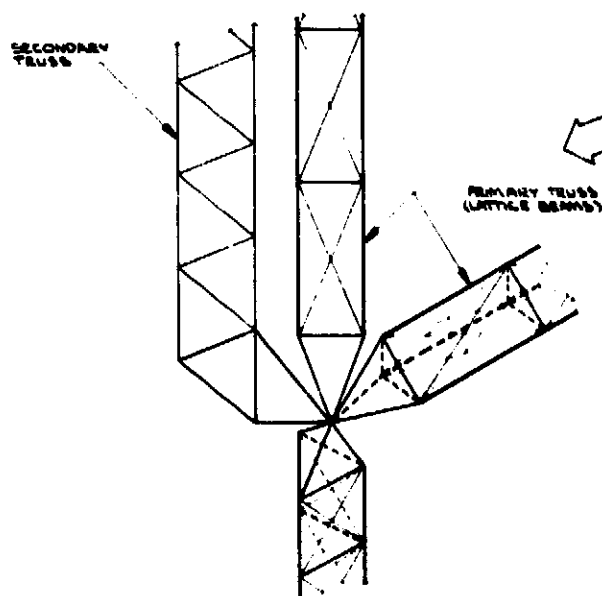
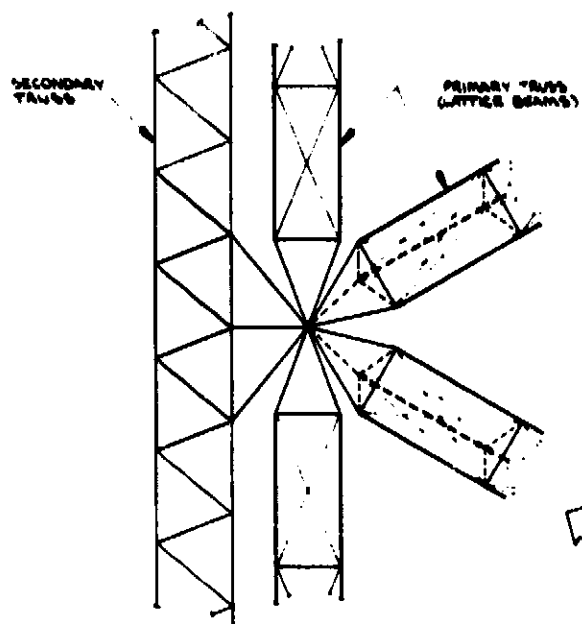
It becomes apparent, for pointing accuracy and figure control, that as the planar area grows to a larger and larger surface, a stiffer support structure is required. The deployable modules would then be thought of as the attachment interface or secondary structure and a deeper supporting truss as the primary structure. An example of this concept is shown in Figure 3.8-9. The secondary truss in this concept is shown tied to a larger tetrahedral truss. The individual modules would be tied at three locations for pointing control, thermal isolation and maintenance/repair provisions. The "module ring", as shown, is mounted to the "irregular" or lower surface of the primary truss. In this example, the upper surface of the primary truss is reduced to a single hexagonal ring which appears to be an efficient support system. An option would be to eliminate the irregular surface members of the primary truss and tie the secondary modules directly to the primary diagonals. If the secondary modules are continuously joined along their boundaries, they would respond like a large plate on a multiple isogrid support.

The primary truss elements in this type of concept would be 100 m or more in length but could be packaged as individual compression members and be erected/assembled on orbit. Assembly trades must be made as a function of final spacecraft size. Figure 3.8-10 shows this concept scaled up to a five-ring primary truss (660 members) and a five-ring module array of over one kilometer on each side (61 basic modules).

This arrangement has been identified as a possible configuration for a large (1 km diameter) microwave antenna for a Solar Power Satellite (S.P.S.)<sup>(8)</sup>. In this configuration the pointing of the subarrays, which are each approximately 100 m<sup>2</sup> in area, is greatly simplified. The subarrays could be pointed at the substructure (tetratruss) level as they are attached in a determinate manner to the deep primary truss.

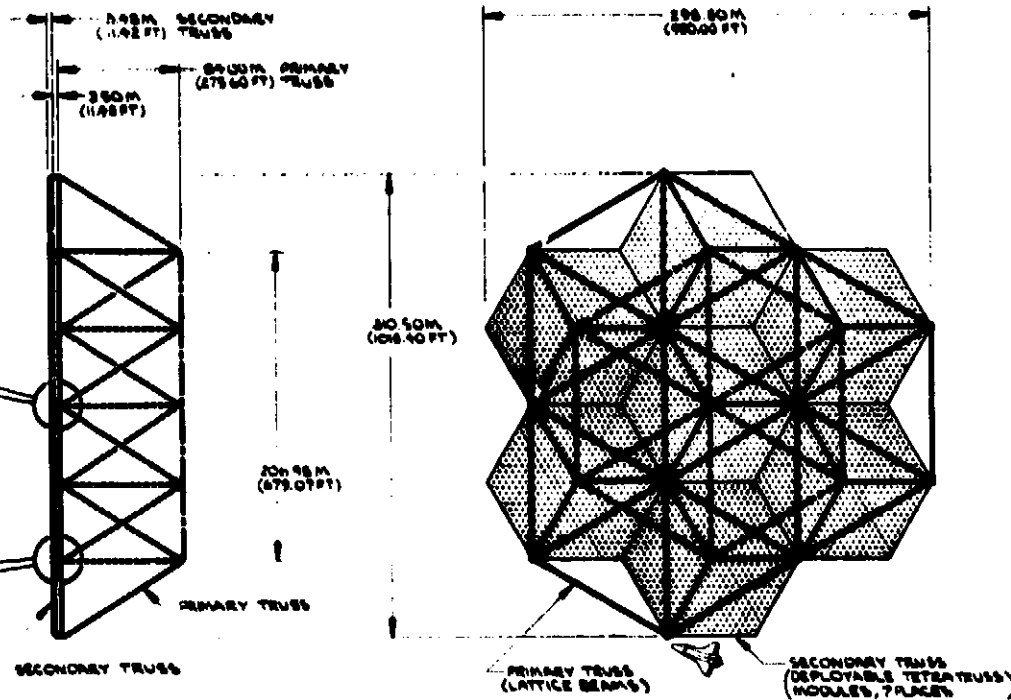
180-2022811

# FOLDOUT FRAME





# FOLDOUT FRAME



0 20 40 60 80 100  
SCALE - METERS  
0 100 200 300  
SCALE - FEET

1180-56568

DESIGN: 100-5-14914		THE SPACE SHUTTLE PROGRAM	
PROJECT: 100-5-14914		PROJECT OFFICE: 100-5-14914	
SUBJECT: TWO TIER SPACE PLATFORM CONCEPT		SUBJECT OFFICE: 100-5-14914	
DESIGNER: J		1180-56568	

Figure 3.8-9. Two Tier Space Platform Concept

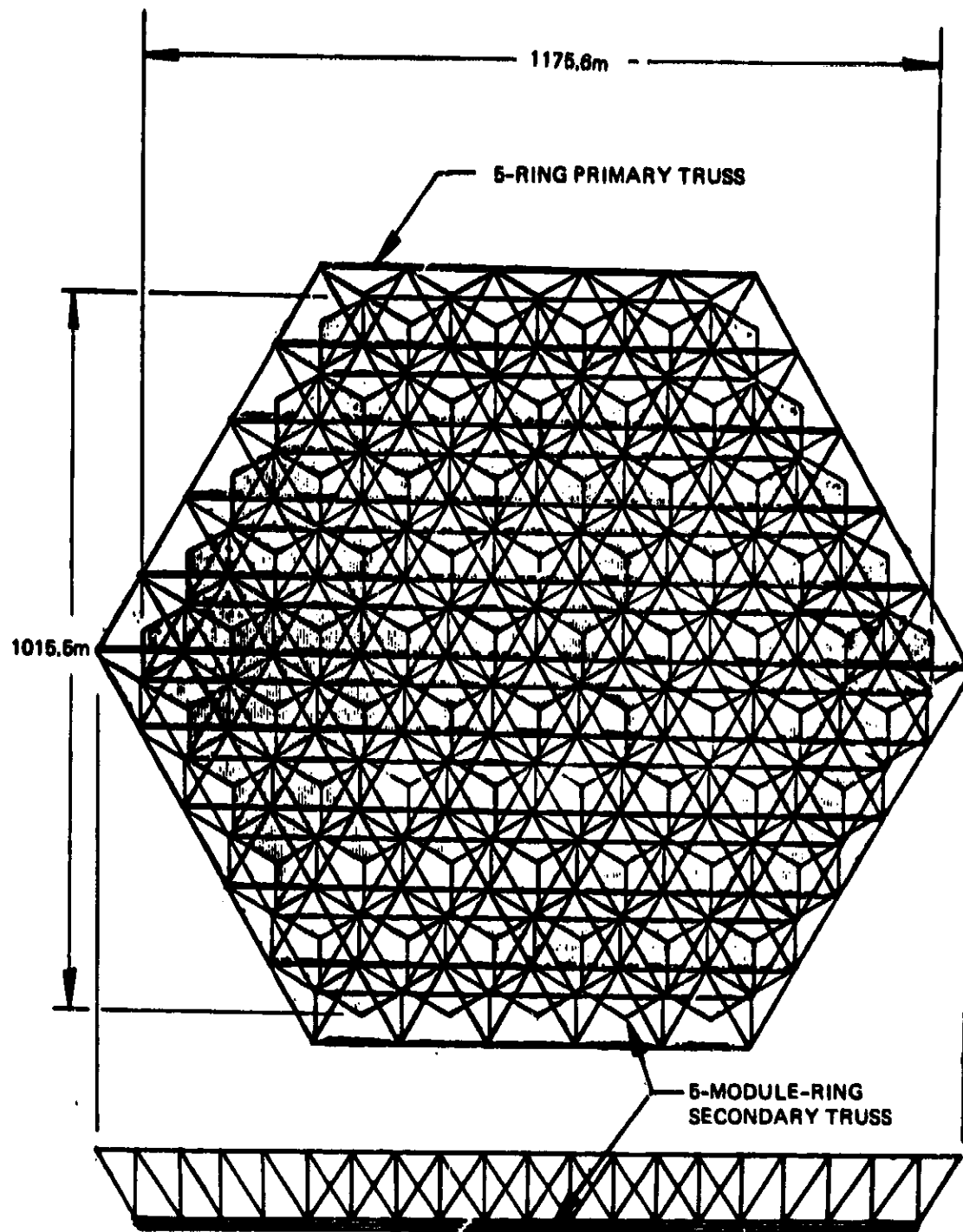






Figure 3.8-10. Multiring Two-Tier Tetrahedral Truss

#### 4.0 COMPRESSION STRUT DEVELOPMENT

A study of building-block approaches to columnar structures was conducted. Various concepts of prepackaged deployable structures were investigated to arrive at near-term approaches to compression loaded members for large area structures applications. Concepts that folded, articulated, coiled or inflated were examined as possible candidates. The desire to be volume and weight compatible with the STS, in the same as the planar array development, demanded a high packaging density (close to  $100 \text{ kg/m}^3$ ) while maintaining a minimum mass per unit length. Applications identified showed a need for compression members from 10 m (32.8 ft) to 1000 m (3280 ft) in length. Some typical strut configurations are shown in Figure 4.0-1.

*Figure 4.0-1: Strut Configurations*

CANDIDATES	CHARACTERISTICS
<p>● CIRCULAR TUBES (RIGID)</p> 	<ul style="list-style-type: none"> <li>● CHEMICALLY MILLED, SEAM WELDED ALUMINUM</li> <li>● FILAMENT WOUND GR/EP COMPOSITE</li> <li>● PULTRUDED GR/EP WITH S - GLASS</li> <li>● POST FORMED GR/THERMOPLASTIC COMPOSITE</li> <li>● TELESOPING TAPERED SECTIONS FOR PACKAGING</li> </ul>
<p>● CHORD BATTEN SECTIONS</p> 	<ul style="list-style-type: none"> <li>● ALUMINUM CHORDS AND BATTENS</li> <li>● GR/EP PULTRUDED CHORDS WITH MOLDED BATTENS</li> <li>● INJECTION MOLDED THERMOPLASTIC JOINTS</li> <li>● GOOD PACKAGING DENSITY</li> </ul>
<p>● CHORD LATTICE SECTIONS</p> 	
<p>● ELASTIC RECOVERY (FLEXIBLE)</p> 	<ul style="list-style-type: none"> <li>● JOINING OF SECTIONS OF CROSS MEMBERS DIFFICULT</li> <li>● PULTRUDED FROM GR/EP OR GR/TP</li> <li>● HIGH PACKAGING DENSITY</li> </ul>

#### 4.1 CONFIGURATION TRADES

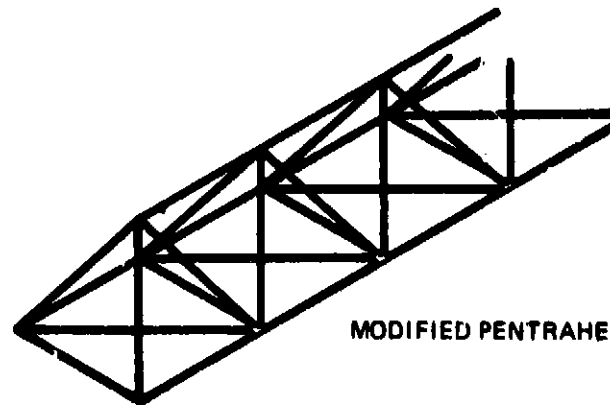
Lattice-stabilized, multi-chord compression elements have long been utilized as efficient support structures for bridges, power line towers, large TV and radio antennas and various construction booms. A triangular cross section provides the maximum stiffness of the various section/chord combinations. The packaging of this concept involves folding or coiling the chord members and hinging or elastically storing the lattice and batten members.

Tubular columns exhibit excellent column behavior and appear to be quite useful in the lower length requirements of from 10 m (32.8 ft) to 20 m (65.6 ft). Cylindrical sections, packaged in a rectangular array in the STS bay, have been shown to reach a packaged density causing weight-critical payloads only in small diameters, i.e., .025 m (1 in) to .038 m (1.5 in). However, tapered columns, nested Dixie Cup fashion, can far exceed the maximum payload of the S.T.S. (Ref. 13).

To develop concepts for application in the 20 m and greater lengths it was evident that lattice members with section depths of 1 m or more would be required.

#### 4.2 PACKAGING CHARACTERISTICS

An articulated lattice truss, a modified pentahedral truss, was configured as shown in Figure 4.2-1, to fill the payload bay to 4.27 m (14 ft). The structural characteristics of this concept are shown in Table 4.2-1. Graphite/epoxy chords were assumed and a D/t of 100 was held constant. While deployed beams of 70 m to 738 m can be packaged, the maximum payload is 1418 kg (3125 lbs), far short of capacity due to the package scheme. An improvement in packaging density was exhibited by the concept shown in Figure 4.2-2. This concept features a triangular cross section with the longerons stabilized by elastic recovery shear ties. The shear ties are fabricated with parabolic curvature and are attached to the longeron by pin joints located at E and B. At locations A, C, D and F the ties are connected to the longeron by a sliding joint. The ties are also pinned for rotation at G and H. Identical shear ties interconnect the three longerons of the strut.



MODIFIED PENTRAHEDRAL TRUSS

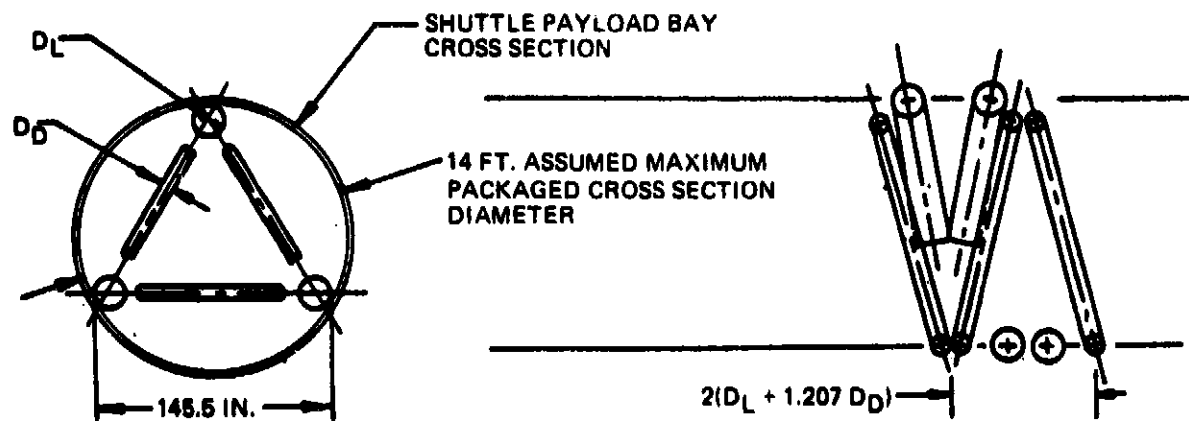


Figure 4.2-1: Articulated Lattice Truss Concept

Table 4.2-1 Structural Characteristics of Strut Assembly

LONGERONS			STRUT							
DIA, $D_L$	LENGTH, $L_L$	NO. OF BAYS	LENGTH, $L_{STRUT}$	$I$	$\rho$	$\frac{L_{STRUT}}{\rho}$	$\sigma_w$	$P_{cr}$	WEIGHT, $W_{STRUT}$	FREQUENCY, $f_{STRUT}$
m (in.)	m (in.)	b	m (in.)	m <sup>4</sup> (in. <sup>4</sup> )	m (in.)		MM/m <sup>2</sup> (psi)	kg (lb.)	kg/m (lb/in.)	HZ
0.0284 (1.1)	3.674 (144.63)	201	738.39 (29,070.63)	6.90 (218.63)	1.22 (48.19)	603.25	4.87 (878.02)	28.88 (83.28)	.2125 (0.0119)	0.0246
0.0308 (1.2)	3.662 (143.78)	100	396.16 (15,578.00)	21.75 (868.13)	1.22 (47.90)	300.13	18.88 (2,739.27)	483.63 (1,072.3)	.8453 (0.0474)	0.1079
0.0782 (3.1)	3.628 (142.80)	68	248.80 (9,718.62)	48.34 (1,903.04)	1.21 (47.61)	204.08	40.85 (5,823.98)	2298.95 (4,974.38)	1.8018 (0.1008)	0.2244
0.1018 (4.0)	3.608 (142.03)	51	183.88 (7,243.53)	84.90 (3,342.80)	1.20 (47.32)	153.08	72.80 (10,630.01)	7128.88 (15,718.20)	3.2442 (0.1817)	0.3987
0.1270 (5.0)	3.585 (141.18)	40	143.42 (5,646.40)	131.04 (5,188.03)	1.19 (47.03)	120.08	118.03 (17,117.74)	18107.84 (39,927.12)	5.1138 (0.2884)	0.6488
0.1624 (6.4)	3.564 (140.30)	34	121.18 (4,770.20)	188.42 (7,339.41)	1.18 (46.74)	102.08	161.31 (23,388.81)	28841.20 (78,588.88)	7.4008 (0.4148)	0.9019
0.1778 (7.0)	3.542 (139.43)	28	102.70 (4,043.47)	250.80 (9,688.01)	1.18 (46.45)	87.05	224.51 (32,881.38)	37818.02 (148,870.81)	8.8831 (0.4934)	1.2807
0.2032 (8.0)	3.519 (138.58)	25	87.88 (3,464.00)	323.23 (12,728.71)	1.17 (46.18)	75.04	241.33 (35,000.00)	84788.84 (209,003.88)	12.8808 (0.7288)	1.7014
0.2388 (9.4)	3.498 (137.70)	22	78.86 (3,089.40)	404.03 (15,608.81)	1.17 (45.89)	68.03	241.33 (35,000.00)	18881.80 (284,818.80)	16.4878 (0.9223)	2.2070
0.2840 (11.2)	3.476 (136.82)	20	68.51 (2,728.80)	492.53 (18,580.78)	1.16 (45.60)	60.03	241.33 (35,000.00)	148104.78 (327,571.08)	20.3830 (1.14218)	2.8834

$$L_{STRUT} = b \cdot L_L$$

$$\sigma_w = \frac{\pi^2 E I}{L^2}$$

$$W_{STRUT} = \frac{\text{TOTAL WT. OF STRUT}}{L_{STRUT}}$$

$$I = 0.333 A_L L^2$$

$$P_o = \sigma_o = 2A_L$$

$$f_n = \frac{1.87}{L_{STRUT}} \sqrt{\frac{388 E I}{W}}$$

$$\rho = \sqrt{1/3 A_L}$$

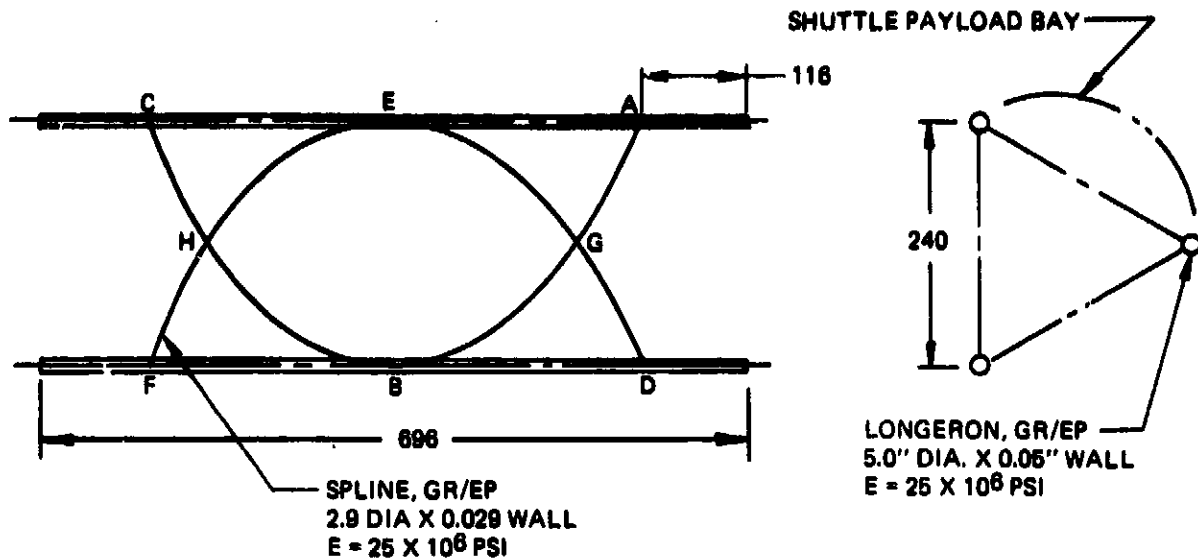
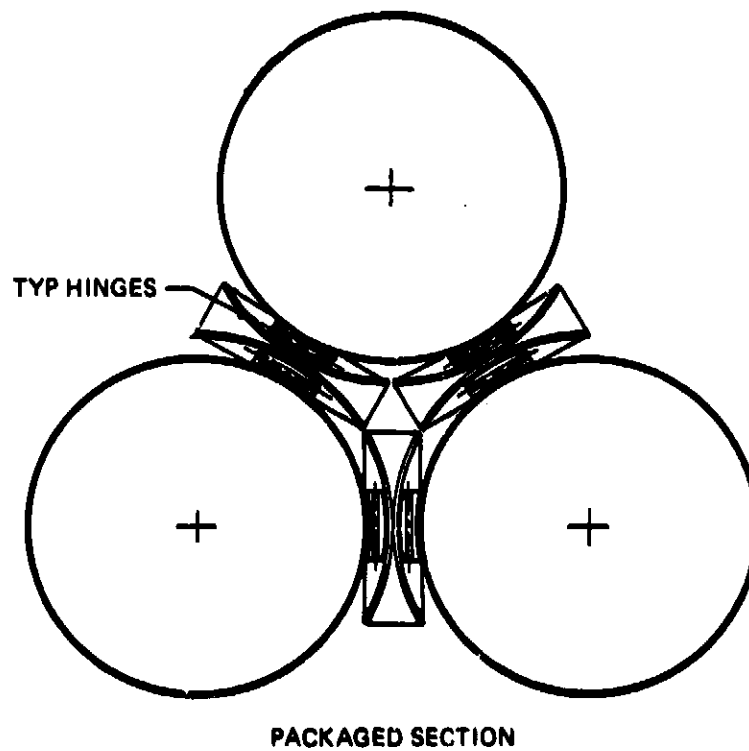
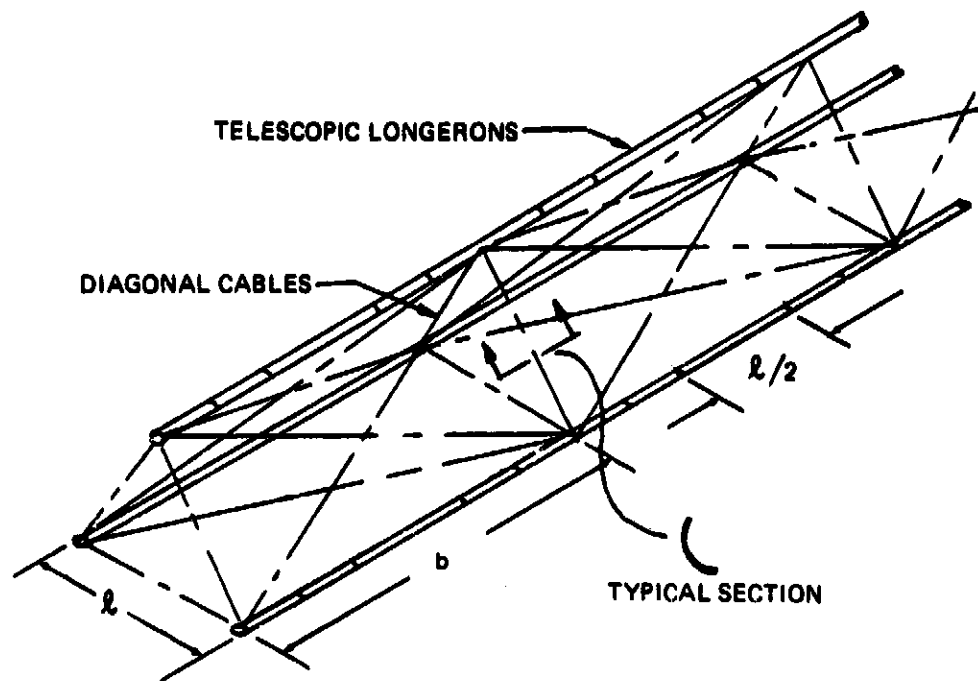


Figure 4.2-2: Collapsible Strut Concept

The packaging of this concept is accomplished by releasing locking devices at A, C, D and F which permits the ends of shear ties to slide along toward the ends of the longerons. The strut section can then be collapsed forcing the shear ties to straighten out. Packaged section approaches a nested longeron stack. Each strut assembly (58 ft long) is assumed to be interconnected with a hinge joint. The hinge joint is not restricted as to orientation, thus rotation of the strut during deployment can occur across different planes of the triangular section. A total of 48 strut sections can thus be packaged for a total deployed length of 848 meters (2784 ft). The weight of this configuration which utilizes .127 m (5.00) dia. Gr/Ep longerons with .127 cm (.050 in.) wall thickness is approximately 8500 pounds. This strut would have an  $L/\rho$  of approximately 400 and would be capable of a compression load of 14,652 N (3294 lbs).

A technique to further improve the packaging density of lattice-column structures was developed. Shown in Figure 4.2-3 is a multi-bay lattice column which consists of three longerons that are stabilized by diagonal cables, in the plane of each bay, and by lateral members that establish the bay length. Each lateral is an open-section member that behaves like a "carpenter's tape" in that it can be folded elastically into a small radius for packaging. The



**Figure 4.2-3. Cable Stayed Foldable Diagonal Concept**

diagonal cables pass through the hinges that attach the laterals to the longerons and are stored in a "reel" device at the end of the bay.

The lattice-column is packaged by folding the laterals and allowing them to "nest" parallel to the longerons. The slack in the cables would be taken into a cable storage device as the longerons are brought closer to each other. This results in a very small packaged cross section. Further densification is available by telescoping the longerons between each bay. The telescoped sections have locking features to prevent linear and rotational motion when the column is in the extended position.

The beam geometry can be established such that the bay length (distance between laterals) is several times larger than the lateral member length. This allows the chords to telescope into one another. Referring to Figure 4.2-3:

$L_p$  = Packaged beam length

$D$  = Chord diameter

$L_D$  = Deployed beam length

$P$  = Load capability of Deployed Column

$b$  = Typical bay dimension

$\ell$  = Distance between chords

$n$  = Number of bays

$$L_p = n \times \frac{\ell}{2}$$

$$L_D = n \times b$$

#### 4.3 STRUCTURAL CHARACTERISTICS AND PAYLOAD EFFECTS

Using chord diameters in the .0508 m (2 in) to .254 m (10 in) range, this concept can be used to package several building-block compression elements. For example, for the two-tier truss approach shown in Figure 3.8-9 the primary member length is 130 m. If a uniform S.T.S. payload density is assumed which fills the payload bay to a diameter of 4.27 m, the mass density can approach  $52 \text{ kg/m}^3$ . Further, if the slenderness ratio is held at 200 the following data will apply to columns constructed from graphite/epoxy:



D (cm)	D/t	$\ell$ (m)	$P/L_D^2$ (N/m <sup>2</sup> )	b (m)
5.08	100	1.6	0.7	3.6
10.16	100	1.6	2.7	13.7

From this data, the payload density and total length of compression member can be determined.

TABLE 4.3-1 LATTICE-COLUMN PACKAGING AND TOTAL DEVELOPED LENGTH

CHORD		PACKAGED CHARACTERISTICS					
DIA (cm)	WALL (cm)	AREA (m <sup>2</sup> )	LENGTH (m)	DENSITY (kg/m <sup>3</sup> )	MASS (kg)	UNITS	TOTAL LENGTH (m)
5.08	.0051	.0077	18	62	11,335	1300	23,400
5.08	.0043	.0077	18	52	13,602*	1847*	33,250
10.16	.0102	.0323	18	20	5,214	443	7,980

\* Maximum mass for C.G. location (4.27 m x 18 m payload)

As shown in Table 4.3-1, compression members with relatively small chord diameters can be packaged up to the maximum mass allowed for full length payloads. Seven units of this strut could be assembled to arrive at a single 130 m long column. A total of 6500 meters of deployable beams is required to provide the primary truss as shown in Figure 3.8-9. One S.T.S. flight could thus deliver enough building-block lattice units to fabricate the truss.

The telescopic feature of this column allows it to be packaged into an even denser payload, e.g.,  $L_p = \ell/2 = .8$  m. Therefore, each bay of 3.6 m could be packaged to .8 m. If the total packaged length is set at 14.63 m and installed in the aft portion of the payload bay, the C.G. of the payload would permit a maximum of 29,484 kg. The number of bays per column would be  $\frac{14.65}{.8 \text{ m}}$  or 18 bays.

The deployed length would thus be 64.8 m. The mass of each beam would be approximately 30 kg, and the total units,  $\frac{29,484}{30}$  or 982. The total length of columns in this case would be 63,634 m. If the 130 m column is the desired unit length, a pair of these columns could be hinged (similar to Figure 6.1-5) and termination fittings added at each end of the column.

A variety of columnar compression elements can thus be packaged, from a basic 18-meter length, to units that telescope to approximately 65 meters and through multiple hinging even greater lengths. The packaging can be adjusted to utilize the total mass delivery to L.E.O. by the S.T.S.

## 5.0 CONCEPT/PERFORMANCE PARAMETRIC STUDY & APPLICATIONS

The work performed under this task was basically a summary of the concept productivity of each building-block design. The productivity was defined as the amount of building-block structure delivered to L.E.O. by a single S.T.S. flight, either cross-sectional area in the case of the tetratruss or developed length when referring to the compression member concepts.

The tetratruss module concept was packaged such that the mass density and CG location permitted a payload of seven modules. This potentially represents a deployed truss frame of  $65,000 \text{ m}^2$  ( $698,000 \text{ ft}^2$ ).

The lattice compression column concept also demonstrated high density packaging. A single flight in this case represents  $63,634 \text{ m}$  ( $208,770 \text{ ft}$ ) of compression elements.

Both building block concepts are scalable to other configurations with similar productivities. The end-item use or application will, of course, impose unique requirements of strength, stiffness, distortion, maintainability, etc., that will determine final member sizes and material choices.

A two-tier truss was identified as a space truss platform fabricable from the building block elements. This concept can be scaled to kilometer size platforms.

### 5.1 EVA Requirements

Construction programatics were not addressed as a part of this study. All building-block elements however, are capable of being deployed to final size by combinations of on-board equipment, stored energy devices and EVA assistance. The role of the astronaut was assumed to be that of assisting in deployment and positioning of the structural elements and repair replacement and inspection of the final spacecraft. The machine assisted assembly in space was viewed as a new technology and not available in the near term time period.

## 6.0 CONCEPT VIABILITY ANALYSIS

A concept viability analysis was conducted to insure that design and analysis techniques were available to properly characterize the structural building block approaches. An additional requirement on the preliminary design details was fabrication precedence or use in, at a minimum, developmental test hardware. A key viability criterion consisted of 1977 manufacturing technology with priority given to practical, low-cost manufacturing processes.

The NASTRAN finite element program was deemed very adequate to analyze the strength, stiffness and isothermal behavior of the tetratruss modules. This program can also analyze the distortion of the truss due to thermal gradients. Boundary conditions verified by 1-g testing are required, however, to accurately describe the behavior of the structure in space. A modification of an existing kinematic analysis program was coded and provided useful spring constant/velocity/acceleration information relative to stored energy and spin deployment of the tetratruss. Element testing described in Section 7.3 to measure joint friction and damping would be used in the kinematic analysis program to verify deployment characteristics.

The lattice strut can be analyzed by several classical methods. Some element in the high D/t range should be done to establish confidence in allowable loads and environmental effects (see Section 7.2).

Chemical rigidization of joints can be accomplished with a polyurethane powder that foams and rigidizes on exposure to ultraviolet rays. Work in this area has been instigated by A.F.M.L. (Ref. 9).

## 6.1 LOW-COST MANUFACTURING OPTIONS

A majority of the detail parts shown in the preliminary design drawings have functional similarities or are replications of existing hardware. The articulating cluster joint and clevis fittings shown in Figure 6.1-1 were developed under Boeing IR&D. Testing of these types of fittings, injection molded from

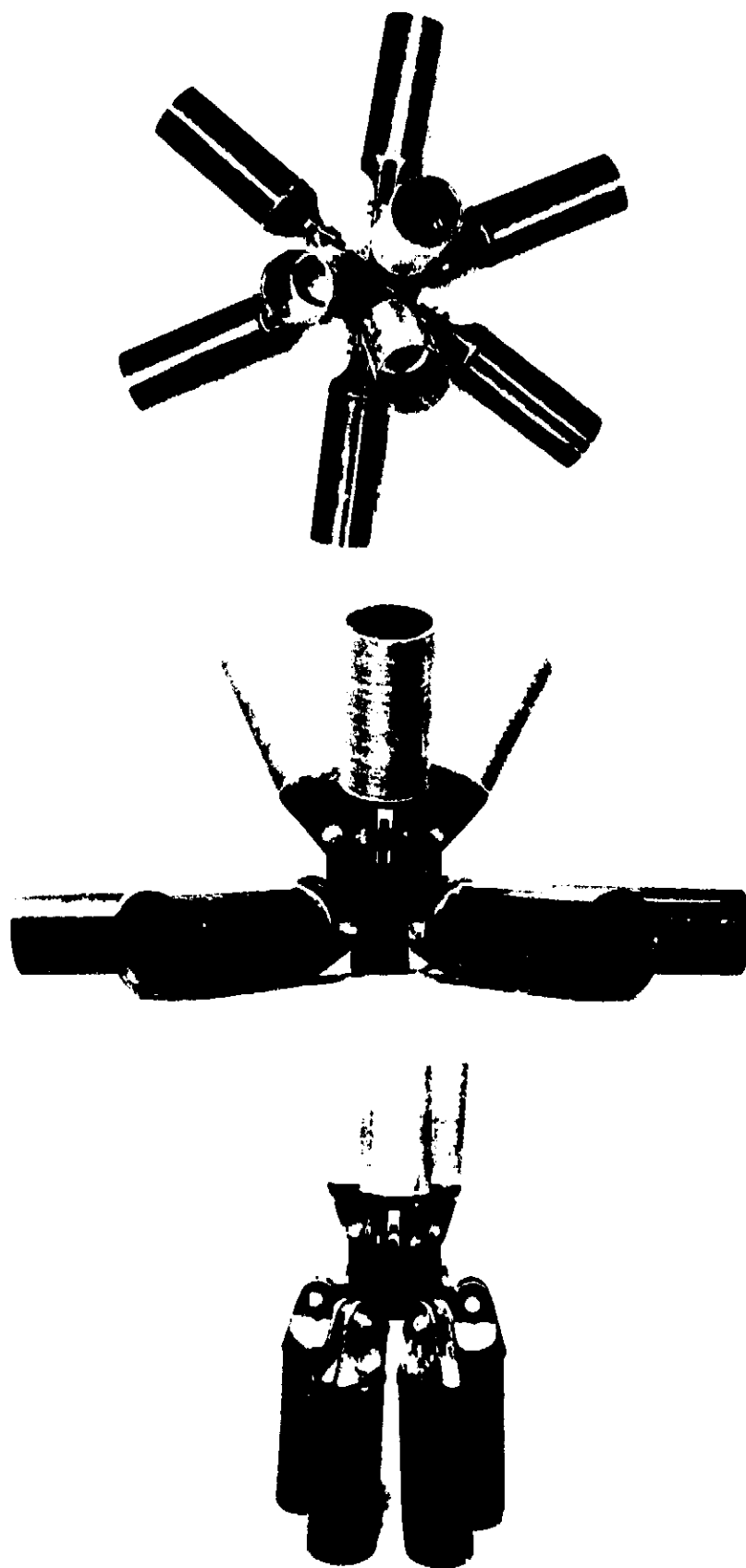


*Figure 6.1-1 Cluster Fitting With Hinged Elements*

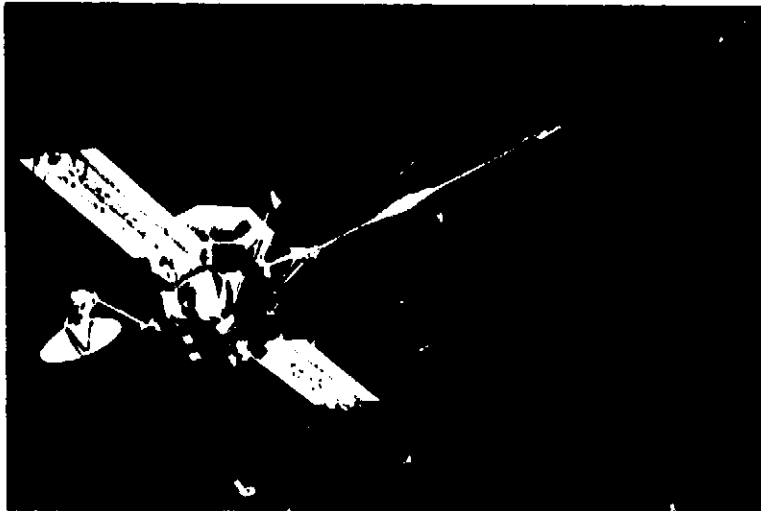
graphite reinforced thermoplastic materials, revealed a low-cost approach to joining stiffness-critical truss members. Long, thin-walled composite tubular struts have been used in a number of contracted and in-house programs, as well as being incorporated into operational spacecraft (Refs. 6, 10, 11). Figure 6.1-2 shows some tubular struts used on various structures that required high stiffness and low thermal distortion. Telescopic struts have been designed, fabricated and tested. Figure 6.1-3 shows a telescopic strut made from fiberglass/epoxy that was used as a payload deployment mechanism under Boeing IR&D. Lattice column concepts have been examined for an number of applications. The open nature of this type of structural member makes it a thermally stable concept by minimizing temperature gradients. This concept, when used with graphite/epoxy chords, can provide a member with essentially zero expansion properties. Several lattice columns have been fabricated and tested under Boeing IR&D as shown in Figure 6.1-4 including multi-chord and spiral lattice configurations. A foldable lattice column, designed for a deployable experiment is shown in Figure 6.1-5 from the fully folded to the deployed position. This unit featured graphite/epoxy chords and fiberglass/epoxy lattice members.

## 6.2 MANUFACTURING APPROACH FOR TETRATRUS MODULE

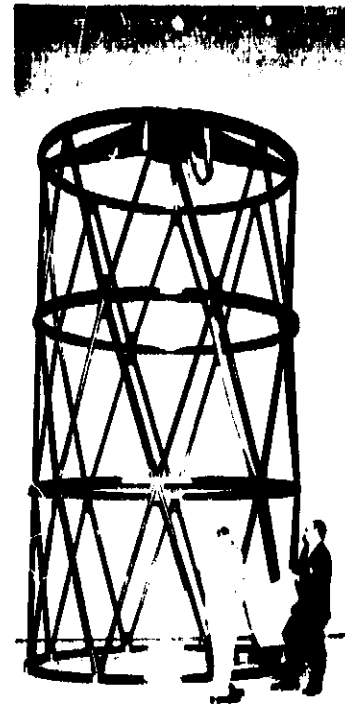
As a guide to cost estimating and concept viability analyses a preliminary manufacturing/fabrication procedure has been prepared to describe a typical module (see Figure 3.8-3) made with graphite/epoxy tubular elements and injection-molded thermoplastic fittings. The details in this procedure have been proven in fabricating the parts described in Section 6.1.

### Module Fabrication Sequence

1. Wind, cure and trim to length strut tubes.
2. Injection mold strut end fittings, knee fittings, and spider fittings.
3. Assemble strut tubes and fittings in bonding assembly tool. Drill and ream attach holes and hinge holes in fittings. Pin fittings to tool and adhesive bond to tubes.



MVM - 73 WITH MAG BOOM EXTENDED



GRAPHITE/EPOXY METERING TRUSS



R. M. S. ARM BOOM CONCEPT



TAPERED COMPOSITE STRUTS  
WITH SNAP-LOCK JOINTS

*Figure 6.1-2 Composite Strut Applications*



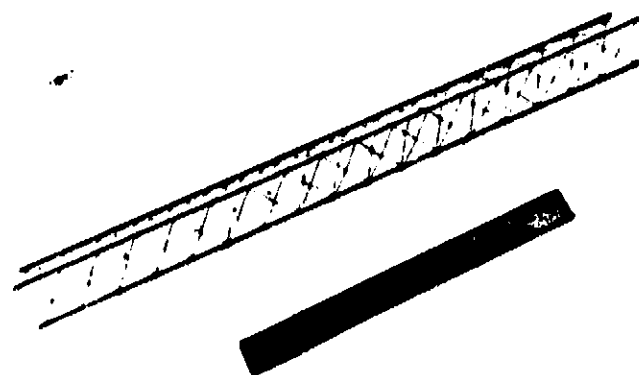
TELESCOPED



DEPLOYED

*Figure 6.1-3 Telescopic Strut Section*





**TRIANGULAR SECTION**



**CIRCULAR SECTION**



**CIRCULAR SECTION**

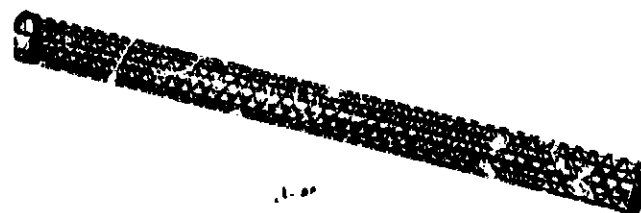
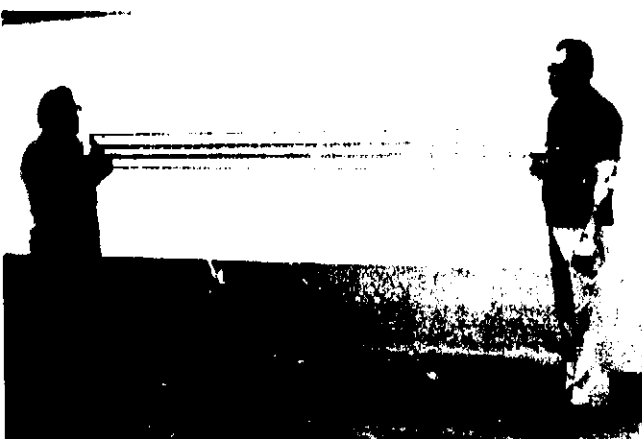
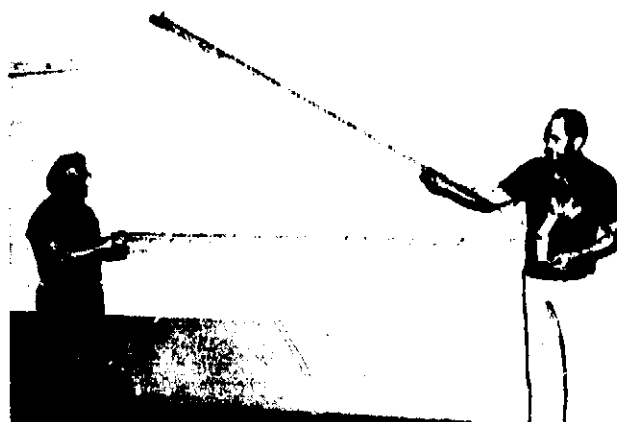


**Figure 6.1-4 Lattice Column Concepts With Graphite/Epoxy Chords and Lattice**



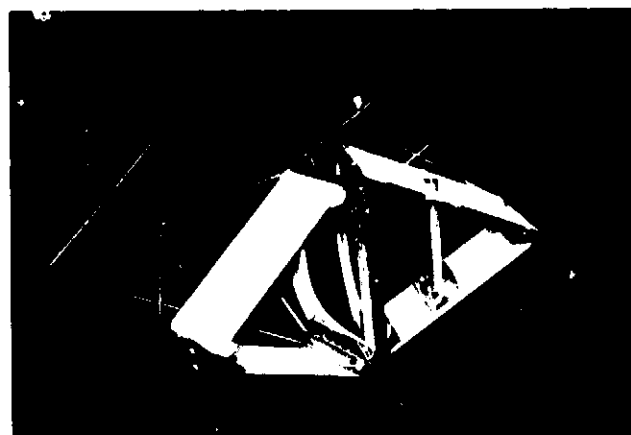
FOLDED



PARTIALLY DEPLOYED



DEPLOYED



HINGE CLOSE-UP

*Figure 6.1-5 Foldable Lattice Column*

4. Install end fitting bushings and knee fitting pin and latch mechanism.
5. Locate and pin spider fittings in assembly tool. Locate and clamp dummy strut between fittings. Drill and ream attach holes. Replace dummy strut with appropriate strut tube. Repeat until all strut tubes are in place in one cell. Remove jig pins and clamps and lift assembly out of assembly tool. Move cell to outside column of assembly tool and assembly next cell. Repeat assembly sequence as required for desired number of cells.

For fabricating a 14-ring truss using 14 foot long tubular members, the following cost estimates have been made:

Detail Part	
Fabrication	\$ 1,160,000
Assembly	533,000
Material	194,000
Tooling	115,000

These values are based on following the proven manufacturing procedures listed above. It was assumed that the 90% learning curve would be followed and that sufficient tooling was available for parallel fabrication lines.

As the number of tubes increases it becomes more advantages to invest in a fully automated tube fabrication facility utilizing pultrusion and filament winding concepts. Such a facility would result in a substantial reduction in tube fabrication costs and greatly increase the rate of production. Some of the assembly operations could also be fully automated but not to the extent of the tube fabrication. The fittings are already injection molded and essentially automated. Tooling cost would increase considerably, reflecting the costs of the automated equipment. This increased cost would tend to disappear as the number of units increased.

## 7.0 STRUCTURE DEVELOPMENT PLANNING

Under Task Four of this study, a program of developmental tests and model verification tests was outlined. The preliminary design concepts and assumed design criteria provided a basis for this program effort. In an actual mission, with particular system requirements, additional verification might be required. For example, trades exist to accomplish a balanced structural/thermal design. Solar flux plus internally generated waste heat will have concept impact and as such, thermal coatings and multilayer insulation usage would have to be examined to satisfy mission-sensitive parameters. While no thermal analysis was funded under this task, a simplified analysis conducted under Boeing IR&D and Contract NAS1-13967 is presented here as data applicable to tetrahedral truss structures and for a point of departure for development planning.

### 7.1 DEVELOPMENT PLAN

A development plan has been conceived which will remove some uncertainties about the structural characteristics of the tetratruss. The plan involves component development tests and tests for analytical model verification. The development tests will be used to provide data for tetratruss static and dynamic analyses, assess component designs, and determine material and structural element capabilities under long-term space environmental conditions. The model verification tests are required to certify the analytical models used to determine static and dynamic characteristics of the tetratruss.

### 7.2 DEVELOPMENT TESTS

Three categories of development tests are proposed for evaluation of materials and component designs. These categories are strength and stiffness of candidate materials and components, module docking concept evaluation, and mechanism characteristics.

The strength and stiffness characteristics tests will be devoted primarily to the evaluation of graphite composite structures. The material testing that must be initiated in the near future is the determination of change in physical characteristics of graphite composites under long-term exposure to vacuum and radiation environment of space. The outgassing and aging effects under long-term space exposure may require modification of the matrix materials being considered for these materials. Also, strength and thermal coefficient of expansion testing of various ply arrangements are required.

Since the LSS will probably be comprised of cylindrical columns with large diameter-to-thickness ( $D/t$ ) ratios, compression and bending tests of these cylinders are required. It is expected that  $100 < (D/t) < 5000$ . There are very little data to support design and analysis of composite tubes in this range. It is proposed that a series of tests of candidate graphite cylinders be performed to determine design allowables for these important structural elements. The initial tests of these cylinders would be performed under controlled environmental conditions of temperature and humidity. The long-term space environmental effects can be determined on additional specimens which have been subjected to vacuum and radiation over various time periods.

The expected scatter in the cylinder tests will mean that a large number of tests must be performed to provide a data base for determining design allowables. The quantity of test specimens has not been determined but the total cost of the test program will be relatively low because the procedure is standard and simple to set up.

The strength and stiffness characteristics of candidate joint designs must also be verified by tests. It is desirable that all joints have the capability to develop the strength of the cylinders. The most severe loading conditions will probably occur during deployment of the tetratruss, but the joints may also require testing for loads imposed during attitude control, orbit transfer, and module docking.

Module docking testing is required to verify load distribution in the tetratruss modules and to determine tolerance requirements when considering fabrication tolerance accumulation and the effect of any thermal expansion of the structure. The docking tests will be performed using portions of the tetratruss which have been instrumented to measure loads and accelerations of the truss elements during the docking maneuver and lockup. All docking tests will be performed under a 1-g environment. Heating elements attached to the test specimens will be used to simulate the solar heating and resulting thermal expansion for various space orientations of the truss.

Mechanism testing will be required to determine joint tolerance requirements and friction characteristics. Joint friction for a quantity of specimens with various tolerances will be determined for use in the deployment analysis. These friction tests will be performed in both air and vacuum to provide data necessary to predicting demonstration deployment of a tetratruss on earth and operational deployment in space. The friction testing will be directed toward achieving a joint design with low friction and a narrow scatter band in the data. Obviously, the joint should be simple in design from cost and weight consideration, but the most important consideration here is the development of reliable low-friction joints with negligible differences in damping characteristics. This is because of the large number of joints and their effect on deployment and stiffness of the tetratruss. It will be necessary to conduct a number of joint friction tests under selected temperature, humidity and load conditions to provide data for deployment analysis of a tetratruss in a 1-g environment. The required development test conditions will be obtained from the deployment analysis model.

### 7.3 MODEL VERIFICATION TESTS

Static and dynamic testing will be required to verify the analytical models used to study behavior of the tetratruss under conditions of deployment, orbit transfer and attitude control. It is expected that all tests can be performed under a 1-g environment. The major test requirement will be that the tests impose boundary conditions identical to those used in the analytical model.

Then if the analytical model provides accurate description of the test specimen behavior on earth, the behavior of the structure in space can be predicted with confidence by using data obtained from development tests. This procedure is common and has been used on many aerospace programs. Models used to predict Saturn vehicle static and dynamics characteristics were developed and verified by nondestructive tests of the vehicles. The Lunar Roving Vehicle was certified for lunar operation analytical models which were verified by testing performed on earth.

Static load tests will be performed to evaluate the tetratruss for steady-state orbit transfer loads imposed by equipment attached to the truss. For example, some truss modules may have to support loads induced by a film or fine mesh stretched over the surface(s) of the truss. Analysis of internal loads and structural deflections can be accurately performed with a computer program such as NASTRAN. Testing which accounts for this preload and any structural temperature gradients would be required to verify the structural model, but these tests could be performed on earth and under ambient conditions. If required, structural temperature gradients can be imposed on the test specimen with heating elements in the same manner used to test the Space Telescope Metering Truss (Reference 6).

Testing will be required to evaluate the deployment analysis. These tests will consider the removal of the truss from the Shuttle payload bay as well as the automatic deployment of the truss. Analysis of RMS and stowed truss motions and loads will be verified by tests which provide data for determination of displacements, accelerations, and internal loads within critical members and attachments during removal from the Shuttle.

The automatic deployment analysis can be verified by 1-g tests of a full-scale two-ring truss. This module would contain 31 cluster joints, 66 tubular mid-joints and 100 tubular elements. The required deployment times will be relatively long to keep inertial loading within structural capability of the lightweight structural elements. This means drag forces should be negligible and the 1-g verification tests can probably be conducted in air under

controlled temperature and humidity conditions. Temperature and humidity may require control if the joint friction development tests show that damping characteristics of the low-friction joints are sensitive to these two parameters.

Vibration tests of the two-ring module will be required to verify the NASTRAN dynamics model of this structure. The NASTRAN model will utilize material and joint damping characteristics and material stiffness determined from the development tests. Dynamic modeling of this type is a recent development under Contract NAS8-31369, Effects of Damping on Mode Shapes (Reference 12). It is expected that the vibration tests will be performed under the same environmental conditions as the deployment tests, but test specimens support conditions will be different.

Instrumentation will generally be the same for the deployment and vibration tests and will consist of strain gages, accelerometers and thermocouples. The quantity and location of measuring devices will be determined from the analyses. In addition to the above instrumentation for dynamic testing, deflection indicators will be required for static testing of the truss.

The plate-element mesh used in the frequency analyses was shown to provide accurate predictions of the first two undamped modes of all models that were studied. A coarser mesh, however, may be capable of providing acceptable results for the multi-module planar arrays. Convergence studies should be performed to define the coarsest mesh which will give acceptable modal data for the multi-module configurations. The coarser models may result in significant savings in computer time. A recommended procedure in development of NASTRAN models of multi-module planar arrays is:

- 1) Develop a detailed finite-element model of the basic module.
- 2) Develop a plate-element model which provides acceptable results for analysis of the basic module.



- 3) Expand the basic module plate-element model to the selected multi-module configuration and obtain results for a selected range of natural frequencies.
- 4) Vary plate-element area and perform convergence studies to find the coarsest acceptable mesh. Use the coarsest acceptable mesh of the multi-module configuration to perform efficient modal surveys involving variations in mass, mass distribution, material damping, etc.

#### 7.4 LARGE SPACE STRUCTURE THERMAL ANALYSIS DEVELOPMENT

A simplified thermal analysis of a representative orbiting large space structure was performed for the purpose of evaluating the character and magnitudes of thermal deformations. Temperature variations in individual members, resulting from natural thermal radiation in orbit, would be used in a NASTRAN analysis of thermal deflections and stresses of an actual mission. The structure chosen for this preliminary analysis was a hexagonal planar planform truss, approximately 100 meters at its maximum dimension, constructed of repeating tetrahedral frame modules. Details of the structure and the orbit selected for this analysis is described in the following paragraphs.

##### 7.4.1 Structure Definition

The thermal analysis was performed on an orbiting platform such as might be used to support the elements of a phased array antenna, an array of sensors, or a continuous planar reflecting surface. The analysis considered only the primary structural members of such a spacecraft and neglected any possible on-board heat sources or non-structural heat sinks.

The structure is hexagonal in planform, with a major planform dimension of 109.96 meters, as illustrated in Figure 7.4-1. The structure is constructed of identical repeating equilateral tetrahedral modules, shown in Figure 7.4-2, forming a planar truss of uniform thickness. The interrelated properties of truss thickness, number of modules, and length of individual members

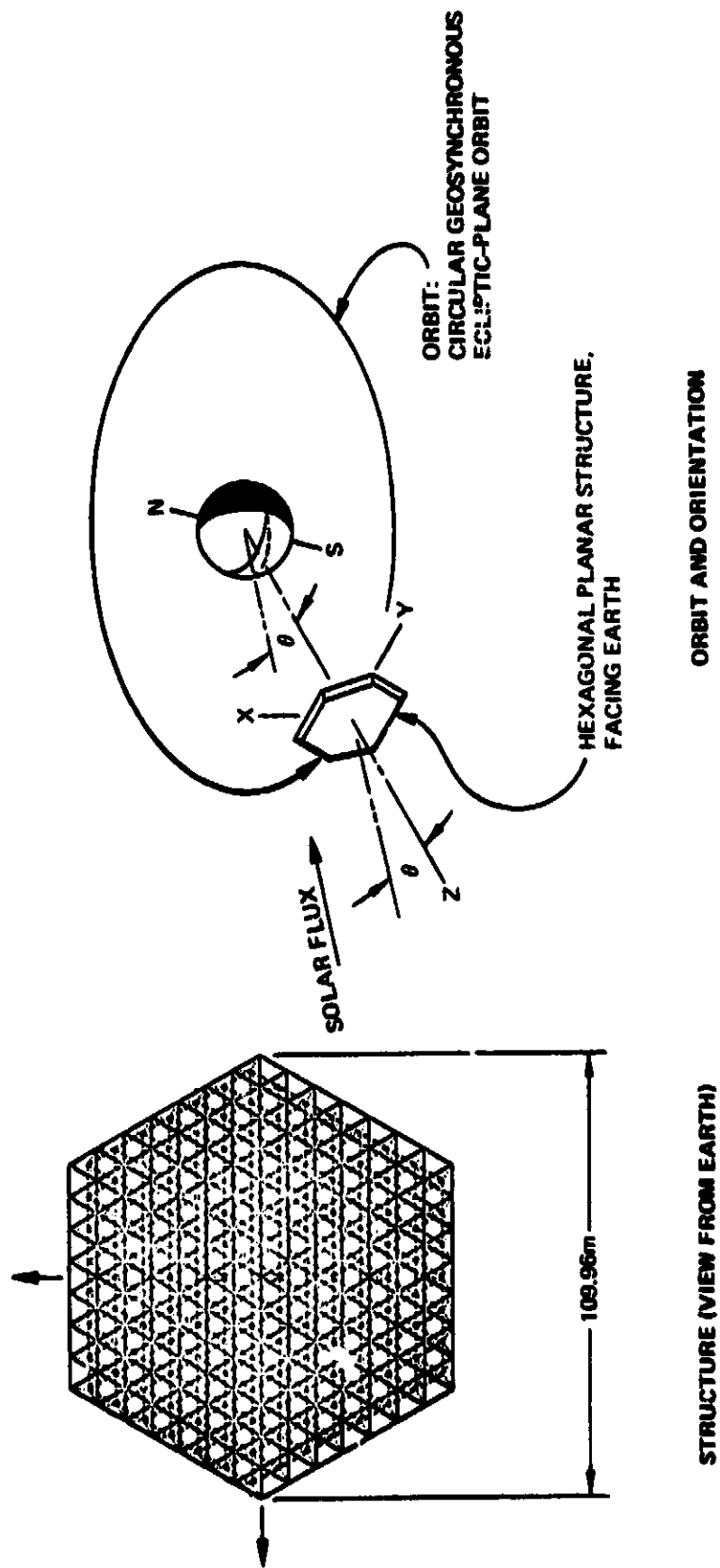


Figure 7.4-1. Orbiting Large Space Structure

are yet to be determined. Likewise the member joint characteristics are yet to be determined.

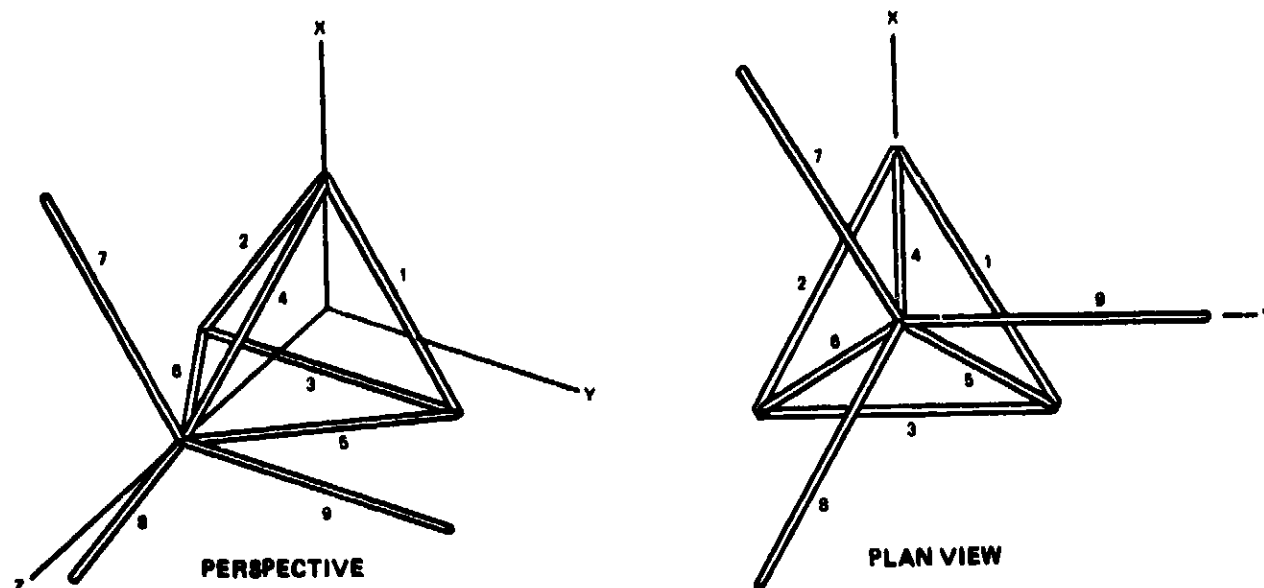


Figure 7.4-2. Tetrahedral Truss Prime Module

All members of the truss are identical tubes of graphite-epoxy composite, 50.8 mm (2.0 in.) in diameter, with 0.508 mm (0.020 in.) wall thickness. Tube surface radiant properties were taken from measurements made at Boeing on MB-0001 (HMS fiber) graphite-epoxy samples. The pertinent values are:

Solar absorptance = 0.916

Emittance = 0.80

#### 7.4.2 Thermal Analysis of Structure in Geosynchronous Orbit

##### Orbit Definition

The orbit selected for the first thermal analysis was a circular geosynchronous orbit in the ecliptic plane. The orbital period was 86164 seconds (24 hours). The structure was assumed oriented so that the normal to the plane of the truss is always directed at the center of the earth. For a structure main-

taining an earth-facing orientation it is expected that a geosynchronous orbit will be more critical to structural thermal deformations because of the absence in geosynchronous orbit of the moderating effect of earth radiation on temperature variations. The structure was oriented so that the larger of its two faces was toward the earth and so that its x-axis was aligned toward solar system north (Figure 4-1).

### Thermal Analysis

Heat input to the structure in geosynchronous orbit was assumed to consist of solar radiation only. Earth-emitted and earth-reflected flux at geosynchronous altitudes are negligible to all but the most detailed thermal environment assessments. Occultation (eclipsing) was ignored for the geosynchronous orbit analysis. Although occultation will occur once each orbit for an ecliptic plane orbit, temperatures computed for an ecliptic plane orbit are accurate approximations of temperatures for a wide range of low-inclination orbits. For most of these other orbits occultation will occur for only a few cycles, at two periods each year. Previous thermal analyses indicated that structural temperatures tend to become uniform during occultation, minimizing the possibility that critical thermal deformations will occur as a result of occultation. Thus, the assumption of no occultation, which has considerable value in simplifying the thermal analysis, does not appear to significantly jeopardize the validity of the results.

The structural member temperatures were computed for a steady-state heat balance between solar radiation absorbed and infrared radiation emitted. The slow rate of change in member orientation relative to the solar flux in a geosynchronous orbit and the absence of any sudden changes in heating due to shading or occultation result in insignificant structural thermal capacitance effects. Thus the steady-state assumption is quite valid for this case.

In keeping with expected launch packaging restrictions, weight limitations, and very low on-orbit loads, it was assumed that the individual members of the truss will be very slender. Thus, with a tube of relatively low longitudinal thermal conductance, only a small portion of each tube's length will be

affected by heat conducted to or from adjoining tubes. Furthermore, the assumed very slender tubes will not be significantly affected by mutual radiation interchange because of very small radiation view factors. Therefore, it was assumed that each tube responds to the thermal environment as an isolated element, leading to predictions of constant temperatures along each member's length. Such an approach is slightly conservative for use in predicting thermal distortions since any inter-member heat exchange that does exist will act to relieve temperature differences and reduce distortions.

The distribution of local values of heat absorbed and heat emitted will in general result in temperature gradients around each tubular member's cross section. These gradients, in turn, will induce bending moments and curvature in the members. With flexible or pinned joints between members the only consequence of this curvature will be a slight change in the member's length. With rigid joints, the induced moments will interact with those from other members, possibly influencing the overall structural distortion. For the present analysis, however, distortions resulting from cross section gradients were assumed secondary to those resulting from member mean temperature variations and longitudinal expansion. Therefore the thermal analysis was performed for isothermal cross sections and yielded only the member mean temperatures.

#### Temperature Results

Structural temperature histories through the geosynchronous orbit are shown as the broken lines (Open Frame) in Figures 7.4-3 through 7.4-7. The figures also show, as solid lines, temperatures for the same structure with an opaque surface on the earth-facing side of the truss. These shielded-frame temperatures were generated under Task III of Contract NAS1-13967. The shield for that analysis had the following properties:

Solar absorptance, truss side	= 0.9
Emittance, truss side	= 0.9
Solar absorptance earth side	= 0.1
Earth-emission absorptance, earth side	= 0.1
Emittance, earth side	= 0.1

The orientation of certain members results in common thermal response, allowing the members to be grouped together on the plots of temperature e.g., members 1, 2, 7 and 8 on Figure 7.4-3.

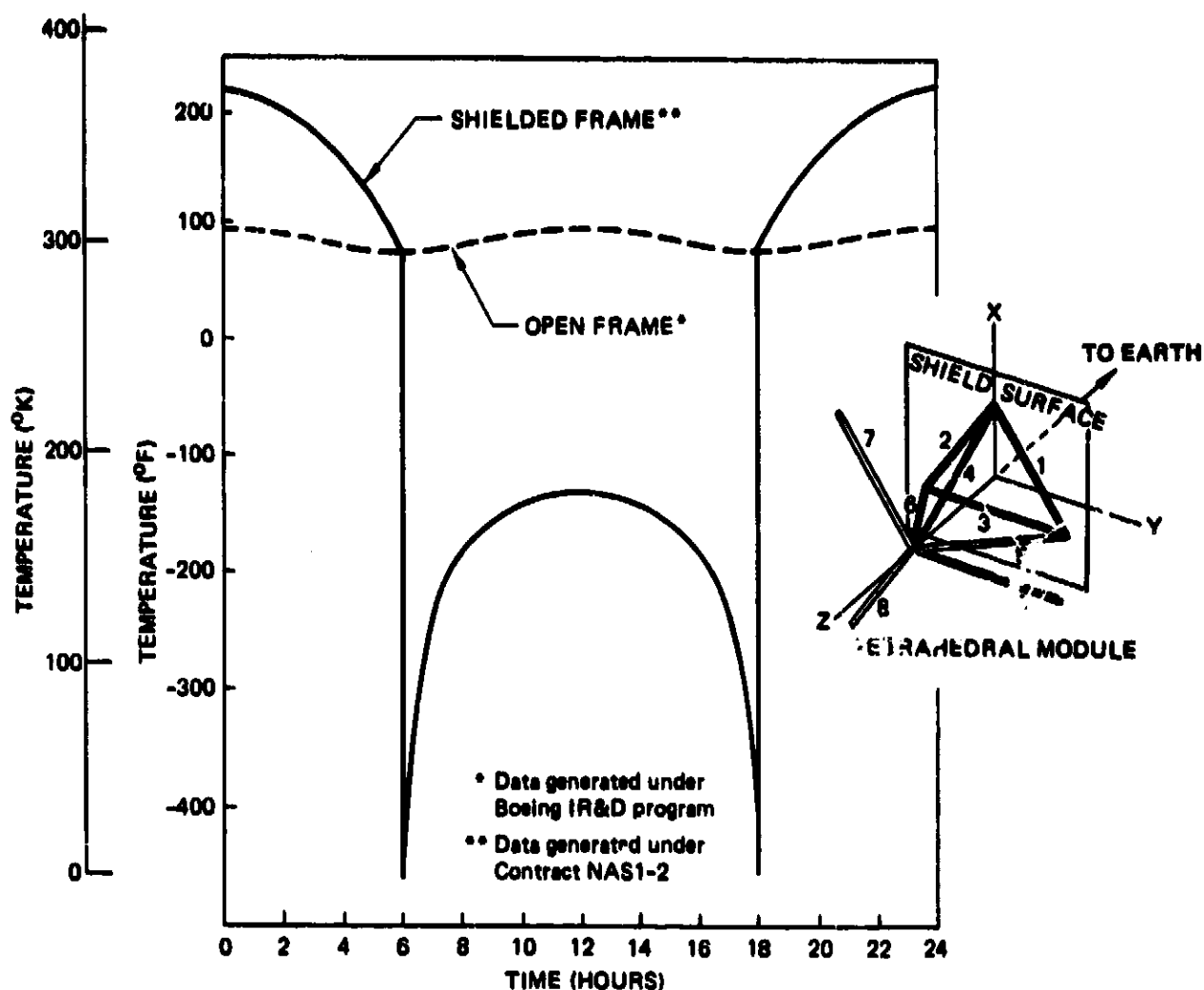


Figure 7.4-3. Temperatures, Geosynchronous Orbit, Members 1, 2, 3, 7, 8

The orientation of members 3 and 9, Figure 7.4-4, is such that these tubes become parallel to the solar flux twice in each orbit, at 6 hours and 18 hours. Under the analysis assumptions of no thermal capacitance and no inter-member heat exchange, the temperatures of these members at these times drop to near the space background level, assumed as 3K (-455°F). In reality, the effects of capacitance and heat flow from other members would probably become significant at these brief periods, moderating the extreme low temperatures that were predicted. A more realistic estimate of these minimum temperatures,

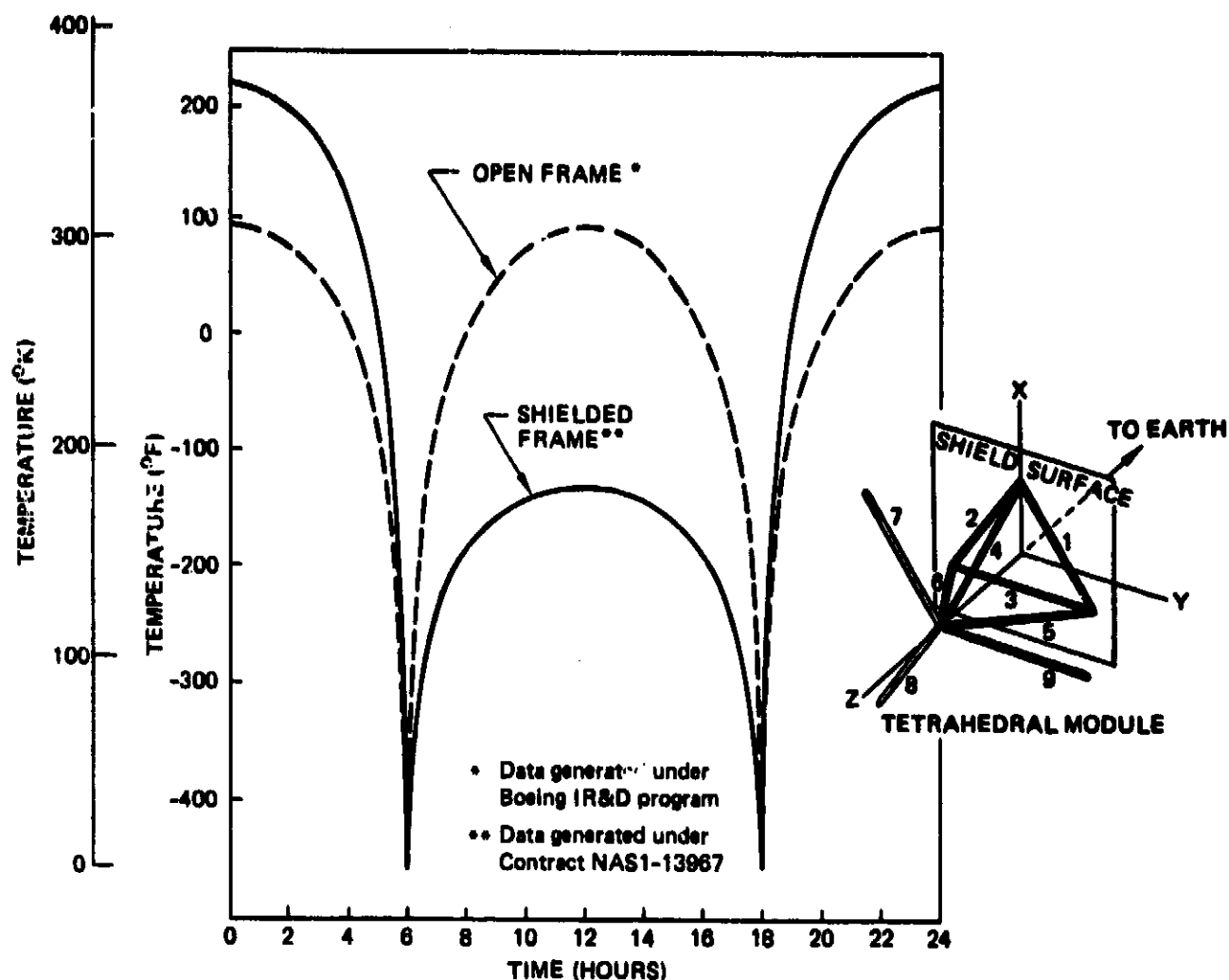


Figure 7.4-4. Temperatures, Geosynchronous Orbit, Members 3, 9

based on a simplified evaluation of the transient response of the members, would need to be incorporated in the deformation analyses of a particular spacecraft.

In summary, the thermal guidelines thus far established should be used as a point of departure when a detailed analysis is done on a particular application. A document that will expand these guidelines titled "Simplified Thermal Analysis for Large Space Structures" will be released at the completion of Task I of NAS1-13967 (Ref. 5).

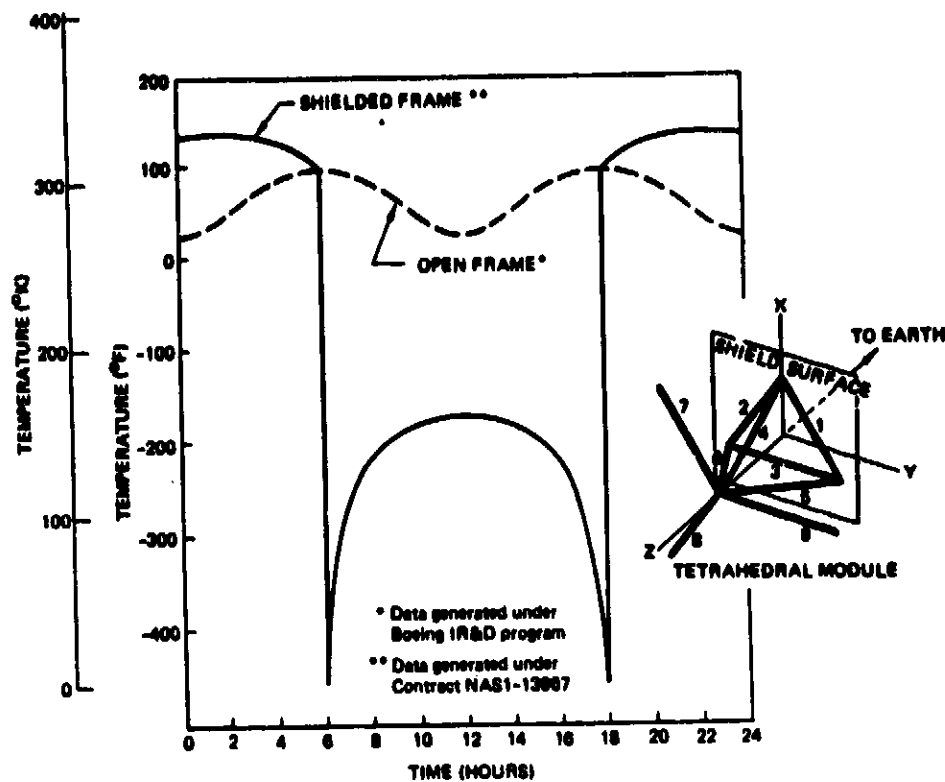


Figure 7.4-5. Temperatures, Geosynchronous Orbit, Member 4

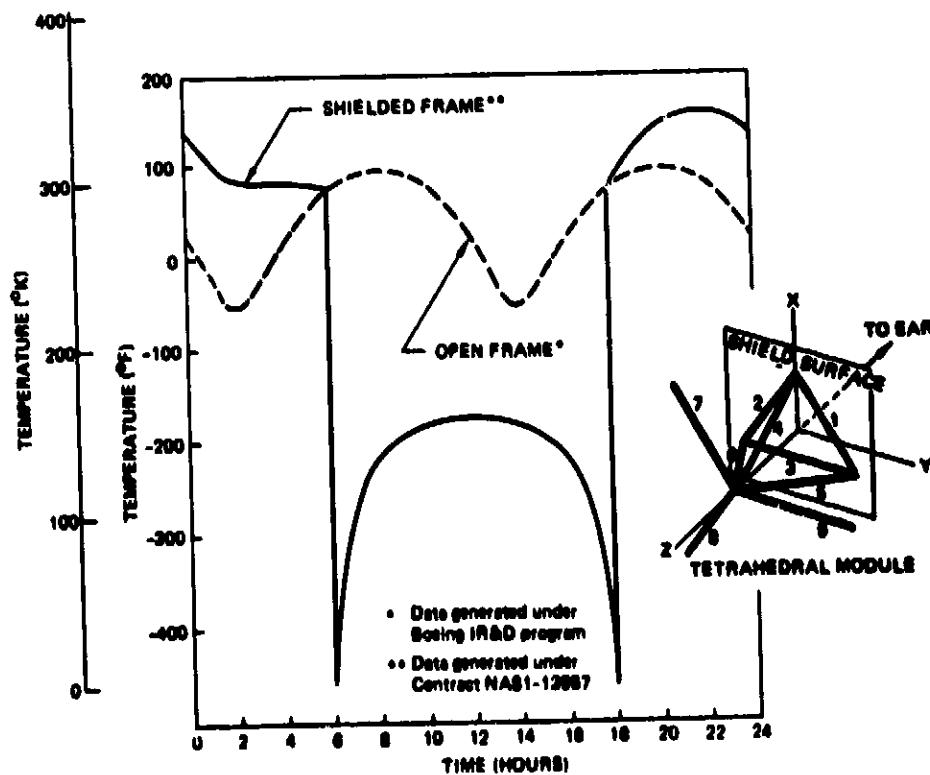


Figure 7.4-6. Temperatures, Geosynchronous Orbit, Member 5



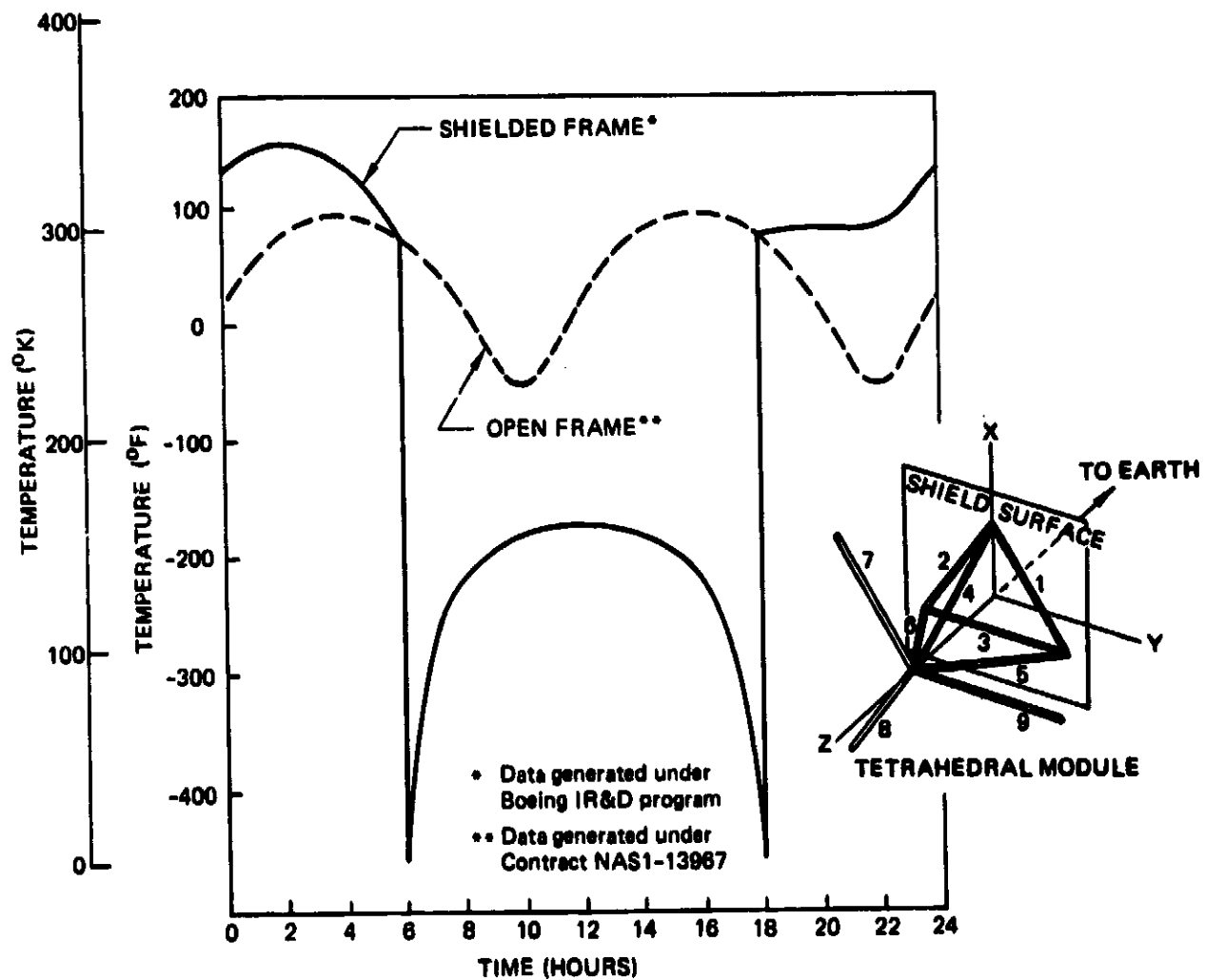


Figure 7.4-7. Temperatures, Geosynchronous Orbit, Member 6

## 8.0

### CONCLUDING REMARKS

Ultra-large structures in space will require, in similar fashion to earth-based construction, a mix of fabrication/assembly schemes. Mission requirements that dictate multi-kilometer sized beams and planar arrays are best satisfied by semi-automated orbiting construction facilities that are fed by heavy lift launch vehicles with basic raw materials. These mass-producing facilities can be thought of as the evolving end product of the "space industrial revolution". In the intervening time period, the construction/assembly learning curve will be established by current S.T.S. transportation and building-block structural concepts amenable to deployment, erection and assembly directed by man with the aid of currently available man-machine tools.

This study has identified two building-block structural concepts that can be utilized in various combinations to construct the structural framework for many large spacecraft configurations. The concepts are S.T.S. compatible in weight and volume goals and represent high on-orbit productivity in terms of structural area or beam length delivered to L.E.O.

A two-tier structural approach utilizing deployable tetratruss modules supported by a deeper tetrahedral truss was conceived as a method of scale-up to large spacecraft applications. The use of relatively "fine grid" deployable truss modules and a primary structure of long lattice compression members simultaneously answers the need for (1) a payload interface with "smaller" hardware and the need for (2) a stiff structure for orbital maneuvers and pointing accuracy.

The construction programmatics were not addressed in depth. Techniques need to be examined such as module removal and deployment from the payload bay assisted by R.M.S., spin table or other deployment - fabrication booms with active erection aids.

A development plan was outlined to show areas of needed data to enable simplified computer-aided analyses to characterize ultra-large structures (megamechanics). High-fidelity modeling of critical interfaces will be required in normal fashion using existing finite element techniques.

The detail design concepts and material choices represent features that have fabrication precedence and require no state-of-art manufacturing technology advances.

## REFERENCES

1. "Outlook for Space", NASA SP-386, January 1976
2. "Orbital Assembly and Maintenance Study", Final Report, NAS9-14319, by Martin Marietta Corp. for NASA L. B. Johnson Space Center, August 1975
3. "Advanced Technology Laboratory Program for Large Space Structures", NAS1-14116-1 by Rockwell International Space Div. for NASA Langley Research Center, August 1976
4. "Orbital Construction Demonstration Study", Final Report, NAS9-14916 by Grumman Aerospace Corporation for NASA L. B. Johnson Space Center, December 1976
5. "Evaluate the Influence of the Operational and System Imposed Requirements on the Structural Design of Large Flexible Spacecraft", Tasks II Monthly Progress Report, NAS1-13967, by Boeing Aerospace Company for NASA Langley Research Center, May 1976
6. "Design Fabrication and Test of a Graphite/Epoxy Metering Truss", Final Report Contract NAS8-29825, by Boeing Aerospace Company for NASA Marshall Space Flight Center, December 1975
7. David W. Twigg, Richard H. Karnes, "Prometheus a User - Oriented Program for Human Crash Dynamics", Contract N00014-72-C-0223, for Office of Naval Research, Nov. 1974, Boeing Computer Services, Inc.
8. Telecon with JSC Contracting Officers Representative, Dr. Fred Stebbins regarding M.P.T.S.
9. J. Spacecraft, V3, No. 4, "Space Rigidized Resin Fiberglass Sandwich Materials", by Hughes Aircraft Company for AFML under Contract F33(657)-11287, April 1966

10. Composite Boom Assembly for MVM-73 Spacecraft Magnetometer Experiment, by Boeing Aerospace Company for J.P.L. under Contract 95300, Tasks 10A and B.
11. Graphite Epoxy Support Truss for Applications Technology Satellite (ATS-F) by Fairchild Industries and Hercules Incorporated under contract to NASA-GSFC, 1971
12. R. M. Gates and D. H. Merchant, Boeing Document D180-20572-1, Effects of Damping on Mode Shapes, Contract NAS8-31369, June 1977
13. Bush, Harold G.; and Mikulas, Martin M. Jr.: "A Nestable, Tapered Column Concept for Large Space Structures", NASA TMX-73927, 1976